UNIVERSIDADE DE SÃO PAULO
ESCOLA DE ENGENHARIA DE SÃO CARLOS

ANDRISE BUCHWEITZ KLUG

Avaliação do dano por fadiga em matrizes de agregado fino preparadas com misturas asfálticas fresadas e resíduo de óleo de xisto

São Carlos, SP
2017

UNIVERSITY OF SÃO PAULO
SÃO CARLOS SCHOOL OF ENGINEERING

ANDRISE BUCHWEITZ KLUG

Evaluation of the fatigue performance of fine aggregate matrices prepared with reclaimed asphalt pavements and shale oil residue

São Carlos, SP
2017

ANDRISE BUCHWEITZ KLUG

Avaliação do dano por fadiga em matrizes de agregado fino preparadas com misturas asfálticas fresadas e resíduo de óleo de xisto

Dissertação submetida ao Departamento de Transportes da Escola de Engenharia de São Carlos – Universidade de São Paulo (STT/EESC/USP) como parte dos requisitos para obtenção do título de Mestre em Engenharia Civil.

Área de Concentração: Infraestrutura de Transportes

Orientador: Adalberto Leandro Faxina (Professor Associado)

VERSÃO DEFINITIVA

São Carlos, SP

2017

Klug, Andrise Buchweitz
K63 / Andrise Buchweitz Klug; orientador Adalberto Leandro Faxina. São Carlos, 2017.

Dissertação (Mestrado) - Programa de Pós-Graduação em Engenharia de Transportes e Área de Concentração em Infraestrutura de Transportes -- Escola de Engenharia de São Carlos da Universidade de São Paulo, 2017.

1. fine aggregate matrices. 2. reclaimed asphalt pavements. 3. viscoelastic continuum damage theory (VECD). 4. shale oil residue. I. Título.

ANDRISE BUCHWEITZ KLUG

Evaluation of the fatigue performance of fine aggregate matrices prepared with reclaimed asphalt pavements and shale oil residue

This dissertation was submitted to the Department of Transportation Engineering of the São Carlos School of Engineering – University of São Paulo (STT/EESC/USP) in partial fulfillment of the requirements for the Master's Degree in Civil Engineering.

Subject Area: Transport Infrastructure

Advisor: Adalberto Leandro Faxina (Associate Professor)

FINAL VERSION

São Carlos, SP

2017

Klug, Andrise Buchweitz
K63 / Andrise Buchweitz Klug; orientador Adalberto Leandro Faxina. São Carlos, 2017.

Dissertação (Mestrado) - Programa de Pós-Graduação em Engenharia de Transportes e Área de Concentração em Infraestrutura de Transportes -- Escola de Engenharia de São Carlos da Universidade de São Paulo, 2017.

1. fine aggregate matrices. 2. reclaimed asphalt pavements. 3. viscoelastic continuum damage theory (VECD). 4. shale oil residue. I. Título.

FOLHA DE JULGAMENTO

Candidata: **ANDRISE BUCHWEITZ KLUG**

Título da dissertação: "Avaliação do dano por fadiga em matrizes de agregado fino preparadas com misturas asfálticas fresadas e resíduo de óleo de xisto"

Data da defesa: 22.08.2017

Comissão Julgadora:	**Resultado:**
Prof. Associado **Adalberto Leandro Faxina (Orientador)** (Escola de Engenharia de São Carlos/EESC)	APROVADA
Profª. Drª. **Verônica Teixeira Franco Castelo Branco** (Universidade Federal do Ceará/UFC)	APROVADA
Profª. Drª. **Jamilla Emi Sudo Lutif Teixeira** (Universidade Federal do Espírito Santo/UFES)	APROVADA

Coordenadora do Programa de Pós-Graduação em Engenharia de Transportes:
Profª. Associada **Ana Paula Camargo Larocca**

Presidente da Comissão de Pós-Graduação:
Prof. Associado **Luis Fernando Costa Alberto**

DEDICATÓRIA

Dedico este trabalho...

A minha perfeita família, nas suas imperfeições:

A meu pai, cujo incentivo e confiança foram essenciais para que eu buscasse meus objetivos de vida sem hesitar;

A minha mãe, que sempre me inspirou por meio de sua bondade, paciência, amor e dedicação.

A meus irmãos, a quem tenho em profunda estima e admiração.

AGRADECIMENTOS

Agradeço...

... ao Professor Adalberto Leandro Faxina a orientação, a dedicação, a paciência, o profissionalismo e a motivação no decorrer desta pesquisa;

... a meus pais o apoio e amor, incondicionais;

... a minha irmã, Marlise, o carinho, a compreensão, a empatia, o amor... porque sua garra e dedicação me são inspiradoras... o seu apoio constante que me motiva e me traz a segurança e a tranquilidade necessárias para manter o foco e a fé nos meus objetivos;

... a meu irmão, Tiago, o carinho, a confiança, o amor e a trilha sonora de muitos momentos... o seu brilhantismo e sua dedicação a tudo que se propõe, porque me são inspiradores... a parceria durante toda a vida, que sempre me trouxe serenidade e segurança;

... a meu irmão, Thales, que pela sua bondade, carinho, otimismo e amor, torna a vida mais leve com sua presença;

... a Josiane Bartz, porque é presente... porque nas especificidades de nossas personalidades, entendi o tamanho do presente que a mim foi dado por meio desta amizade... porque torna a vida indiscutivelmente melhor;

... a Thieli, Micheli e Samara, porque existem na minha vida, porque nossos momentos são sempre para somar;

... a Vó Vanda o apoio e contribuição direta ao longo de toda a vida. Aos avós Bruno e Elda, porque cumprem o papel de avós com zelo, dedicação e amor;

... a Andressa Ng a parceria e a amizade, o que enriqueceu o trabalho e trouxe leveza e alegrias durante a caminhada;

... a Anthony Gomes o carinho, a amizade, o incentivo e o apoio constantes;

... a Bruno Faglioni, Carolina Kubiaki, Angélica Meireles e Murilo Santos o “pode contar comigo”, o ombro amigo;

... a Matheus Silva, Ramane Cristina, Fernando Piva, Rosuel Krum, Elaine Ribeiro, Júlia Savietto, Bruno Medeiros, Felipe Bethonico, Monigleicia Orioli e Adrian Grasson Filho os abraços, as palavras amigas, os sorrisos;

... aos colegas do Departamento de Transportes, especialmente à galera da Toca do STT, os bons momentos compartilhados;

... a Donaldo e Clécia, Írio e Elaine as portas e braços abertos;

... aos professores do Departamento de Transportes o conhecimento compartilhado;

... à equipe dos laboratórios e aos demais funcionários do Departamento de Transportes, especialmente a Aline do Vale, Ygor Mello e João Domingos Pereira Filho o suporte direto e constante no decorrer dos trabalhos.

A todos meu Muito Obrigada!!

RESUMO

KLUG, A. B. (2017). **Avaliação do dano por fadiga em matrizes de agregado fino preparadas com misturas asfálticas fresadas e resíduo de óleo de xisto**. Dissertação (Mestrado em Engenharia Civil) – Departamento de Engenharia de Transportes, Escola de Engenharia de São Carlos, Universidade de São Paulo, São Carlos, SP.

A incorporação de misturas asfálticas fresadas na produção de misturas asfálticas novas é uma alternativa útil à utilização de materiais novos, gerando benefícios econômicos e ambientais. A reciclagem de pavimentos criou um ciclo sustentável de reuso de recursos naturais não-renováveis, reduzindo a demanda por agregado mineral e asfalto novos. No entanto, a adição do material fresado, especialmente em proporções altas, provoca aumento na rigidez da mistura asfáltica, causado pela alta rigidez do asfalto envelhecido. Uma elevada rigidez pode tornar a mistura asfáltica mais propensa ao trincamento por fadiga. Para contornar tal desvantagem e permitir a adição de maiores quantidades de material fresado, asfaltos de baixa consistência e agentes de rejuvenescimento podem ser adicionados à mistura. Os asfaltos de baixa consistência atuam para reduzir a rigidez do asfalto envelhecido e os agentes de rejuvenescimento atuam para restaurar as propriedades originais do asfalto envelhecido, aproximando-as das exigidas pelas especificações para asfaltos virgens. O resíduo de óleo de xisto é um dos agentes rejuvenescedores mais utilizados no Brasil e, segundo a literatura, resulta em desempenho comparável ao desempenho de outros agentes rejuvenescedores comerciais, com a vantagem de apresentar maior poder de rejuvenescimento devido à sua maior aromaticidade. O processo de trincamento por fadiga principia nas microtrincas presentes na matriz de agregado fino (MAF) da mistura asfáltica. Uma abordagem para avaliar o comportamento à fadiga das misturas asfálticas é baseada na teoria do dano contínuo em meio viscoelástico, pela qual o processo de trincamento do material é representado por variáveis de estado interno associadas à redução na integridade do material. Neste estudo, ensaios em amostras de MAF foram feitos para caracterizar o desempenho à fadiga, e os dados foram analisados utilizando a teoria do dano contínuo em meio viscoelástico. O objetivo da pesquisa foi avaliar o desempenho à fadiga de MAFs produzidas com três proporções de material fresado (20, 40 e 100%), dois asfaltos com diferentes graus de desempenho (PG 64-22 e PG 58-16), e três combinações (100/0, 50/50, 0/100) de asfalto PG 64-22 e agente de rejuvenescimento (resíduo de óleo de xisto). Dentre as MAFs preparadas com material fresado, duas apresentaram desempenho à fadiga superior à mistura de controle (composta apenas com materiais novos): a MAF composta com 40% de material fresado e PG 64-22 e a MAF composta com 20% de material fresado e PG 58-16. O resíduo de óleo de xisto não atuou como rejuvenescedor do asfalto envelhecido, para a maioria dos casos avaliados, provavelmente devido à baixa taxa de difusão do material no asfalto envelhecido.

Palavras-chave: Matrizes de agregado fino, misturas asfálticas fresadas, dano contínuo em meio viscoelástico (VECD), resíduo de óleo de xisto.

ABSTRACT

KLUG, A. B. (2017). **Evaluation of the fatigue performance of fine aggregate matrices prepared with reclaimed asphalt pavements and shale oil residue**. Master's Dissertation (Master of Civil Engineering) – Department of Transportation Engineering, São Carlos School of Engineering, University of São Paulo, São Carlos, SP. Brazil.

The incorporation of recycled asphalt pavements (RAP) in the production of new asphalt mixtures is a useful alternative to the use of virgin materials, leading to economic and environmental savings. Pavement recycling created a sustainable cycle of reuse of nonrenewable natural resources, reducing the demand for new mineral aggregate and binder. However, the addition of RAP, especially at higher percentages, increases the stiffness of the asphalt mixture, because of the high stiffness of the aged binder. High stiffness makes the asphalt mixtures more prone to fatigue cracking. In order to overcome such limitation and allow the incorporation of higher percentages of RAP, soften binders or rejuvenating agents are added to the mixture. The former act to reduce the high stiffness of the aged binder and the latter act to restore the aged binder properties to those required by the binder specifications. The shale oil residue is one of the most used rejuvenating agents in Brazil, and, according to the literature, its performance is comparable to other commercial rejuvenating agents, with the advantage of presenting higher rejuvenating potential, what is due to its higher aromaticity. The fatigue cracking process starts as micro cracks in the fine aggregate matrix (FAM) of the full asphalt mixture. One approach to investigate the fatigue process of the asphalt mixtures is based on the viscoelastic continuum damage theory (VECD), in which the process of micro cracking of a material can be represented by internal state variables associated with the reduction of the material integrity. In this study, tests on FAM samples were performed in order to evaluate the fatigue performance, and the results were analyzed by means of the VECD theory. The objective of this research was to evaluate the fatigue performance of FAMs produced with three RAP contents (20, 40 and 100%), two binders of different performance grades (PG 64-22 and PG 58-16), and the combination of new binder (PG 64-22) and rejuvenating agent (shale oil residue) at different binder/agent rates (100/0, 50/50 and 0/100). Out of the FAMs prepared with RAP, two presented fatigue performance superior to the control mixture (compounded with only new materials): the FAM prepared with 40% of RAP and PG 64-22 and the FAM prepared with 20% of RAP and PG 58-16. The shale oil residue did not play its role of rejuvenating the aged binder for most cases, probably because of the low diffusion rate of the material into the aged binder.

Keywords: Fine aggregate matrices, reclaimed asphalt pavements, viscoelastic continuum damage theory (VECD), shale oil residue.

TABLE OF CONTENTS

1. INTRODUCTION 17
1.1. Reclaimed asphalt pavements (RAP) 17
1.2. Use of rejuvenating agents and soft asphalt binders 19
1.3. Tools to evaluate the incorporation of RAP into new HMA mixtures 20
1.4. The viscoelastic continuum damage theory 21
1.5. Objectives of this research 21
1.6. Experimental plan and method of analysis 22
1.7. Structure of this master's dissertation 22
2. LITERATURE REVIEW 25
2.1. Reclaimed asphalt pavements (RAP) 25
2.1.1. RAP applications around the world 25
2.1.2. Environmental and economic perspectives 26
2.1.3. Technics used to incorporate RAP in asphalt mixtures 27
2.1.4. Long-term performance of asphalt mixtures containing RAP 30
2.1.5. RAP asphalt binder 36
2.1.6. Design of asphalt mixtures using RAP 41
2.1.7. Some Brazilian research works with RAP 49
2.2. Fine aggregate matrix (FAM) 52
2.2.1. Mechanisms of damage of asphalt concrete mixtures 55
2.2.2. Micromechanical computational modeling 60
2.2.3. Viscoelastic continuum damage theory – VECD 62
2.2.4. Reclaimed Asphalt Pavements – RAP 64
2.2.5. Rheological properties 65
2.3. Theory of viscoelastic continuum damage – VECD 66
2.3.1. The Work Potential Theory 67
2.3.2. Elastic-Viscoelastic Correspondence Principle 69
2.3.3. Viscoelastic Continuum Damage Model 71
2.3.4. Mechanistic Fatigue Life Prediction Model 75
2.4. Linear viscoelasticity 76
3. MATERIALS AND METHOD 79
3.1. Mineral aggregates 79
3.1.1. New mineral aggregates 79

3.1.2. Reclaimed asphalt pavements (RAP) 79
3.1.3. Aggregate gradation 80
3.2. Asphalt binders 81
3.3. Rejuvenating agents 82
3.4. FAM mixtures 83
3.4.1. FAM design method and preparation of the mixtures 83
3.4.2. Compaction method 84
3.4.3. Sample preparation 84
3.5. Tests in the DSR 85
3.5.1. Linear-viscoelastic range 86
3.5.2. Fingerprint test – linear-viscoelastic properties 87
3.5.3. Damage tests 89
3.6. Procedure of analysis 90
3.6.1. Damage analysis 90
3.6.2. Prediction of fatigue life 91
4. RESULTS 93
4.1. Characterization of the samples 93
4.2. Linear viscoelastic properties 93
4.3. Relaxation properties and damage evolution rate 95
4.4. Characteristics curves – *CxS* 100
4.5. Fatigue models 103
4.6. Comparison of the fatigue lives of the FAMs at different strain levels 108
4.6.1. FAM 1 (only RAP) and FAM 2 (only new materials) 109
4.6.2. FAM 1 (only RAP), FAM 2 (only new materials) and FAM 7 (20%RAP+PG64) 110
4.6.3. FAM 1 (only RAP), FAM 2 (only new materials) and FAM 8 (40%RAP+PG64) 112
4.6.4. FAM 1 (only RAP), FAM 2 (only new materials) and FAM 9 (20%RAP+PG58) 113
4.6.5. FAM 1 (only RAP), FAM 2 (only new materials) and FAM 10 (40%RAP+PG58) 114
4.6.6. FAM 1 (only RAP), FAM 2 (only new materials) and FAM 11 (20%RAP + 50/50 – PG64/rejuvenator) 115
4.6.7. FAM 1 (only RAP), FAM 2 (only new materials) and FAM 12 (20%RAP + 0/100 – PG64/rejuvenator) 116

4.6.8. FAM 1 (only RAP), FAM 2 (only new materials) and FAM 13 (40%RAP + 50/50 – PG64/rejuvenator) 118
4.6.9. FAM 1 (only RAP), FAM 2 (only new materials) and FAM 14 (40%RAP + 0/100 – PG64/rejuvenator) 119
4.6.10. FAM 7 (20%RAP+PG64) and FAM 8 (40%RAP+PG64) 120
4.6.11. FAM 9 (20%RAP+PG58) and FAM 10 (40%RAP+PG58) 121
4.6.12. FAM 7 (20%RAP+PG64) and FAM 9 (20%RAP+PG58) 123
4.6.13. FAM 8 (40%RAP+PG64) and FAM 10 (40%RAP+PG58) 124
4.6.14. FAM 11 (20%RAP + 50/50 – PG64/rejuvenator) and FAM 12 (20%RAP + 0/100 – PG64/rejuvenator) 126
4.6.15. FAM 13 (40%RAP + 50/50 – PG64/rejuvenator) and FAM 14 (40%RAP + 0/100 – PG64/rejuvenator) 127
4.6.16. FAM 7 (20%RAP + 100/0 – PG64/rejuvenator), FAM 9 (20%RAP + 100/0 – PG58/rejuvenator), FAM 11 (20%RAP + 50/50 – PG64/rejuvenator) and FAM 12 (20%RAP + 0/100 – PG64/rejuvenator) 129
4.6.17. FAM 8 (40%RAP + 100/0 – PG64/rejuvenator), FAM 10 (40%RAP + 100/0 – PG58/rejuvenator), FAM 13 (40%RAP + 50/50 – PG64/rejuvenator) and FAM 14 (40%RAP + 0/100 – PG64/rejuvenator) 131
4.6.18. Final rank order 132
5. CONCLUSIONS 139
5.1. Major findings 139
5.2. Final remarks 145
5.3. Suggestions for future studies 146
6. REFERENCES 149

1. INTRODUCTION

1.1. Reclaimed asphalt pavements (RAP)

The use of reclaimed asphalt pavements (RAP) in the construction of new asphalt layers has been a current practice in several countries, including Brazil, where this technique has been used for decades, but at a very limited rate as compared to the amount of RAP used in the construction of new pavements in other countries. The rationale behind this technique is the reuse of deteriorated asphalt layer materials aiming at minimizing the environmental effect caused by the extraction of new materials, especially mineral aggregates, and also reducing the construction costs as compared to those related to the construction of an asphalt layer with new mineral aggregates and virgin asphalt binder (Li, Williams, & Clyne, 2008; Copeland, 2011). For example, an asphalt mixture containing 50% of RAP could reduce its overall asphalt binder content requirement by 2–3 % (Lavin, 2003). Recycling does not only save money and resources, but also eliminates a waste product that otherwise would require proper disposal. The use of RAP turns the construction of pavements into a sustainable activity over time because of the reduced consumption of both energy and natural resources (Maupin Jr., Diefenderfer, & Gillespie, 2009) and represents an important strategy to ensure economic competitiveness of flexible pavement construction (Al-Qadi, Elseifi, & Carpenter, 2007). If properly designed, it is expected that the asphalt mixtures produced with RAP present a similar service life compared to those produced with new materials (Aurangzeb & Al-Qadi, 2014; Poulikakos et al., 2014; Mogawer et al, 2015).

According to Asphalt Institute (2010), RAP has been used extensively in new HMA pavements for several decades and has consistently exhibited equal performance to mixtures made with only new material. The first register of the employment of RAP dates back to 1915 (Kandhal, 1997; Salman et al., 2017). There are historical registers of RAP use also in 1923, in Singapure, and in 1948, in Bombay, India (Taylor, 1978). Nevertheless, the technique gained popularity in the 1970s when the cost of asphalt binder increased expressively due to the petroleum crisis that forced the generalized use of recycling techniques as a way to reduce the costs related to new asphalt binders (Kandhal, 1997; McDaniel & Anderson, 2001). At that time, non-proprietary methods were developed allowing the use of RAP in HMA applications (Salman et al., 2017). Prior to that time (Newcomb et al., 2007), very little asphalt mixture

was reutilized since there was very little incentive to recycle. As also discussed by Newcomb et al. (2007), before the oil embargo, the price of asphalt cement was so low that the cost of removing, stockpiling, and recycling old asphalt pavements was higher than that for purchasing, mixing, and placing new materials.

The popularization of the milling machines in the 1980s turned the removal of the asphalt layers into an easier task, boosting the popularization of the recycling techniques – according to Terrel et al. (1997), the first milling machines were developed by a contractor in the State of Utah, in the United States. In Brazil, Balbo (2007) reported that the milling process of deteriorated asphalt layers got popular by the end of the 1980's due to the convenience of the method, once that it avoids the alteration of the thickness of the layer in relation to the sidewalk and the consequent problems with the drainage equipment, bridge clearance, at-grade intersections and so forth. Milling machines are convenient because they are able to remove any amount of material and produce any desired grade and it does not produce so much pollution since heat is not required. Another advantage of the milling process, as discussed by Newcomb et al. (2007) is the fact that the material removed by the milling machine does not have to be crushed after removal, since it is fine enough to be used right afterwards, and also that the milled surface can be opened to traffic temporarily until the overlay is finished.

Another fact that propelled the recycling of asphalt layers was the introduction of drum-mix plants in the late 1970's. Before the advent of drum-mix facility, engineers did not know how to recycle in a batch facility, once that the materials could not be fed through the dryer since this would overheat the asphalt and cause a major pollution issue. In one of the drum mix processes, RAP is added about halfway down the drum where it is mixed with the new aggregate and new asphalt binder. After the development of the drum-mix facility, the Minnesota process was developed for the batch facility, which encompasses superheating of the new aggregate in the dryer, in such a way that the superheated aggregates retransmit heat to the RAP (Newcomb et al., 2007).

Newcomb et al. (2007) also discussed on the scenarios for possible employment of recycling. As they mentioned, any project that requires an overlay or major reconstruction is a candidate for recycling, but, on the other hand, some pavements may be repaired more economically only with an overlay. It is the case of thin asphalt layers, in that the milling machine may break the old layer into chunks, which will likely require additional crushing for use in a recycled mixture. Also because of the removal of chunks, it is difficult to

maintain the grade and major rework of the base course may be needed. For such a case, it would be simpler and cheaper to apply an overlay. In other words, the overall condition of the existing pavement is the major issue that must be addressed prior to repair. Also according to Newcomb et al. (2007), a pavement showing alligator cracks has a structural problem and, for such case, a reinforcement is needed. When only one layer is considered enough to provide sufficient reinforcement to the existing pavement, the underlying material may need to be removed for best performance, mainly because cracks are likely to reflect through the overlay if the existing mixture is not removed.

Recycling may not be indicated if the mineral aggregate in the old asphalt mixture does not meet specifications. It is the case of uncrushed aggregates in the old asphalt mixture, once that the recycling is going to produce a new mixture with a significant amount of uncrushed aggregates, and also the case of the existence of a high percentage of filler in the old asphalt mixture, once that the milling operation is going to create additional filler – in this case, it is going to be harder to meet the requirements for fine materials in the mixture. It is also the case of materials with tendency to suffer polishment, once that they may create problems if the mixture is designed for the surface course. According to most of these problems can be overcome if low RAP contents are used (Newcomb et al., 2007).

The techniques employed to recycle old asphalt layers have been developed over time, either in terms of the machines or the methods of incorporating RAP into new asphalt layers. The results of this progress are seen in terms of the use of rejuvenators, stabilizers, warm-mix agents, and higher RAP proportions. Test procedures to characterize the HMA mixture prepared with RAP and control parameters had been gradually introduced, in parallel with the assessment of the performance of the asphalt layers constructed with RAP. After overcoming the initial challenges of the implementation of the technique, engineers are moving, nowadays, towards the development of tools that allow them to evaluate the mechanical behavior of the HMA mixture compounded with RAP regarding the traditional pavement failure mechanisms.

1.2. Use of rejuvenating agents and soft asphalt binders

It is widely known that the aged binder of the old asphalt mixture causes an increase in the mixture stiffness and, consequently, an increase in the rutting resistance of the mixtures containing RAP (McDaniel e Anderson, 2001; West et al., 2009; Ali et al., 2016).

On the other hand, the stiffening process that occurs after the addition of a proportion of RAP can compromise the fatigue performance of the mixture (Zhang et al., 2015; Ghabchi et al. 2016). In order to overcome such issue and to spread the use of larger proportions of RAP, soft binders and rejuvenating agents have been employed to produce new HMA mixtures.

The addition of a soft binder has been used to compensate for the high stiffness of the RAP binder, and because of that the new binder has to be selected based on the stiffness level of the aged binder (Tavakol et al., 2017). In turn, rejuvenating agents act in order to restore the physical and chemical properties of the RAP binder (Newcomb, et al. 2007) by means of a diffusion process (Carpenter & Wolosick, 1980), leading to a binder with reduced viscosity and stiffness and increased ductility (Terrel & Epps, 1989; Shen et al., 2005; Brownidge, 2010; Ali et al., 2016). Studies concerning the use of softening and rejuvenating agents indicate that the fatigue cracking resistance of HMA mixtures containing RAP may be improved, when the aged binder is correctly rejuvenated (Ali et al., 2016) or the rejuvenator is adequately selected (Little et al., 1981; Mohammadafzali et al., 2015).

1.3. Tools to evaluate the incorporation of RAP into new HMA mixtures

One approach to evaluate the properties of HMA containing RAP is the employment of rheological tests performed on the extracted and recovered aged binder (Peterson et al., 2000; Ma et al., 2011). However, the solvents utilized during the extraction process can lead to an alteration on the binder properties (Ma et al., 2011), i. e., an increase of binder stiffness (Burr et al. 1991). An alternative approach to characterize the RAP mixtures is to analyze its mechanical properties by performing rheological tests on samples composed of fine aggregate matrix (FAM) (Nabizadeh, 2015; He et al., 2016; Zhu et al., 2017).

The damage process on the asphalt mixtures initiates on the material discontinuities, like air voids, micro cracks between binder-aggregate interface (adhesive micro cracks) or micro cracking of the binder (cohesive micro cracks). Based on this knowledge, researchers started to utilize the FAM scale to estimate the mechanical behavior of HMA mixtures (Kim et al., 2003a,b). A protocol to evaluate the FAM properties was developed by Kim and Little (2005), which consists of performing oscillatory tests on cylindrical samples, by following two steps: (i) low strain tests, in order to identify the

viscoelastic properties of the material; ii) high strain tests, to evaluate the damage evolution process on the material. The findings of studies that correlate the results of tests performed on FAM samples with the ones of tests performed on full mixture samples indicate that the FAM scale can provide reasonable information to predict the full mixture behavior (Nabizedeh, 2015; Freire et al., 2017).

1.4. The viscoelastic continuum damage theory

In order to evaluate the resulting data of FAM tests and to characterize the damage behavior of asphalt concrete mixtures, the viscoelastic continuum damage theory (VECD) has been widely used (Lee, 1996; Park et al., 1996; Lee & Kim, 1998a; Lee et al., 2000; Daniel & Kim, 2002; Palvadi, 2011; Palvadi et al., 2012; Karki et al., 2014; Karki et al., 2016; Freire et al., 2017). According to the continuum mechanics theory, a body with internal discontinuities and a given stiffness may be represented by a body without discontinuities with a reduced stiffness. Furthermore, the microstructural changes that occur during a damage process are uniformly distributed within the body and are quantified by internal state variables (Schapery, 1984, 1990).

The theory was extended by Schapery (1990) to evaluate the viscoelastic behavior by means of the application of correspondence principles, in order to eliminate the time dependency, typical of viscoelastic materials. The artifice utilized was to transform the stress-strain relationships of a viscoelastic dominium in a pseudo dominium that corresponds to a hypothetical elastic material, by considering that the constitutive equation for viscoelastic materials ($\sigma=E_R\varepsilon^R$) is identical to the one for elastic materials (Hooke's Law), but the variables are pseudo variables: pseudo stress (σ^R) or pseudo strain (ε^R) (Schapery, 1990). The damage evolution of a viscoelastic material can be described as a function $C(S)$, in which a reduction on the material pseudo stiffness (C) is associated to an internal state of the material (S) (Lee & Kim, 1998a; Lee et al., 2000; Kim & Little, 2005).

1.5. Objectives of this research

The main objective of this research is to investigate the effects of the following variables on the fatigue performance of specimens of fine aggregate matrix (FAM):

(i) different proportions of RAP;

(ii) two binders of different performance grade;

(ii) the addition of new binder or rejuvenating agent or a mixture of both.

This research was designed to improve the existing knowledge on the fatigue behavior of asphalt mixtures prepared with RAP regarding the effects of two common variables: the impact of higher proportions of RAP and the use of a soft virgin binder versus the use of a rejuvenating agent or a combination of both.

1.6. Experimental plan and method of analysis

Fine aggregate matrices were produced utilizing the particles lower than 2.00 mm of a basalt rock and a source of RAP of unidentified origin, two asphalt binders (PG 58 and PG 64) and one rejuvenating agent (shale oil residue). The mixtures were produced with RAP contents of 0, 20, 40, and 100 percent, and binder/rejuvenating ratios of 100/0, 50/50 and 0/100. Ten FAM mixtures were produced with the combinations of the materials. The loose mixtures were compacted in the Superpave gyratory compactor, and the compacted samples had their end cut in order to have a more homogeneous air-voids distribution. Cylindrical FAM samples of 40 mm in height and 12.5 mm in diameter were extracted from the compacted specimens, by means of a diamond drill.

Frequency sweep tests, in controlled stress mode of loading (15 kPa), at 25°C, were performed in order to obtain the linear viscoelastic properties of the samples. The same samples were submitted to time sweep tests in stress control at 1 Hz and 25°C, with tension ranging from 50 to 350 kPa, in order to obtain the damage characteristics of the FAMs. The ten FAM were combined into nineteen groups, in order to compare the effect of the variables under study (RAP content, type of binder, and binder/rejuvenator ratio). The characteristic curves of the materials were built and a power-law model was adjusted to the data in order to obtain the coefficients of the mechanistic fatigue prediction model. Such model is based on the VECD theory, and was utilized to predict the fatigue lives of FAMs as a function of the applied strain.

1.7. Structure of this master's dissertation

This dissertation is divided into five chapters. Chapter 1 consists of the contextualization of the research and contains a brief description of: (i) the use of RAP on

the production of new asphalt mixtures; (ii) the use of rejuvenating agents and soft asphalt binders; (iii) tools to evaluate the incorporation of RAP into new HMA mixtures; (iv) the viscoelastic continuum damage theory; (v) the objectives of the research; (vi) the experimental plan and the method of analysis; and (vii) the structure of the dissertation.

Chapter 2 consists of a literature review, which presents the relevant studies covering the following topics: (i) the use of reclaimed asphalt pavements (RAP) in the design and construction of recycled asphalt mixtures; (ii) the fine aggregate matrix (FAM) of asphalt mixtures and its rheological characterization; and (iii) the development of the theory of viscoelastic continuum damage (VECD) and its application to the characterization of the fatigue behavior of asphalt mixtures.

Chapter 3 contains the materials and method utilized to predict the fatigue behavior of the FAMs mixtures. First, a detailed description of the materials and procedures utilized to fabricate the FAM samples is presented. Then, the test procedure for determining the linear viscoelastic characteristics and the damage properties of the FAM mixtures are described. Finally, the analysis method utilized to evaluate the data from the tests is presented.

Chapter 4 presents the results obtained from the experiments performed in this study. The viscoelastic characterization of the samples is presented, followed by the damage characteristics and the fatigue behavior of each FAM. Then, the comparisons among the FAMs are presented, in order to evaluate the effect of the variables of interest. Chapter 5 provides the conclusions of the research and the recommendations for future studies. At the end of the document, the references used along the document are presented. Detailed information of the tests is presented in Appendix A.

2. LITERATURE REVIEW

The literature review of this dissertation is divided in three parts. The first part provides an overview of the use of reclaimed asphalt pavements (RAP) in the design and construction of recycled asphalt mixtures. The second item is devoted to studies of the fine aggregate matrix (FAM) of asphalt mixtures and its rheological characterization. The third section of this chapter describes the development of the theory of viscoelastic continuum damage (VECD) and its application to the characterization of the fatigue behavior of asphalt mixtures.

2.1. Reclaimed asphalt pavements (RAP)

2.1.1. RAP applications around the world

The technical adequacy of RAP use is such that several countries reported the gradual increase of the RAP amount used in the construction of new asphalt layers. In 2008, a survey of the U.S. state DOTs (Copeland, 2008) showed that the average RAP content used in the construction of new asphalt layers ranged between 10 and 20%, with an average use of 12%. It was also reported that very often states did not allow RAP contents greater than 25% in the surface layer (Salman et al., 2017). The main reason for such limited percentage was the uncertainty regarding the long-term performance of asphalt layers constructed with RAP (Copeland, 2008). Three years later, a new survey of the U.S. state DOTs (Hansen & Newcomb, 2011) showed that not only the total amount of RAP used in new asphalt layers increased but also the average proportions of RAP added to new asphalt layers increased to approximately 17%.

Recent data of RAP production in Europe (Olard & Pouget, 2014) show that the total production of RAP in 2014 was 276,4 million tons against 49,6 million ton in 2012, indicating that the incorporation of an average proportion of 18% of RAP is enough to employ 100% of the available RAP. Also according to Olard and Pouget (2014), a similar scenario is seen in France: 6,5 million ton are available annually and the annual production of new asphalt mixtures reaches 35,3 million ton, what is equivalent to 18,4%. Differently from many countries, in France about 40% of the available RAP are employed in the construction of granular layers and in cold recycling using emulsions, foam asphalt or Portland cement (Olard & Pouget, 2014).

According to the European Asphalt Pavement Association (EAPA, 2015), Europe employs 82,8% of the annual amount of RAP available (47.3 million tons in 2015), while in the United States this percentage of reuse reaches 91% (with an annual production of about 69,7 million tons). In France, the percentage of reuse reaches 68%, in Germany, Finland, Great Britain, Hungary, Iceland, Luxemburg, Slovakia, Slovenia, Spain, Sweden and Turkey it is 100%, in The Netherlands it is 80%, and in Italy it is about 70% (EAPA, 2015). In China (Xu et al., 2014), the paved road systems are comprised by 4,420,000 km and the estimated amount of RAP available is of the order of 160 million ton, which led the Transportation Ministry to approve a plan with the objective of employing 95% of the total amount of RAP available in proportions up to 50% in the next five years.

In Japan, 100% of the available RAP is used in the construction of new HMA layers, not only because economic and environmental reasons, but also because of lack of space for disposal of the discarded materials (Kubo, 2014). In New Zeland, the allowed proportion of RAP to be used in the construction of new asphalt layers ranges from 15 to 30%, with the proportion of 15% as the most usual, and there is the need of a governmental approval to use higher RAP proportions by means of studies showing the adequate performance in experimental tracks (Lo Presti et al., 2012; Kodippily et al., 2015). In Brazil, apparently, there are not statistics regarding of the amount of RAP obtained from roads, what makes it difficult to estimate the amount of RAP available to construct new asphalt layers.

2.1.2. Environmental and economic perspectives

The use of RAP in the construction of new asphalt layers is also an object of economic and environmental analyses that demonstrate its technical viability. Kandhal and Mallick (1997) estimated that the use of a RAP content between 20 and 50% can provide a saving from 14 to 34%, considering only material and construction costs. Aurangzeb and Al-Qadi (2014) used life-cycle cost analysis (LCCA) and life-cycle assessment (LCA) in order to evaluate the economic and environmental impacts of using high RAP contents in the construction new asphalt layers. The analyses compared the life-cycle cost and the life-cycle environmental impact of four pavement sections comprised of virgin and recycled asphalt mixtures at the RAP contents of 30, 40, and 50%. The authors observed cost reduction, energy savings and reduction of gases that contribute to the greenhouse effect with the use of high RAP contents. The LCA analysis conducted by Aurangzeb and Al-Qadi

(2014) showed a reduction of up to 28% in the environmental impact caused by the construction of the asphalt layer when RAP is used to substitute part of the virgin materials.

Visintine (2011) compared HMA mixtures compounded with 30 and 40% of RAP and showed savings at the network level of about 19% when 30% of RAP is used and saving ranging from 30 to 36% when 40% of RAP is used in the production of new asphalt layers. In a study conducted by the Federal Highway Administration (FHWA) using the life-cycle cost analysis, Moya et al. (2011) compared the performance of trial sections constructed with and without RAP and concluded that the long-term costs of using RAP in thicker reinforcements would be equivalent to the costs of constructing HMA mixtures with new materials. Ventura et al. (2008) evaluated the use of increasing contents of RAP (0, 10, 20, and 30%) in hot-mix recycling to construct binder layers and showed that, except for the toxicity and ecotoxicity indicators, the whole set of indicators evaluated in their study showed the tendency of reduction of potential environmental effects with the increase of the RAP content used.

The Green Group of the National Center of Asphalt Technology (NCAT) used the life-cycled assessment method considering the material consumption and the construction activities related to the construction of four new trial sections using RAP and comparing such scenarios to the production of new HMA mixtures with virgin materials (Willis, 2015). The study pointed out that the use of recycled materials to replace new materials (mineral aggregates and asphalt binder) reduces both the energy consumption (savings between 9 and 26%) and the CO_2 emissions (reduction between 5 and 29%) produced during extraction and processing of raw material. The study also showed that the combined use of recycled materials and local materials reduces the energy required to haul the raw materials and the asphalt mixture (savings between 19 and 42%) and the CO_2 emissions are reduced in 6 to 39%. Willis (2015) also concluded that using lower temperatures due to the incorporation of WMA technologies will reduce the energy consumption in 12 to 17% and the CO_2 emissions in 6 to 9%.

2.1.3. Technics used to incorporate RAP in asphalt mixtures

The recycled HMA mixtures are used in a variety of applications in several engineering solutions for paving (Silva, 2011): HMA mixes, cold-mix asphalts, warm-mix asphalts and granular material for bases, subbases and subgrade reinforcement. The technics employed to recycle RAP are generally divided in two categories (Costa & Pinto,

2011): hot-mix recycling and cold-mix recycling, which in turn can be processed in situ or in a central plant. For plant hot-mix recycling, two types of plants are used: drum-mixer plants and batch plants. For plant cold-mix recycling, plants like those to produce soil mixtures are used. Cold in-place recycling is an environmentally friendly activity and it advantages include significant remedial corrections of most pavement distresses and complete reuse of the existing pavement (Lavin, 2003).

Asphalt Institute (1986) defines hot-mix recycling as the process of combining RAP with aggregates and new asphalt binder and/or a recycling agent in a central plant in order to produce a new HMA mixture. The production of asphalt mixtures containing RAP is similar to the production of asphalt mixtures using only new materials, where the RAP is treated as an aggregate and some slight modifications must be done to the way it is fed through the HMA facility (Newcomb et al., 2007). The amount of RAP used in an HMA mix is related to the plant type being used, the gradation of the RAP aggregates, and the properties of the RAP binder. The ratio of RAP to virgin aggregates is typically 15 to 25% for batch plants and up to 30 to 50% for drum-mixer plants. In turn, the in situ hot-mix recycling is a process of correction of superficial distresses, generally by means of milling the old asphalt mixture, mixing with rejuvenating agent, virgin mineral aggregate, and virgin asphalt, and subsequent distribution of the recycled mixture over the pavement, without removal of the RAP from the place and hauling to a central plan (Costa & Pinto, 2011).

When the recycling process occurs with no use of energy to heat the materials, it is designated as cold-mix recycling (Momm & Domingues, 1995) and materials as asphalt emulsions, mineral aggregates, rejuvenating agents or chemical stabilizers can be mixed at room temperature of about 25°C. The final product is generally used to build base courses that must be covered with a superficial treatment or an asphalt concrete before the traffic is opened. According to Costa and Pinto (2011), the cold-mix recycling can be used either to build a base course stabilized with asphalt, if the base and the wearing courses are milled and mixed together with the employment of asphalt binder as a binder agent, or to build a base course stabilized with hydraulic agent (or chemically stabilized), if the base and the wearing courses (or even the subbase) are milled and mixed together with the employment of hydraulic stabilizers as lime, Portland cement or fly ashes. Similarly to the hot-mix recycling, the cold-mix recycling can be carried out in situ or in a central plant (Costa & Pinto, 2011) and, for the latter case, plants like those used to prepare soil mixtures can be used. In situ cold-mix recycling is often performed using a

recycling train, for large or long roadway projects, and consists of pulverizing, screening, crushing and mixing units (Lavin, 2003). The in situ cold-mix recycling used first the milling-recycling machines Caterpillar and Wirtgen – the machines were able to mill the wearing course, add the asphalt emulsion, homogenize the material and lay it down. Such a technique (Costa & Pinto, 2011) is widely used in Europe and the percentage of RAP incorporated into the new mixtures reach about 90%. In Brazil, according to Pinto et al. (1994), the first road segment using the in situ cold-mix recycling was constructed in 1993 on BR-393 Highway, between Além Paraíba City and Sapucaia City, in the Rio de Janeiro State, in a construction work conducted by the National Transportation Department – DNIT.

According to Lavin (2003), in batch mixing plants, the heat transfer is carried out by conduction, which consists of using heat from the new mineral aggregate to increase the temperature of the RAP. The temperature of the new mineral aggregate must be increased to account for heat transfer to the RAP. As the RAP is not preheated in the process, higher percentage of RAP will require a higher temperature for the new aggregate at the time of mixing (Newcomb et al., 2007) and this can be a factor limiting the amount of RAP used to produce the new HMA mixture. With a drum-mixer plant (Asphalt Institute, 1986), the RAP is introduced directly into the drum-mixer dryer after the virgin aggregates are introduced, what means that RAP is being introduced into the drum similarly to the virgin aggregates. Inside the drum-mixer, the virgin aggregates are heated and such heated aggregates are then used to dry and heat the RAP, in order to produce the new recycled hot mix at the required final temperature. According to Newcomb et al. (2007), the RAP is fed into the outer drum away from the flame, in order to prevent the generation of smoke and emission problems. In a parallel flow drum facility, the RAP is added about half way down the drum, and the aggregate protects the RAP from the direct contact with the flame.

In a drum-mixer plant (Asphalt Institute, 1986), one or more cold-feed bins are dedicated for RAP and a separate belt scale is used to measure the quantity of RAP introduced into the system. The control system uses this scale to control the ratio of RAP to virgin aggregates, along with the quantity of new binder based on the quantity of usable binder in the RAP. According to Newcomb et al. (2007), higher RAP contents are difficult to deal with in such type of facility, once that there will not be enough aggregate to shield the RAP from the flame and, in this case, excessive pollution occurs and the RAP binder is subjected to damage. Because of that, the amount of RAP that is commonly recycled in a

drum-mixer facility is typically no more than approximately 30%, although theoretically these facilities are able to deal with higher RAP amounts.

According to Lavin (2003), the RAP gradation and the heat transfer ability of the mixing plant limit the amount of RAP that can be used in an asphalt mixture. During the milling or crushing process, agglomerates of coarse aggregate particles and mastic are formed, and a significant amount of fine material can be generated, and these materials must be accounted for in the final gradation of the asphalt mixture. The ability of the mixing plant in transferring enough heat to dry the RAP should also be taken into account, once that the heating of the RAP in the mixing plant extracts most of the asphalt binder from it and allows it to be blended throughout the new asphalt mixture. Some modern drum mixing plants, such as double drum plants, have been designed to incorporate up to 70% RAP or more. Usually, batch mixing plants can only incorporate up to 30% RAP in the new HMA mixture.

2.1.4. Long-term performance of asphalt mixtures containing RAP

RAP is almost exclusively used for dense graded mixtures, once that the RAP gradation typically prevents its use in gap-graded mixtures (Lavin, 2003). Providing that specific performance criteria are met, asphalt mixtures produced with RAP can be used both at intermediate layer and wearing courses. Theoretically, a recycled asphalt mixture should be designed to produce a new asphalt mixture having the same properties as that in a mixture produced with new materials and also should present a service life similar to those produced with new materials (Lavin, 2003; Newcomb et al., 2007; Mogawer et al, 2015; Aurangzeb & Al-Qadi, 2014; Poulikakos et al., 2014). The equivalence in performance between an asphalt mixture prepared with RAP and an asphalt mixture prepared with only new materials is a requirement of most state DOTs (Newcomb et al., 2007). Asphalt layers incorporating small amounts of RAP (less than 20%) have performed similarly to those produced with only virgin materials (Mogawer et al., 2011). But, in practice, one of the biggest challenges to the use of increasing amounts of RAP in the construction of new asphalt mixtures was, or still is, the belief that the performance of the asphalt layer compounded with RAP is worse than the performance of the asphalt mixture compounded with virgin materials.

Some of the challenges that initially delayed the application of higher RAP proportions in the construction of new asphalt layers (Willis and West, 2014) were the

lack of recommendations regarding of the design of the asphalt mixture and its preparation process, as well as the lack of availability of performance data to show how this type of asphalt mixture responds in the field (Salman et al., 2017). Although such hurdles had been realistic some years ago (Willis and West, 2014), more recent detailed evaluations showed that asphalt mixtures compounded with RAP, when adequately designed and produced, can perform similarly to asphalt layers produced with virgin materials, if the RAP proportions ranges from 10 to 30% (Kandhal et al., 1995; Sullivan, 1996; McDaniel et al., 2000; Shah et al., 2007; Li et al., 2008; Mogawer et al., 2011; Shen et al., 2007a). The NCHRP 9-46 project completed in 2013 (West et al., 2013) has investigated the best practices related to RAP management in field production and construction and provided guidance for adoption of higher RAP contents in HMA mixtures, including the development of a mix design and evaluation procedure that provides satisfactory long-term performance for HMA mixtures prepared with high RAP content (between 25 and 50% or more) and the proposal of changes to the current AASHTO standards in order to accommodate higher RAP contents.

Besides the technical and economic advantages associated to the recycling of old asphalt mixtures, environmental laws in several countries have been promoting the use of higher RAP proportions (above 50% of the total mass), based on results from studies carried out in the laboratory and in the field with asphalt mixtures produced with high RAP proportions that show the viability of the technique (Kim et al., 2009a,b; West et al. 2009; West et al., 2013; Willis e West, 2014; Mogawer et al., 2015). Other investigations showed the technical viability of employing 100% RAP (Silva et al., 2012; Zaumanis et al., 2014b) with the asphalt mixtures performing similarly to asphalt mixtures compounded with virgin materials, particularly after the addition of rejuvenators.

In the United States, nowadays, the proportion of RAP allowed to be used in the production of asphalt mixtures by the State DOTs is generally limited to 25% (Boriack et al., 2014). Most of the State DOTs specify that 15% of RAP, or less, in mass, can be added, assuming that such amounts will not change the performance grade of the asphalt binder (McDaniel and Anderson, 2001; Newcomb et al., 2007; Willis e West, 2014). For RAP proportions between 15 and 25% in mass, the grade of the virgin asphalt binder needs to be adjusted in order to account for the stiffened, aged binder present in the aged asphalt mixture. In such case, it is recommended to reduce the performance grade of the asphalt binder in one degree (Boriack et al., 2014; Newcomb et al., 2007). An analysis of the

combined asphalt (aged and virgin ones) is done when the amount of RAP exceeds about 25% (Newcomb et al., 2007).

When the RAP proportion is superior to 25%, such mixtures are considered mixtures with high RAP proportions and a detailed project is needed in order to select an asphalt binder with adequate properties and for that blending charts are used (Copeland, 2011; McDaniel & Anderson, 2001; Boriack et al., 2014). In parallel to the recommendations concerning the aged asphalt binder (Willis & West, 2014), the NCHRP Project 09-46 (West et al., 2013) indicated that the volumetric parameters of the HMA mixtures are not enough to evaluate the performance and call everybody's attention to the need of evaluating the low-temperature properties, the rutting resistance, the fatigue resistance, the moisture damage, and the stiffness.

The state DOTs are generally reluctant in using high RAP proportions in the production of new asphalt mixtures because of the aged asphalt binder (Li et al., 2008; Al-Qadi et al., 2009; Mogawer et al., 2012; Mogawer et al., 2015). It is well established that the prediction of the performance of asphalt mixtures containing high RAP proportions is very tough, because of the complex interaction between the aged and the new asphalt binder in the new asphalt mixture (Daniel et al., 2010; Maupin Jr. et al., 2008). It is also well established that the aged binder in asphalt mixtures containing high RAP proportions increases the stiffness of the mixture and consequently the rutting resistance, but, on the other hand, such high stiffness can reduce the fatigue resistance of the mixtures (McDaniel et al., 2000; McDaniel and Anderson, 2001; Karlsson & Isacsson, 2006; West et al., 2009; Al-Qadi et al., 2012; Mogawer et al., 2012; Boriack et al., 2014, Ali et al., 2016), besides of the increased risk of moisture damage caused by the excessive stiffening of the HMA, while part of the binder is actually not contributing to viscoelastic properties, resulting in under-asphalted mixtures (Al-Qadi et al. 2007). The Kansas Department of Transportation (KDOT), for example, is currently allowing Superpave HMA mixtures with higher percentage of RAP materials, but recently premature cracking has become prevalent on HMA pavements constructed with high percentages of RAP (Sabahfar et al., 2016). On the other hand, other research works reported that RAP might provide stronger moisture resistance than the virgin HMA mixtures, once that the mineral aggregates are already naturally protected by the old binder (Karlsson and Isacsson, 2006).

The studies conducted by Sargious and Mushule (1991), Mohammad et al., (2003), Huang et al. (2004), Pereira et al. (2004), Mogawer et al. (2011), Silva et al. (2012), West

et al. (2013), Islam et al. (2014) and Li et al. (2014), and Zhang et al. (2016) pointed out the increase of the rutting resistance after the addition of RAP to the new asphalt mixtures. According to Mogawer et al. (2011), the incorporation of RAP in small quantities (about 5% to 10%) provides HMA mixtures with rutting performance similar to HMA mixtures prepared with virgin materials, but the improved rutting resistance becomes more noticeable when higher RAP proportions are used. Tam et al. (1992), McDaniel et al. (2000), Li et al. (2008), and Islam et al. (2014) observed reduction of the resistance to thermal cracking after the addition of RAP to the new asphalt mixtures. Conversely, Li et al. (2014) and Sabahfar et al. (2016) observed the increase of such resistance. Ghabchi et al. (2016) observed that the low-temperature cracking potential increased for mixtures produced with RAP and a blend of RAP and recycled asphalt shingles (RAS). Tam et al. (1992), McDaniel et al. (2000), Mohammad et al., (2003), Mannan et al. (2015), and Zhang et al. (2016) pointed out reduction in the fatigue resistance and the opposite was pointed out by Huang et al. (2004), Pereira et al. (2004) and Silva et al. (2012). Ghabchi et al. (2016) observed that the fatigue life can increase or decrease with the addition of RAP or a blend of RAS and RAP, depending on the binder grade used (increased with the PG 64-22 and decreased with the PG 70-28). The following research studies indicated increase of the resistance to moisture-induced damage: David (2006), Al-Qadi et al. (2012), Aurangzeb et al. (2012), Silva et al. (2012), and Li et al. (2014). Nonetheless, the research works by Hu et al. (2012), West et al. (2013), and Sabahfar et al. (2016) showed reduction of such resistance. A null effect on the resistance to moisture-induced damage was mentioned by Amirkhanian and Williams (1993), Sondag et al. (2002), Aurangzeb et al. (2012), Islam et al. (2014) and Poulikakos et al. (2014). As can be seen, results are widely mixed and no clear conclusion can be draw from such high number of studies.

A study published by Islam et al. (2014) also reported that the addition of RAP increases the dynamic modulus of the HMA mixtures and their tensile strength. Increase in tensile strength was also reported by Huang et al. (2004) while testing the effect of increasing amount of RAP in asphalt mixtures, and by Ghabchi et al. (2016) while testing the effect of RAP and a blend of RAP and RAS – for the latter case, the use of 6% RAS resulted in the maximum increase in ITS values. Conversely, Kandhal et al. (1995) reported decrease of the tensile strength of recycled mixtures as compared to the reference one. Increases in dynamic modulus with increasing RAP contents were also reported by Pereira et al. (2004), Silva et al. (2012) and Tavakol et al. (2017), as compared

to HMA mixtures produced with virgin materials. Increase in dynamic modulus and flexural stiffness was also observed by Ghabchi et al. (2016) with mixtures produced with RAP or a blend of RAP and RAS. Regarding fatigue and low-temperature cracking potential, West et al. (2013) reported that high RAP contents resulted in lower fracture energies at test temperatures used to evaluate such susceptibility and pointed out that careful attention should be given to the selection of the grade of the virgin binder, in order to minimize the risk of occurrence of cracking at long term.

Boriack et al. (2014) carried out a study aiming at evaluating the optimum binder content as a function of the RAP content in the HMA mixture. Mixtures with 0, 20 and 40% RAP and three percentages of added binder (design asphalt binder, design + 0.5%, and design + 1.0%) were used. Additionally, a mixture containing 100% RAP with four additional asphalt binder contents (0.0, 0.5, 1.0 and 1.5%) was evaluated in order to determine the binder content that optimizes the mixture performance. The mixtures prepared with 0 and 20% RAP had their fatigue and rutting resistances improved with an increase of 0.5% in binder content, with a slight decreases of dynamic modulus. The mixtures prepared with 40% RAP and various quantities of binder suffered a decrease in both rutting and fatigue resistances, indicating that the original amount of binder was sufficient. The mixtures prepared with 100% RAP showed very high dynamic modulus and rutting resistance at all binder quantities, but the fatigue resistance resulted comparable to the 20% RAP mixture when 1,5% binder was added to the 100% RAP mixture.

Winkle et al. (2016) reported an experience of construction of trial sections using high RAP proportions (30, 35 and 40%) in which the RAP was fractionated in such a way that the fine materials (passing sieve #8 mm) were eliminated. A field surveying carried out eight months after construction showed that the section with 40% RAP presented the best performance, followed by the section with 35% RAP and the one with 30% RAP. The authors also reported reduction of approximately 34% in the quantity of transversal cracking in those sections when the RAP content increased from 30 to 40%. Mannan et al. (2015) also studied HMA mixtures prepared with a RAP content similar to those used by Winkle et al. (2016) and observed that the addition of 35% RAP resulted in a reduction of the fatigue life of the HMA mixture in comparison with an HMA mixture prepared with virgin materials. On the other hand, the study of the recovered aged binder by Mannan et al. (2015) showed that the presence of RAP binder increased the fatigue life of the asphalt binder. Mannan et al. (2015) attributed such discrepancies to the week interaction

between the RAP aggregate and the virgin binder, once that, according to those authors, the fatigue cracking occurs mostly at the binder-aggregate interface.

Ghabchi et al. (2016) carried out a research on the use of RAP and RAS and concluded that: (i) the fatigue life of asphalt mixes with a PG 64-22 binder increased with use of RAP or a blend of RAS and RAP, the maximum increase in fatigue life was obtained with a blend of 5% RAS and 5% RAP, and the fatigue life decreased when 6% RAS was used compared to that of virgin mix with the same asphalt binder; (ii) the use of RAP and/or RAS resulted in a decrease in fatigue life when a PG 70-28 asphalt binder was used, and the maximum decrease in fatigue life, compared to that of virgin mix with the same type of asphalt binder (PG 70-28), was obtained with 6% RAS; (iii) the use of a polymer-modified asphalt binder (PG 70-28) was found to be an effective way to increase the fatigue life of the mix, specifically when RAS and/or RAP were used; (iv) the flexural stiffness of the asphalt mixes increased using RAS and RAP and the RAS content was found to have a greater contribution to increasing the flexural stiffness; (v) the addition of RAS and/or RAP increased the dynamic modulus for both asphalts (PG 64-22 and PG 70-28), what may result in a better rutting performance; (vi) the low-temperature cracking potential increased; (vii) the indirect tensile strength of the asphalt mixes increased and the use of 6% RAS resulted in the maximum increase in ITS values.

Zhang et al. (2016) evaluated ten mixes with different percentages of RAP and concluded that (i) the addition of RAP significantly affected the volumetric of the asphalt mixtures and increased the rutting resistance; and (ii) the fatigue cracking resistance of mixes with a low percentage of RAP was comparable to that of the control mix without RAP, and the effects of a high percentage of RAP (more than 17%) on fatigue cracking depended on the target PG of binder – when the target virgin binder PG was relatively low, e.g. PG 58-28, bumping down the grade of the virgin binder did not affect the fatigue resistance of the high RAP mixes, but when the target virgin binder PG was relatively high, e.g., PG 70-28, the high RAP percentage decreased the fatigue resistance of the asphalt mixes. These authors hypothesized that bumping down the grade of the virgin binder may have led to the elimination or reduction of the degree of polymer modification, which could have compromised the fatigue resistance of the high RAP mixes. They recommended to keep the high temperature grade of the target PG for the virgin binder without grade bumping to achieve good fatigue resistance of RAP mixes.

2.1.5. RAP asphalt binder

Binder aging occurs during the construction of asphalt layers and develops along pavement lifespan. During the aging process, malthenes oxidize and the ratio of malthenes to asphalthenes is reduced (Asphalt Institute, 2010). Some investigations showed that the level of aging depends on the level of damage of the recycled asphalt layer (Smiljanic et al., 1993) and also that HMA mixtures with high air void contents, as the case of porous HMA, presented greater stiffness than regular HMA (Kemp & Predoehl, 1981). Stockpiling is also another factor affecting the level of aging, as the material is more prone to exposition to air (McMillan & Palsat, 1985). The level of moisture damage on the old asphalt layer is also an issue of concern and, as a rule of the thumb, stripped HMA should not be recycled (Karlsson and Isacsson, 2006), due to the probability of reoccurrence of the phenomenon, although Amirkhanian and Williams (1993) had showed that the use of an anti-striping agent combined with a RAP content from 15 to 20% is able to yield HMA mixtures with strength and moisture resistance comparable to HMA mixtures totally produced with new materials.

The aged, hard binder of the RAP mixture is capable of increasing the viscosity of the resulting binder of the recycled mixture and such increase is more expressive as the amount of RAP used in the mixture increases. Such viscosity increase can create difficulties to the compaction of the asphalt layer. The Lousiana DOT, for example, after a study conducted in 1981 to evaluate the condition of four projects involving RAP implemented constraints on the allowable reclaim/virgin ratio and in the consistency of the virgin asphalt cement, in order to meet specification limits for the maximum allowable viscosity of plant produced mix. An AC-30 grade asphalt cement was required for mixtures utilizing up to 20% RAP and an AC-10 grade asphalt cement was required for reclaimed materials between 20 and 30% RAP (Carey & Paul, 1982; Paul, 1996). According to Paul (1996), a further restriction was later placed on wearing course mixes limiting the maximum allowable RAP proportion to 15%, and, subsequently, this amount was reduced to 10%. Supplemental specifications in 1987 eliminated the use of reclaimed material in wearing course mixes because it was reported that the viscosities of recovered asphalt cement from recycled mixes on a majority of projects were greater than the 12,000 poise limit. Since most projects during this period were of small tonnage, projects were being completed prior to central lab testing to determine the plant produced viscosity. After the fact tests indicated recovered viscosities between 12,000 and 20,000 poises.

According to Ali et al. (2016), more recently, most of the state DOTs in the United States allow the use of RAP in the preparation of HMA mixtures in proportions ranging from 15 to 45% and the reason for such low RAP proportions in use is basically the RAP aged binder. When high RAP contents are used, the RAP binder can reduce the mixture performance in terms of fatigue, low-temperature and reflective cracking, once that the aged binder is more brittle than a non-aged binder. In an attempt to mitigate the excessive hardening of the asphalt mixtures caused by the presence of the aged asphalt binder in the recycled asphalt mixtures, the state DOTs have been recommending the use of a softer asphalt binder when RAP contents ranging from 15 to 20% are used. In this case, the new binder must be selected based on the stiffness level of the aged binder and such determination is made using the so-called blending charts. In a study conducted by Tavakol et al. (2017), a total of nine mixtures with varying virgin binder contents and containing higher percentages of recycled materials (RAP and RAS) were developed using blending charts and assessed for fatigue cracking susceptibility using dynamic modulus and direct tension fatigue tests. Based on the results of this study, 65-85% was recommended as the acceptable range of virgin binder content for mixtures.

Although soft binders have been used to compensate for the stiffness imparted to the mixture due to the RAP binder, several studies have shown that asphalt rejuvenators can allow more recycled materials to be incorporated in asphalt mixtures than soft binders alone, without compromising the performance of the asphalt mixtures (Shen et al., 2005; Al-Qadi et al., 2007; Shen et al., 2007a;b; O'Sullivan, 2011; Ali et al., 2016; Mogawer et al., 2015). According to Im et al. (2014), rejuvenators may be a cost effective way to enhance the overall performance of the HMA mixtures containing recycled materials. The primary purpose of the rejuvenators is to restore the aged binder to requirements of binder specifications (Newcomb et al., 2007). In some state DOTs, soft asphalt binders have been used exclusively as recycling agents, but some state DOTs, mainly in the western U.S., permit the use of rejuvenators (Newcomb et al., 2007). Even with these benefits, some state agencies have limited the use of rejuvenators because of potential rutting-related concerns (Shen et al., 2007b).

According to Newcomb et al. (2007), there is a slight difference in the differentiation between rejuvenating agents and softening agents: the former attempt to restore the physical and chemical properties of the aged asphalt binder to that of a new asphalt binder, while the latter lower the viscosity of the aged asphalt binder. As also mentioned

by Ali et al. (2016), Shen et al. (2005), and Brownidge (2010), the rejuvenators act to restore the performance-related properties of the RAP asphalt binder by means of a diffusion process (Carpenter & Wolosick, 1980), restoring its colloidal structure and chemical components, which in turn leads to reduced viscosity and stiffness and increased ductility (Terrel & Epps, 1989; Shen et al., 2005; Brownidge, 2010; Ali et al., 2016).

The structural properties of HMA mixtures using RAP and rejuvenators are generally satisfactory when the rejuvenator is selected adequately (Little et al., 1981; Epps et al., 1980). According to Ali et al. (2016), if the RAP binder is rejuvenated, more percentages of RAP can be used to produce HMA mixtures without compromising their performance. In turn, Mohammadafzali et al. (2015) affirmed that, if correctly selected, the rejuvenator can extend the service life of an aged asphalt binder by up to 10 years. On the other hand, Mohammadafzali et al. (2015) warned that the recycled RAP binder, even when it meets the requirements of a performance-based specification, is less durable than the virgin one, once that the aging rate of recycled binders does not reduce after a 20-hour exposition in the PAV. Ongel and Hugener (2015) also observed that aging of rejuvenated binders is faster than the virgin ones.

The use of rejuvenators is not encouraged by some state DOTs because of the concern with rutting development (Shen et al., 2007b; Mogawer et al., 2015). One alternative is the use of modified asphalt binders instead of soft asphalt binders, aiming at alleviating the concerns regarding rutting (Mogawer et al., 2012; Mogawer et al., 2015). Research studies have illustrated that polymer modification is able to provide HMA mixtures produced with high RAP percentages with similar or better performance than the mixture prepared with virgin materials and that it is also able to provide mixture performance benefits including: increased strength at high temperatures, improved adhesion properties, and increased resistance to fatigue cracking, rutting, bleeding, and low temperature cracking (Mogawer et al., 2012). Mogawer et al. (2015) studied the effects of five rejuvenating agents on the performance of HMA mixtures prepared with 50% RAP and modified asphalt binders and concluded that modified binders were able to compensate for the loss of performance due to the use of rejuvenators. The recycled mixtures using rejuvenators showed a fatigue resistance greater than the control mixture (produced with virgin materials) and the 50% RAP mixture produced with a soft binder.

Mohammadafzali et al. (2015) studied the long-term aging of artificially aged binders rejuvenated with four recycling agents (water-based emulsion, heavy paraffinic

distilled solvent extract, petroleum natural distillate and oil base bio-rejuvenator) and observed that while some samples aged significantly slower than the original binder, other aged faster: the water-based emulsion and the heavy paraffinic distilled solvent extract reduced the aging rate, while the petroleum natural distillate and the oil base bio-rejuvenator increased it. Mohammadafzali et al. (2015) also called people's attention to the fact that the highest aging rates were observed for the binder rejuvenated with the bio-rejuvenator, which points out the importance of taking the effect of long-term aging into account when such sort of product is used as a rejuvenating agent.

Mogawer et al. (2013) reported that the rejuvenators were able to reduce the resulting binder stiffness and increase the resistance of the HMA to cracking formation. Im et al. (2014) studied the impact of several commercial rejuvenators on the performance of asphalt mixtures containing RAP and RAS and observed that the mixtures containing rejuvenators showed higher resistance to rutting, cracking, and moisture-induce damage. Other researchers also confirmed the efficiency of some rejuvenators: Asli et al. (2012), Silva et al. (2012), Hajj et al. (2013), Hill et al. (2013), Zaumanis et al. (2013), Yu et al. (2014), and Zaumanis et al. (2014b). Such studies present conflicting results about the effect of rejuvenators on the rutting resistance and are unanimous in reporting the positive effect of the rejuvenators on the fatigue and thermal-cracking resistances.

Some researchers had studied the effect of different rejuvenators in the light of performance-based specifications and developed blending charts based on the Superpave binder tests, using conventional and modified asphalt binders (Shen et al., 2007b; Zaumanis et al., 2014a). Shen et al. (2007b) worked with concentrations of rejuvenating agents varying from 0 to 14% and used the Superpave parameters as a tool to obtain the ideal concentration of rejuvenating agent aiming at achieving a certain binder performance grade. Shen et al. (2007b) concluded that the average content of rejuvenator, calculated with the individual contents obtained for each specification parameter, is appropriate as dosage parameter. Regarding the HMA mechanical properties, Shen et al. (2007b) reported that they resulted better or equivalent to the HMA mixtures prepared with virgin components. In general, Shen et al. (2007b) concluded that the rutting resistance parameters decreased with the increase of the proportion of the rejuvenating agent and the fracture properties were improved.

Zaumanis et al. (2014a) compared six rejuvenating agents (an aromatic extract and waste engine oil, both petroleum-based products, and four organic products, namely,

waste vegetable oil, organic oil, waste vegetable grease and distilled tail oil) and developed a dosage procedure aiming at achieving a certain binder PG. They pointed out that the organic oils required lower contents when compared to the petroleum-based materials to produce equivalent softening of the aged binders. They also claimed that the dosage of the rejuvenator can be optimized in order to yield performance grades and penetration values equivalent to the ones of the virgin binder – this would be advantageous for the initial selection of the rejuvenator content, before carrying out the performance tests. According to those authors, the rejuvenator content can be optimized by means of the proposed procedure, in order to guarantee conformity to the design PG for a variety of RAP binders – in the mixture design, such tool allows taking into account the inevitable variability of RAP obtained from different sources and/or pavements with distinct aging levels.

Dosage procedures based on empirical properties were also published in the literature (Silva et al., 2012; Zaumanis et al., 2013). Silva et al. (2012) determined the rejuvenator proportions with basis on the values of penetration, softening point and viscosity of the RAP binder mixed with three rejuvenator contents (3, 6 and 12%). Zaumanis et al. (2013) had claimed that the penetration index can be used as a simple and efficient measurement of the performance of the rejuvenators, once that the penetration index (PI) results varied significantly depending on the rejuvenator and supported the low-temperature mixture test results.

Mogawer et al. (2013) presented a procedure to determine the rejuvenator dosage, aiming at keeping the original PG of the RAP binder. Three locally used rejuvenators with different chemical composition were selected for the study (BituTech RAP, SonneWarmix RJT, SonneWarmix RJ). For this study, a rejuvenator content of 9% by weight of RAP was determined to be appropriate. The use of a softer binder (PG 58-28) in high RAP mixtures has proved to be inadequate, once it did not yield acceptable mixture volumetric properties. The mixture volumetric properties improved and met specification limits only when rejuvenators were added, suggesting that an under-asphalted condition may occur when high amounts of RAP are added without rejuvenators. Rutting performance of mixtures prepared with RAP and rejuvenators resulted poor, compared to the control mixture, but the use of polymer-modified binders alone or in conjunction with rejuvenator was capable of correcting those deficiencies. The fatigue performance increased with the

use of rejuvenator, as compared to the control mixture, and the level of improvement was greater when polymer-modified asphalts and rejuvenators were combined.

According to Mogawer et al. (2013), addition of rejuvenators was also needed to produce mixtures with resistance to low-temperature cracking comparable to the control mixture. The use of polymer-modified binders alone was not able to always yield a resistance to low-temperature cracking comparable to the control mixture and the combination of polymer-modified binder and rejuvenator had a varied effect on the resistance to low-temperature cracking, even though all the mixtures performed better than the control one. The main conclusion of the research carried out by Mogawer et al. (2015) was that rejuvenators and modified asphalts must be combined in order to produce an HMA mixture with high RAP contents that presents performance similar or superior to an HMA mixture prepared with virgin materials.

2.1.6. Design of asphalt mixtures using RAP

The procedure outlined below is based on AASHTO M 323 – "Superpave volumetrix mix design" – and the NCHRP Report 452 – "Recommended use of Reclaimed Asphalt Pavement in the Superpave mix design method: technician's Manual" (McDaniel & Anderson, 2001). The procedure addresses the use of RAP in the Superpave mixture design of HMA mixtures. Some pertinent comments and additional instructions provided here were obtained from Lavin (2003), Newcomb et al., 2007; Al-Qadi et al. (2007) and Asphalt Institute (2010).

According to McDaniel and Anderson (2001), a distinct shortcoming of the original Superpave method is that it makes no specific provision for the use of RAP in the mix design process and, in practice, such shortcoming has hindered the use of RAP by state agencies that have adopted the Superpave mix design method. To remedy such situation, the Superpave Mixtures Expert Task Group of the Federal Highway Administration used past experience to develop interim guidelines for the use of RAP in the Superpave method. Those guidelines reflected the fact that the effect of the aged binder on the performance of the virgin binder depends upon the amount of RAP in the HMA mixture, namely, if the RAP amount is low, its effect is minimal and the RAP behaves like a "black rock" that influences the volumetric properties and the performance by means of its aggregate gradation and properties. As the level of RAP in the mixture increase, the aged binder blends with the virgin material in sufficient quantity to significantly affect its

performance. The NCHRP Project 9-12 – "Incorporation of Reclaimed Asphalt Pavement in the Superpave System" (McDaniel et al., 2000) – was later created with the aim of developing guidelines for incorporating RAP in the Superpave mix design method and preparing a technician's manual to implement those guidelines in routine laboratory operations. The NCHRP Report 452 was final product of the research efforts done by the NCHRP Project 9-12.

According to McDaniel and Anderson (2001), the research findings largely confirmed current practice as exemplified by the firts interim guidelines of the Superpave Mixtures Expert Task Group. Low amounts of RAP, typically 10 to 20%, can be used without characterization of its recovered binder properties, once that there is not enough of the old, hardened aged binder present to significantly change the properties of the asphalt binder, and the RAP may be solely accounted for as a component of the mineral aggregate. When RAP is added in amounts greater than 20 percent, recovery and testing of its binder is recommended, along with the use of blending charts to determine what performance grade of virgin asphalt binder should be used in the mix design. The RAP aggregate properties should be considered as if the RAP is another aggregate stockpile. In the Superpave mix design, the RAP aggregates should be blended with the virgin aggregates so that the final blend meets the Superpave consensus properties. The results of the research largely agree with the usual practice of most state highway agencies and this agreement should give highway agencies and contractors greater confidence in more widely extending the use of RAP in HMA, regardless of the mix design method used.

According to McDaniel and Anderson (2001), the materials in the RAP most likely meet the specifications at the time of construction. However, because Superpave specifications are tighter than the previous hot-mix specifications, controls in particular on aggregate gradation and shape are frequently tighter than before. For example, if the RAP gradation is very different from the Superpave specifications, the amount of RAP that can be used may be limited. Another example is the allowable gradation, that may be different for Superpave mixtures as compared to Hveem or Marshall mixtures: for Superpave mixtures, frequently, lower fines contents are required. Past experience with RAP in Marshall and Hveem mixtures has shown that properly designed and constructed RAP mixes can perform as well as, or even better than, mixtures made with all new materials. The same should be true for Superpave mixtures made with RAP.

One of the challenges and performance risks associated with the use of RAP and RAS is the variability in aggregate and binder properties of recycled stockpiles (Ozer et al., 2017). The variability of RAP material is generally high because it may come from different layers in the pavement structure (which may include base, intermediate and surface courses, along with patches, chip seals, and other maintenance treatments) or from stockpiles of materials from different sources, although this mixing is not encouraged (McDaniel & Anderson, 2001; Asphalt Institute, 2010). It is important that the RAP sample be representative of the RAP that will be used by the mixing plant (Lavin, 2003) and because of that the first step in a project that will include RAP in the HMA mix is to obtain a representative sample of the RAP that is going to be used. Good stockpiling practices (like distinct stockpiles for materials from different sources) or processing the RAP by crushing and/or screening (when different sources of RAP are placed together in the same stockpile) will reduce the variability (McDaniel & Anderson, 2001; Asphalt Institute, 2010). Because of variability concerns, some states limit the amount of RAP that can be included in new mixtures. Some states allow the use of higher percentages of RAP if the material is milled off the same project where the new mix will be placed, and if RAP is used from a stockpile that includes material from several projects, less RAP may be used. If the RAP varies widely in properties, such as gradation or asphalt content, the resulting hot-mix asphalt may also be variable, and, because of that, variability is a concern for both the agency and the contractor (McDaniel & Anderson, 2001).

After sampling the RAP source, asphalt and mineral aggregate should be separated, in order to obtain information like gradation and shape (e.g., angularity and flat and elongated ratio) and binder content. Any deficiency in the gradation can be corrected by blending the appropriate fractions of virgin and reclaimed aggregate to meet the gradation requirements of the final HMA mixture (Asphalt Institute, 2010). According to McDaniel and Anderson (2001), to calculate the voids in the mineral aggregate (VMA) or to use the Superpave method for estimating the binder content of a mixture, it is necessary to know the combined aggregate bulk specific gravity (virgin aggregates and RAP). Calculating the combined bulk specific gravity requires knowing the bulk specific gravity of each aggregate component, however, it can be difficult to accurately measure the bulk specific gravity of the RAP aggregate. Measuring the RAP aggregate specific gravity would require extracting the RAP, sieving it into coarse and fine fractions, and determining the specific gravity of each fraction. The extraction process, however, can change the

aggregate properties and also may result in a change in the amount of fine material, which in turn could also affect the specific gravity.

Two approaches are used to measure the bulk specific gravity (McDaniel & Anderson, 2001; Asphalt Institute, 2010). Asphalt Institute (2010) discusses on the advantages and disadvantages of each approach. The first approach consists of splitting the extracted aggregate into fine (minus #4) and coarse (plus #4) fractions, and determining the bulk specific gravity (G_{sb}) of each fraction. The advantage of this method is that it provides a direct measure of the specific gravity of the aggregate. On the other hand, the extraction process (chemical or ignition) can change the aggregate properties or samples can contain asphalt or solvent, which will make it difficult to accurately measure the specific gravity. The second method consists of determining the maximum specific gravity of the RAP (G_{mm}), determining the asphalt content of the RAP, and then calculating the effective specific gravity (G_{se}) of the aggregate. The advantage of this method is that it is more accurate than the determination of the bulk specific gravity of the individual fractions. The disadvantage is that using G_{se} rather than G_{sb} of the RAP aggregate will result in an overestimate of the combined bulk specific gravity and will artificially raise the VMA of the HMA mix. The error will increase with higher percentages of RAP.

According to McDaniel and Anderson (2001), the RAP aggregate may also be tested to determine its consensus properties as is done with virgin aggregates for Superpave mixtures. It is important to remember, however, that the Superpave consensus properties apply to the total blend of aggregates (RAP plus virgin in this case), not to the individual aggregate components. It is helpful to know the properties of the RAP aggregate because that knowledge can help the mix designer determine how much RAP can be added to the new mix and still meet the consensus properties for the blend. The coarse aggregate (retained on #4 sieve) should be analyzed for coarse aggregate angularity. The fine aggregate angularity can be determined on the aggregate from the RAP that passes #8 sieve, but one should be aware that the fine aggregate angularity of the RAP aggregate may be changed (usually decreased) by the extraction process. The percentage of particles that are flat and elongated must also be determined. If the RAP aggregate has a high percentage of flat and elongated particles, it can be blended with more cubical aggregate so that the resulting blend meets the requirements.

Another important issue for the project of the mixture is the determination of the moisture content present in the RAP. According to McDaniel and Anderson (2001), when determining batch weights for RAP at the plant, the weight of the moisture in the RAP must be accounted for, just as it is for virgin aggregates, otherwise actual weight of RAP added will be lower than required. The RAP moisture content can also be a limiting factor for plant production, once that high moisture contents take a long time and a lot of energy to dry, and this can severely affect production. In batch plants, high moisture contents can produce steam clouds in the pugmill that need to be vented.

Regarding the RAP binder, the NCHRP Report 452 (McDaniel & Anderson, 2001) recommends that it is not necessary to test the RAP binder for low RAP contents (10 to 20%), once that there is not enough of the old, hardened RAP binder present to change the total binder properties. At higher RAP contents, however, the RAP binder will have a noticeable effect, and it must be accounted for by using a softer binder. For intermediate ranges of RAP, the virgin binder grade can simply be dropped one grade. For higher percentages of RAP, extraction and recovery of the RAP binder will be needed to determine its properties. Table 2.1 shows recommended tiers for Superpave RAP mixtures and the appropriate changes to the binder grade, where the limits of these tiers depend on the RAP binder grade. With softer RAP binders, higher percentages of RAP can be used. The first tier establishes the maximum amount of RAP that can be used without changing the virgin binder grade. The second tier shows the percentages of RAP that can be used when the virgin grade is decreased by one grade on both the high- and low-temperature grades. The third tier establishes that for higher RAP contents, it is necessary to extract, recover, and test the RAP binder and to construct a blending chart.

Table 2.1. Binder selection guidelines for RAP mixtures

	RAP percentage		
	recovered RAP grade		
recommended virgin asphalt binder grade	**PG xx-22 or lower**	**PG xx-16**	**PG xx-10 or higher**
no change in binder selection	<20%	<15%	<10%
select virgin binder one grade softer than normal*	20-30%	15–25%	10–15%
follow recommendations from blending charts	>30%	>25%	>15%

*For example, select a PG 58-28 if a PG 64-22 would normally be used.

In accordance with the NCHRP Report 452 (McDaniel & Anderson, 2001), to construct a blending chart, the desired final binder grade and the physical properties (and critical temperatures) of the recovered RAP binder are needed, along with one of the following pieces of information: (i) the physical properties (and critical temperatures) of the virgin binder, or (ii) the percentage of RAP in the mixture. Once the RAP binder has been extracted and recovered, its properties need to be determined in the dynamic shear rheometer (DSR) at high temperatures in order to determine its continuous grade (i.e, temperature at which $G^*/sen\delta$ = 1.0 kPa), and the remaining RAP binder must be aged in the rolling thin film oven (RTFO) for tests in the DSR and bending beam rheometer (BBR). The continuous grade of the RTFOT-aged residue is then determined, which is used in conjunction with the continuous grade of the original RAP binder in order to determine its performance grade. The RTFOT-aged residue is also subjected to tests in the DSR at intermediate temperatures, in order to determine the fatigue critical temperature. The same RTFOT-aged residue is also used to determine the low-temperature performance grade of the RAP binder in the BBR.

Once the physical properties and critical temperatures of the recovered RAP binder are known, two blending approaches may be used. In one approach (designated Method A), the percentage of RAP that will be used in an asphalt mixture is known, and the appropriate virgin asphalt binder grade for blending needs to be determined. In the second approach (designated Method B), the maximum percentage of RAP that can be used in an asphalt mixture while still using the same virgin asphalt binder grade needs to be determined. When the RAP percentage to be used in the project is known, it is needed to determine the grade of the binder that must be blended with the RAP to obtain a particular grade for the blend of old and new binder. For such determination, it is necessary to know the final blended binder grade, the percentage of RAP, and the recovered RAP properties. When the performance grade of the virgin binder to be used in the project is fixed, it is needed to determine the RAP percentage that must be added to obtain a particular grade for the blend of old and new binder. For such determination, it is necessary to know the final blender binder grade, the virgin binder grade, and the recovered RAP properties (McDaniel & Anderson, 2001).

The properties of the virgin asphalt binder needed to satisfy the assumptions can be determined by using the following equation for the high, intermediate, and low critical

temperatures separately, where T_{virgin} is the critical temperature[1] of the virgin asphalt binder, T_{blend} is the critical temperature of the blended asphalt binder (final desired), %RAP is the percentage of RAP expressed as a decimal (i.e., 0.30 for 30%), and T_{RAP} is the critical temperature of the recovered RAP binder. An example is provided in NCHRP Report 452 (Chapter 3) where the use of a RAP binder with a continuous PG of 86-11 (or 82-10 as per AASHTO MP1) requires, after calculations, the addition of a virgin binder with a continuous PG of 54-26 (or 58-28 as per AASHTO MP1), in order to obtain a blended binder grade of PG 64-22 and considering that the RAP percentage in the mixture is 30% (McDaniel & Anderson, 2001).

$$T_{virgin} = \frac{T_{blend} - (\%RAP x T_{RAP})}{1 - \%RAP} \quad (2.1)$$

For the cases in which a particular virgin binder grade is desirable for the recycled mixture, for economic reasons or availability or even because of the specifications for a given project, the amount of RAP that can be used with that specific virgin binder grade, and still meeting the final blended binder properties, must be determined. The percentage of RAP needed to satisfy the assumptions can be determined by using the following equation for the high, intermediate, and low critical temperatures separately, where $\%_{RAP}$ is the percentage of RAP expressed as a decimal (i. e., 0.30 for 30%), T_{virgin} is the critical temperature of the virgin binder, T_{blend} is the critical temperature of the blended asphalt binder (final desired), and T_{RAP} is the critical temperature of the recovered RAP binder. An example is provided in NCHRP Report 452 (Chapter 3) where the use of a virgin binder with PG 58-28 requires, after calculations, the addition of a RAP percentage between 14 and 40%, in order to obtain a blended binder grade of PG 64-22 and considering that the recovery binder RAP is a PG 82-10. A RAP percentage lower than 66% would be needed to meet the intermediate-temperature grade (McDaniel & Anderson, 2001).

$$\%_{RAP} = \frac{T_{BLEND} - T_{VIRGIN}}{T_{RAP} - T_{VIRGIN}} \quad (2.2)$$

[1]Critical temperatures are the temperatures at which a binder meets the specified Superpave criteria, for example, 1.00 kPa for unaged binder high temperature stiffness (G*/sinδ).

Regarding the design of the mixture containing RAP, one major decision that must be made early in the process is the approximate amount of RAP that is intended to be used. This decision is made based on the prevailing state specifications, the aggregate gradation and properties, economics, and, sometimes, the binder properties. The amount of RAP to add to the new mixture may be limited by many different factors, including (i) specification limits for mix type, plant type, or other reason; (ii) gradation; (iii) aggregate consensus properties; (iv) binder properties; (v) heating, drying, and exhaust capacity of the plant; (vi) moisture content of the RAP and virgin aggregates; (vii) temperature to which the virgin aggregate must be superheated; (viii) ambient temperature of the RAP and virgin aggregate; and other factors. Overall, however, the situation when using RAP in Superpave mixtures is similar to the situation when using RAP in Marshall or Hveem mixtures, i. e, the blend of materials has to meet certain properties, and the plant must be capable of drying and heating the materials. Many of the techniques used to evaluate the RAP are similar to previous techniques, but other, particularly the binder evaluation, are quite different (McDaniel & Anderson, 2001).

Once the RAP aggregate gradation has been determined, that aggregate must be blended with the virgin aggregates to meet the overall mixture gradation requirements: the total blend must pass between the control points and the restricted zone should be avoided. The Superpave mix design procedure recommends that at least three trial blends be evaluated, and when RAP is used these blends may include different percentages of RAP or may be different combinations of virgin stockpiles with a set percentage of RAP. The proposed aggregate blends must meet the gradation requirements as well as the consensus aggregate properties, along with the required mixture volumetric properties (i.e., VMA, VFA, dust proportion, and densification properties) at 4% air voids (McDaniel & Anderson, 2001).

According to McDaniel et al. (2000), the overall Superpave mix design process is very much the same regardless of the inclusion of RAP. The differences include the following: (i) the RAP aggregate is treated like another stockpile for blending and weighing, but must be heated gently to avoid changing the RAP binder properties; (ii) the RAP aggregate specific gravity must be estimated; (iii) the weight of the binder in the RAP must be accounted for when batching aggregates; (iv) the total asphalt content is reduced to compensate for the binder provided by the RAP; and (v) a change in virgin binder grade may be needed depending on the amount of RAP, desired final binder grade, and RAP

binder stiffness. When batching out the RAP aggregates, it is important to remember that part of the weight of the RAP is binder. It is necessary to increase the weight of RAP and decrease the amount of virgin binder added to take this RAP binder into account.

The steps required when doing a Superpave mix design with RAP are described in the NCRHR Report 452 (McDaniel & Anderson, 2001) and will be entirely reproduced here. The steps outlined in that report are based on the 1999 AASHTO specifications, which require compacting specimens to N_{design} (design number of gyrations) rather than to N_{max} (maximum number of gyrations), once that N_{max} is verified only for the final mix design.

2.1.7. Some brazilian research works with RAP

Some research works developed in Brazil and involving recycling of HMA mixtures are listed below, aiming at pointing out the importance of this topic in the country. Domingues and Balbo (2006) studied HMA mixtures prepared with 100% RAP, with emphasis on the use of rejuvenating agents. Balbo and Bodi (2004) studied the use of RAP (milled material) or material in blocks in hot-mix recycling using 100% recycled materials for the construction of high-modulus base courses for perpetual pavements and rigid base courses for areas under reconstruction. Balbo and Bodi (2004) obtained recycled mixtures with high Marshall estability values, high resilient modulus and high indirect tensile strength values, as compared to standard limits. Baldo and Bodi (2004) also reported that the new asphalt should be added at reduced proportions if a high modulus mixture is desired.

Almeida et al. (2014) evaluated the volumetric and mechanical properties of recycled mixtures, aiming at studying the effect of different contents of asphalt emulsion and Portland cement in cold-mix recycling. These researchers observed that the increase of the emulsion proportion, for a fixed proportion of 1% Portland cement, did not present a clear trend on mixture apparent density, but, on the other hand, the increase of emulsion proportion was able to reduce the resistance to uniaxial compression. Almeida et al. (2014) also observed that the apparent density and the resistance to uniaxial compression increased with the increase in the cement proportions, for a fixed proportion of 3% asphalt emulsion. The mixtures prepared with 2% cement and 3% emulsion showed the highest apparent density and the highest resistance to uniaxial compression.

Vasconcelos and Soares (2003) studied the effect of low and high amounts of RAP (10 and 50%) on the performance of HMA mixtures, using a 50-60 pen-grade binder and

a rejuvenating agent (AR-75). These authors obtained similar optimum binder contents, regardless of the presence of a high amount of RAP in one of the mixtures. They also mentioned that the procedure to determine the theoretical maximum density is capable of yielding different binder contents and recommended the adoption of the procedure ASTM D 2041 to determine such density. In terms of mechanical properties of the HMA mixes, Vasconcelos and Soares (2003) observed increased resilient modulus and indirect tensile strength values for the mixtures prepared with RAP as compared to the control mixture.

In a subsequent work, Vasconcelos and Soares (2004) evaluated the effect of short-term aging of recycled mixtures with increasing RAP percentages (0, 10, 30 and 50%). Aging was simulated in oven, before compaction, for periods of 0, 1, 2 and 4 hours at compaction temperature (144 to 149ºC). The results obtained for the volumetric parameters showed great variation in the recycled mixtures, probably due to heterogeneity issues caused by RAP. The optimum binder content tends to increase with short-term aging, due to asphalt absorption. Except for the mixture prepared with 10% RAP aged for 1 h, all the others presented increased binder contents with the increase of time in the oven. The mixture prepared with only new materials presented the lowest variation in binder content with the increase of time in the oven. Additionally, small variations in binder content were observed for 2 and 4 hours of exposure for all the mixtures. This might indicate that the absorption of binder happens mainly during the first two hours in the oven and that, after that period of time, the actual interaction between the RAP and the new binders take place, which is able to reduce the optimum binder content slightly for higher RAP contents.

David (2006) studied the mechanical behavior of mixtures produced by means of cold-mix recycling for the construction of base courses, using an asphalt emulsion (cationic, slow set, RL-1C), an emulsified recycling agent (ARE-75), and new mineral aggregates. David (2006) concluded that (i) the mixtures produced with the emulsion RL-1C presented higher tensile strength values than the mixtures prepared with the agent ARE-75, (ii) the addition of filler from new aggregates increased the specific density of the mixtures prepared with both agents with no marked influence of the agent type, and (iii) the mixture RAP+filler+RL-1C presented higher tensile strength ratios, even though the mixture RAP+RL-1C had also presented adequate results.

Moreira (2005) studied cold-mix recycling, using three RAP contents (25, 50 and 75%) and observed a negative effect of the increase of the RAP content on the mechanical

properties of the recycled mixtures, even though the mixture prepared with 25% RAP had shown acceptable performance. The mixtures studied by Moreira (2005) presented low tensile strength values as compared to conventional mixtures, which mean that they are not adequate to high-traffic-volume roads. On the other hand, the mixtures presented results compatible with those expected for hot asphalt-sand mixtures, which is an evidence of their adequacy for roads of intermediate- and low-volume traffic.

Silva (2011) studied the application of cold-mix recycling in laboratory-made samples and field trials and observed better performance for the mixtures prepared with SBS-modified, slow-set cationic asphalt emulsions than for the mixtures prepared with conventional (non-modified) asphalt emulsions. Data from back analysis of field deflection measurements yielded resilient modulus for the asphalt layer produced with recycled material between 1,000 and 2,000 MPa, which are similar to those obtained in laboratory in the triaxial test. Silva (2011) also mentioned that the layer produced with recycled material did not present the same level of stiffness of an asphalt concrete, although containing 1% Portland cement, but it performs as a material stiffer and more cohesive than the one used in an unbound granular layer.

Nascimento et al. (2013) evaluated the performance of asphalt mixtures prepared with different RAP proportions and observed that the compaction method affects the final results. The compaction in the gyratory compactor produced mixtures with lower air voids, leading to resilient modulus and indirect tensile strength values higher than those observed for the mixtures compacted by means of the Marshall procedure. In turn, Lima (2003) studied the performance of hot-mix recycled mixtures prepared in the laboratory with the addition of rejuvenating agent (AR-75) and increasing RAP contents (0, 10, 30 and 50%) and observed an increase of stiffness of the resulting mixtures. Such increase in stiffness led to an increase in the resilient modulus (between 3,200 and 8,900 MPa), in the indirect tensile strength (between 1.2 and 1.6 MPa) and in the fatigue life measured by means of diametral compression (in stress control). Triches et al. (2000) studied the field performance of a cold-mix recycled mixture prepared with a medium set asphalt emulsion (RM-1C) used in the construction of a wearing course in a road of intermediate traffic volume. The authors did not evaluate the diffusion process of the emulsion into the aged binder but claimed that such emulsion would be able of diluting the aged binder because of its naphthenic nature. Triches et al. (2000) reported that the use of RAP by means of

cold-mix recycling with conventional emulsion (non-modified) led to a durability 70% higher as compared to a double superficial treatment.

Bessa et al. (2016) evaluated the design of cold recycled mixes through different compaction methods, by varying asphalt emulsion and cement contents, and by employing different curing temperatures and periods, and proposed a design method. Mechanical tests performed indicated that specimens compacted by the Marshall hammer provide similar results when varying asphalt emulsion and cement contents, while the Proctor hammer compaction presented variation on their mechanical behavior as asphalt emulsion and cement contents were varied. The design procedure should include at least three asphalt emulsion contents. Five samples for each emulsion content should be prepared, with variation on their water content to obtain the optimum moisture content. The water present in the asphalt emulsion should be considered. Unconfined compressive strength tests are then performed to design the mix. In relation to the curing procedure, it is recommended that the specimens are submitted to a curing temperature of 60 °C during only one day.

As far as environmental regulations are concerned, in spite of some advancement in the Brazilian legislation related to handling of solid residues, as the CONAMA Resolution number 5 and the Brazilian Federal Law 9.985/200, no specific guidance is offered in any of these regulations in terms of handling of materials originated from paving construction. One exception to this rule is the Municipality of the Sao Paulo City, by means of the Law number 14.015/2005 that requires the presentation of an environmental handling plan and prohibits the disposal of such materials at any sort of landfill, sanitary landfill or public or private plots accredited for such aim, and the removal to areas outside of the geographic limits of the municipality. Recycling is the preferential alternative and it should be executed within the limits of the municipality. As a matter of comparison, some documents available online describes the pavement recycling policies of some countries (Schimmoller et al., 2000; Piarc, 2008).

2.2. Fine aggregate matrix (FAM)

The fatigue cracking mechanism of asphalt pavements starts from invisible micro cracks that occur in discontinuities of the material. Such micro cracks are followed by the crack propagation process, leading to the formation of macro cracks, until a complete

degradation of the material. An accurate prediction of the fatigue behavior of the asphalt mixtures has been the goal of many studies, in order to improve the asphalt mixture design and, consequently, the performance of flexible pavements. Studies on the response of asphalt mixtures to fatigue are divided into two categories: (i) the full asphalt mixture, which contains asphalt binder, coarse aggregates, fine aggregates and mineral fillers; and (ii) the fine aggregate matrix (FAM), composed by part of the fine aggregates, minerals fillers and asphalt binder.

The changes of the material microstructure are the beginning of the fatigue process, and these changes are influenced substantially by properties of the mastic (combination of binder, filler, and entrapped air), once these changes occur by means of adhesive micro cracks (cracking between aggregates and binder) and cohesive micro cracks (cracking of the binder) (Kim & Little, 2005). Based on this premise, Kim, Little and Lytton (2003a) and Kim, Little and Song (2003b) started to study the fatigue behavior of asphalt mixtures using the FAM approach.

In studies with FAM mixtures, the first assumption is that it reproduces the internal structure of the fine portion of the aggregate gradation of a full HMA mixture. Another assumption is that the physic-chemical interactions between aggregate and binder are replicated in the FAM specimen. In order to separate the fine gradation of the aggregates, researches in the USA have been using aggregates passing sieve #16 (1.18 mm), which is part of the sieve series of the American standard for HMA mixtures (Zollinger, 2005; Masad et al., 2006; Arambula, Masad, Epps-Martin, 2007; Bhasin et al., 2008; Caro et al., 2008; Masad et al., 2008; Castelo Branco et al., 2008; Castelo Branco, 2008; Caro et al., 2010; Vasconcelos et al., 2010; You, Adhikari & Kutay, 2009; Palvadi, 2011; Vasconcelos et al., 2011; Caro et al., 2012; Palvadi et al., 2012; Im, 2012; Izadi, 2012; Souza et al., 2012; Tong et al., 2013; Arega et al., 2013; Kim & Aragão, 2013; Kanaan et al., 2014; Aragão et al. 2014; Tong et al., 2015; Im et al., 2015; Gudipudi & Underwood, 2015; Nabizadeh, 2015; Karki et al., 2015a,b; Cravo, 2016; Karki et al., 2016; Haghshenas et al., 2016, Cucalon et al., 2017).

Some researchers adopted different nominal maximum aggregate sizes (NMAS) to produce FAM samples. In a study conducted by Aragão et al. (2010), an image treatment process was utilized to capture digital images from the mixture. The particles smaller than 0.30 mm were considered as the fine aggregate matrix phase because the portion of the aggregate gradation finer than 0.30 mm was not distinctively captured by the digital

image processing. The aggregates passing sieve #50 (0.30 mm) were adopted in order to characterize the FAM microstructure by means of X-ray images and to characterize the FAM linear viscoelastic properties (Aragão et al., 2010). Motamed, Bhasin and Izadi (2012) utilized glass beads with MNS of 1.00 mm (#18), 0.5 mm (#35) and 0.1 mm (#140) to evaluate the binder properties without the interaction with the mineral aggregate.

Underwood and Kim (2013) investigated the effect of different NMAS in the FAM microstructure, by performing tests with FAM samples produced with aggregates particles passing sieve #8 (2.36 mm), #16 (1.18 mm) and #30 (0.06 mm). Underwood and Kim (2011) justify the use of aggregate particles passing sieve #8 based on the packing theory presented by Vavrick et al. (2001). According to Vavrick et al. (2001), the void space created by three of the nominally largest sized coarse particles touching in the most optimal arrangement is the ideal aggregate diameter to a primary control sieve. For mixtures with a NMAS of 9.5 and 12.5 mm, this dimension is approximately 2.36 mm, and the FAM material should be fabricated with aggregates particles smaller than 2.36 mm.

A series of studies investigating the fatigue properties (Underwood & Kim, 2011; Gong et al., 2016; He et al., 2016; Zhu, et al. 2017) and creep stiffness (Dai & You, 2007) of asphalt mixtures utilized FAMs produced with NMAS of 2.36 mm (#8). Aggregate particles smaller than 1.18 mm (#16) to produce the FAM samples was considered a non-practical size, due to the large amount of material that needs to be separated and discarded to prepare the FAM samples (He et al., 2016; Zhu et al., 2017).

In Brazil, sieve #16 (1.18 mm) is not part of the sieve series of Brazilian standards for HMA mixtures, and because of that the FAMs are produced with aggregate particles passing sieve #10 (2.00 mm) (Coutinho, 2012; Pazos, Sacramento & Motta, 2015). Brazilian researchers investigated the influence of different NMAS, i.e., #16 (1.18 mm), #10 (2.00 mm) and #5 (4.00 mm), in the fatigue properties of FAMs (Freire et al., 2014; Freire, 2015 and Freire et al., 2017). The NMAS of #10 (2.00 mm) was considered suitable, because the fatigue curves of the FAMs presented slope similar to the curves for the HMA mixture. Another reason to adopt sieve #10 is the ratio between the aggregate size and sample diameter of 1:6, which is higher than the minimum of 1:3 recommended by Kim et al. (2004).

FAM represents an intermediate scale between the asphalt mastic and the complete asphalt mixture. It presents an internal structure that is more homogeneous than the one represented by the full HMA mixture, and provides a more realistic characterization of the

fatigue response of full asphalt mixtures than the one provided by tests performed on the mastic. Another advantage of utilizing FAM samples in fatigue testing is that the reduced size of the samples requires a smaller amount of material compared with the amount required to produce samples of full asphalt mixtures, demanding a reduced laboratory work to prepare the samples.

2.2.1. Mechanisms of damage of asphalt concrete mixtures

Kim et al. (2003a) evaluated the fatigue and healing process of asphalt mixtures by performing dynamic mechanical analysis (DMA) tests using FAM samples produced with sand asphalt. The sand-asphalt samples were fabricated with mineral aggregates particles lower than 1.18 mm (#10) and with a binder content of 8%. The asphalt content was an arbitrary value selected to produce a "film thickness" of approximately 10 microns. The mixture was compacted in a specific mold in order to produce a cylindrical specimen with 50 mm in length and 12 mm in diameter. The test results indicated that the introduction of rest periods increased the fatigue life for the analyzed conditions. The researchers suggested that the testing method could result in a specification-type test method for asphalt mixtures characterization because its efficiency, reproducibility and reliability.

Kim et al. (2003b) evaluated the effect of mineral fillers on the fatigue resistance of asphalt mixtures composed with two asphalt binders (AAD-1 and AAM-1) and two fillers (limestone and hydrated lime), utilizing the same procedure used by Kim et al. (2003a). The cylindrical sand-asphalt samples were tested under controlled-strain torsional mode of loading, and, for such mode of loading, the results indicated that the fillers contributed to increase the fatigue life, especially for the mixture containing hydrated lime and asphalt AAD-1. Such mixture presented a greater improvement on fatigue life, indicating that the physicochemical interaction between binder and filler depends on the type of material.

Due to the successful development of the FAM testing method, Kim and Little (2005) proposed a protocol to assess the impact of fine aggregates and mineral fillers on fatigue damage, performing dynamical mechanical tests using the dynamic mechanical analyzer (DMA). Dynamic tests were performed under controlled-strain mode of loading, in two steps: 1) low strain levels for validation of the linear viscoelastic behavior; 2) high strain levels for fatigue damage simulation. The protocol developed during the study was considered effective to provide acceptable data to characterize the fatigue behavior of the materials evaluated in their investigation.

Studies concerning fatigue behavior, moisture damage and healing characteristics of the asphalt mixtures by performing tests on FAM samples utilizing the DMA have advanced, mainly due to the efforts of the researchers from the Texas A&M University (Zollinger, 2005; Masad et al., 2006; Bhasin, 2006; Arambula, Masad & Epps-Martin, 2007; Masad et el., 2008; Caro et al., 2008; Castelo Branco, 2008; Vasconcelos, Bhasin & Little, 2010; Vasconcelos et al., 2011). An important contribution presented by this research group refers to the compaction method of the FAM samples. The samples fabricated by compacting the loose mixture in a cylindrical mold (Kim et al., 2003a; Song, 2004) have been presenting higher air voids on the top of the samples, as reported by Zollinger (2005), and it could result in cracks in the sample edges. A new procedure to produce FAM samples was developed by Zollinger (2005), in order to overcome such problem. The method consists of the following steps: i) to compact the loose mixture, utilizing the Superpave gyratory compactor, producing samples of 85 mm in height, 152 mm in diameter and 11% air-voids content; ii) to trim the top and bottom parts of the specimen off, reducing the height to 50 mm; iii) to extract cylindrical samples of 50 mm in height and 12,5 mm in diameter, using a coring barrel.

The susceptibility to moisture damage of the adhesive bond of aggregates and asphalt and the cohesive strength of the binder was evaluated by Zollinger (2005) and Masad et al. (2006), with the objective of determining procedures to be used to select combinations of aggregates and binders that might reduce such susceptibility. A problematic combination of aggregates and binders can be identified by means of the ratio of the adhesive bond energy under dry conditions to the adhesive bond energy under wet conditions, $\Delta G^{a(w)}/\Delta G^{a(D)}$, and a wet/dry ratio lower than 0.8 was defined to separate the good from the poor combinations of materials.

Once the moisture damage in asphalt mixtures cause a reduction in fatigue life, N_f, the effect of moisture can be assessed by performing fatigue tests (Zollinger, 2005). FAM samples under dry and wet conditions were tested and another parameter for moisture damage evaluation, defined as the ratio of the number of cycles to failure under wet to dry condition, $N_{f(W)}/N_{f(D)}$. For such parameter, the findings indicated that the higher the wet/dry ratio, the better the mixtures performs, as the wet fatigue life is closer to the dry fatigue life. The ratio of the shear modulus at failure to the initial shear modulus, G'/G, captures the amount of the mastic dynamic modulus that can decrease while still accumulating damage. The mixtures evaluated with good resistance to moisture damage

presented lower ratios for G'/G at failure than the mixtures with poor resistance. The findings of the study also indicated that a fixed value of 50% reduction in stiffness does not represent the fatigue failure of all materials evaluated in those investigations (Zollinger, 2005; Masad et al. 2006).

In a study of the impact of fine aggregate matrix on the fatigue behavior of asphalt mixtures, Kim and Little (2005) performed dynamic sweep tests at several strain levels high enough to produce damage. The dissipated energy (hysteresis loop area between measured stress and measured strain) was calculated by monitoring loss modulus at each loading cycle. By analyzing the hysteretic stress-strain behavior of the fatigue tests, it was observed that the stress-strain loops downward when the dissipated energy reduces. The results of damage accumulation were also investigated by means of the VECD theory, and the changes in the dissipated pseudo strain energy and pseudo stiffness of the hysteresis loop during the loading indicated that micro damage has occurred. The cumulative dissipated pseudo strain energy (CDPSE) was employed as a quantitative indicator to define fatigue resistance.

Kim and Little (2005) also evaluated the changes in the normalized nonlinear dynamic modulus due to damage accumulation and observed two inflection points in the *normalized nonlinear dynamic modulus vs. number of cycles* curve: i) a first inflection point (FIP), which is associated to the micro cracking and ii) a second inflection point (SIP), which is possibly associated to the macro cracking (Figure 2.1). A transition point, N_t, between the two inflection points was also observed. These three points, FIP, SIP and N_t, were considered as potential fatigue failure points, and were compared with the criterion proposed by Reese (1997), which considers the maximum phase angle (MPA) value as a reasonable fatigue failure point. The analysis presented a minimum deviation error for the comparison between N_t and MPA, leading the researchers to adopt the N_t as a fatigue failure point. The materials evaluated during the study presented 60 to 85 percent stiffness reduction at the failure point.

The fatigue criterion defined as a 50 percent reduction of pseudostiffness (Park et al., 1996, Lee; 1996) was also adopted by Kim and Little (2005) to evaluate the fatigue life of the mixtures investigated in their study. For a given mixture, the fatigue response was calculated for a representative data set of 0.4 percent strain level and different indicators of fatigue failure were evaluated (stiffness reduction; pseudo-stiffness reduction; CDPSE; dissipated energy changes; FIP, SIP and N_t). The results indicated that the ratio of each

indicator to a certain number of loading cycles have a similar reduction. The findings showed that these three damage parameters are effective to characterize fatigue damage during torsional loading: (i) a decay in pseudostiffness; (ii) a loss of nonlinear dynamic modulus; (iii) a change in dissipated strain energy.

Figure 2.1. Plots of normalized nonlinear dynamic modulus and phase angle versus number of loading cycles in fatigue testing.

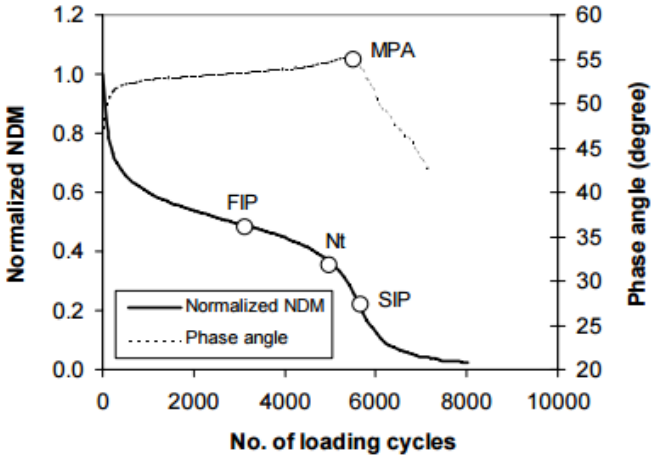

Source: Kim and Little (2005, p.44)

Song (2004) developed a methodology to characterize the damage behavior in asphalt concrete mixtures based on nondestructive imaging techniques (X-ray CT), principles of viscoelastic continuum damage mechanics, and principles of micromechanics. For the digital image analysis method, a damage parameter, ξ, that quantifies the percentage of cracks and air voids in a specimen was defined. For the continuum damage mechanics approach, DMA tests on FAM samples were performed and the damage parameter at each load cycle, S, was calculated. Another parameter adopted to quantify damage was the dissipated pseudo strain energy (DPSE) or W_R, which is the area within the hysteresis loop in the stress-pseudo strain domain. The hysteresis behavior was obtained from the DMA fatigue tests. The parameters were compared and the results indicated good correlation among the parameters evaluated.

Zollinger (2005) and Masad et al. (2006) suggested that the DPSE or W_R parameter should be calculated as the area of the hysteresis loop divided by the volume of the material that is capable to dissipate energy. Furthermore, the DPSE or W_R should not be calculated based only on the changes in the viscoelastic properties (W_{R1}), because the accumulation of permanent deformation was not uniform during loading. Masad et al.

(2008) proposed a method that can separate the dissipated energy due to permanent deformation from viscoelastic energy. Masad et al. (2008) assumed that the damage process, mathematically, consists of three components: (i) a component that is associated with an increase in the phase angle between loading cycles (W_{R1}), (ii) a component that accounts for the changes in the phase angle for the same loading cycle due to permanent deformation (W_{R2}), (iii) a component that accounts for the changes in the pseudostiffness of the material before and after damage (W_{R3}). A proper partitioning of the energy between nonlinearity and damage allows to unify the results of the controlled-strain and controlled-stress modes of loading, and the ratios of W_{R1} and W_{R3} are the same when the results of both mode of loading are unified.

Two new parameters to characterize fatigue damage were proposed by Masad et al. (2008): (i) the projected crack radius, $\Delta R(N_f)$, at a fixed number of cycles, and (ii) the ratio of $\Delta R(N_f)$ to $ln(N)$. Castelo Branco et al. (2008) and Castelo Branco (2008) applied this method to investigate the fatigue cracking of asphalt mixtures under different levels of strain and stress. The values for the crack growth index are similar for tests performed on both modes of loading: controlled-stress or controlled-strain mode. The moisture susceptibility of asphalt mixtures can be evaluated based on the ratio $\Delta R(N_f)_{(WET)}/\Delta R(N_f)_{(DRY)}$, by performing tests on wet and dry samples (Caro et al., 2008).

A controlled-stress repeated direct tension (RDT) test method to identify the fatigue crack growing caused by moisture in flexible pavements was developed by Tong, Luo and Lytton (2013). The new test procedure and data analysis were based on the pseudo strain energy equivalence theory, in order to characterize the fatigue crack growth of FAM samples that were conditioned at different levels of relative humidity (RH). The crack propagation at the tertiary stage (decrease of the modulus magnitude and increase of the phase angle as the load cycles increased) of the RDT tests was analyzed and the fatigue properties of the samples were determined according to the strain energy equivalence principles, which states that the dissipated strain energy and the recoverable strain energy in the asphalt mixture specimen are equivalent to their counterparts in the undamaged material. The newly RDT test methodology was considered more efficient than the torsional tests because the stress state complexity within the specimens is greatly reduced.

Tong et al. (2013) and Tong, Luo and Lytton (2015) utilized the RDT test method to evaluate the effect of moisture and aging damage in asphalt mixtures. Moisture-

conditioned and aged specimens were tested and the crack growth evolution was analyzed. The findings indicated that the saturated vapour pressure in the bulk samples significantly increases the fatigue cracking of the asphalt mixtures. An increase of the rate of asphalt fatigue cracking after aging was also observed, for both warm mix and hot mix asphalts. Moreover, the results of the moisture-conditioned samples present a higher fracture parameter, *n'*, than that for aged specimens, indicating that WMA mixtures are more susceptible to moisture compared to HMA mixtures.

The healing mechanism has a significant effect on the performance of asphalt mixtures and a better understanding of the healing process can provide a better prediction of the fatigue behavior of such materials. The DMA technology was utilized by Bhasin et al. (2008) to investigate the healing properties of six FAM samples produced with two types of aggregates and three types of bitumen. In order to quantify the FAM healing, nine rest periods of four minutes were introduced during the cycle tests and the data were compared with data from tests without rest periods. Each rest period was introduced after cycles that correspond to 2.5, 5, 10, 15, 20, 25, 30, 40, and 50 percent of the fatigue life for a sample tested without rest periods. The healing properties of the three different bitumen were investigated by tests performed on the dynamic shear rheometer (DSR). The effect of healing on the performance of the bitumen samples presented a good correlation with the relative increase in the fatigue life of the FAM mixtures due to the introduction of rest periods.

2.2.2. Micromechanical computational modeling

The analytical micromechanics has been utilized to determine the viscoelastic properties of asphalt mixtures and to predict the dynamic modulus of the material, G^*, in order to compute the mechanical responses of asphalt pavements to fatigue damage. Although the method does not require performing the set of time-consuming tests that are required, for example, by the DMA approach, some researches pointed out that the analytical micromechanics approach presents some limitations (Kim, Allen, & Little, 2005; Aragão et al., 2010). The homogenization methods required to apply the theory do not account for geometric heterogeneity of the mixes and interactions among the mixture elements, leading to some unreliable results. The overcome these limitations, computational micromechanical modeling has been used in order to predict damage in asphalt mixtures. The computational methods take in account the heterogeneous

geometric characteristics and the inelastic behavior of the material. Because of that, the material microstructure and its response to the stresses and strains can be analyzed more realistically (Aragão et al., 2010).

Aragão et al. (2010) conducted a study to compare micromechanical models (analytical and computational) with dynamic modulus tests results obtained from cylindrical specimens of full asphalt mixtures. The asphalt concrete microstructure of the asphalt mixtures was obtained by using a digital image process and samples compacted in the Superpave gyratory (150 mm in diameter and 170 mm height). The images were converted to a binary format (black and white, representing the asphalt matrix phase and the aggregates, respectively). The black portion was considered as the blend of binder with particles smaller than 0.30 mm, once it was not possible to capture the aggregate gradation finer than 0.30 mm by the digital image process. FAM samples were produced using aggregates particles smaller than 0.30 mm, in order to obtain the linear viscoelastic properties of the material. The dynamic modulus was predicted considering the percentage of voids in mineral aggregates (VMA), the percentage of voids filled with asphalt (VFA) and the aggregate contact volume (Pc), which were estimated from the images of the asphalt concrete microstructure. The comparisons between the data from the micromechanical models and the data from experimental tests indicated that: (i) the prediction models present reasonable agreement with the test results; (ii) the Hashin's analytical prediction model presents the worst performance, which can be explained because geometric simplifications were assumed; (iii) the computational micromechanics modeling approach presented better predictions to higher loading frequency than to lower loading frequency; (iv) the computational micromechanics modeling approach, incorporated with the testing protocol, seems to be an attractive alternative to fatigue characterization because it requires a reduced time of laboratory work.

In a later study, Aragão et al. (2011) refined the micromechanical computational model to predict fracture behavior of heterogeneous viscoelastic asphalt mixtures, using the finite-element method and a cohesive zone fracture model. The linear viscoelastic material properties and fracture parameters were obtained from laboratory tests performed on the fine aggregate matrix. The FAM samples were produced with a blend of binder and aggregate particles smaller than 0.28 mm. The viscoelastic parameters were then incorporated to a finite element model that represents the mixture cohesive zone (matrix phase: combination of asphalt binder, air voids, fine aggregates and filler). The

results from model simulations were compared to results from performed laboratory tests for the calibration and validation of the model. A good agreement between the simulations results and the experimental results was observed.

Aragão and Kim (2012) proposed a new procedure to characterize the mode I fracture behavior of asphalt concrete mixtures subjected to loading conditions at an intermediate service temperature. This new method consists in testing the matrix phase under different ranges of loading rates (1, 5, 10, 25, 50, 100, 200, 400, and 600 mm/min) at an intermediate temperature (i. e., 21ºC) in order to evaluate the effects of rate dependency and temperature sensibility. Semi-circular bending (SCB) samples with an introduced notch were tested at the conditions aforementioned, and a digital image correlation (DIC) system was incorporated into the fracture tests to capture specimen deformations during the tests. The first image captured represents the SCB undamaged structure. New images of the sample were being collected during the deformation process and the notch was monitored. The DIC compares the undamaged structure image to the images of the deformed structure and calculates the displacement and deformation of the specimen. The researchers obtained good agreement between DIC results and numerical simulations and concluded that the FAM fracture properties are clearly rate-dependent at intermediate temperatures.

2.2.3. Viscoelastic Continuum Damage theory – VECD

The fatigue life, N_f, of asphalt mixtures is defined as the number of loading cycles at which the material failure occurs. Li (1999) defined the failure criterion as a specific crack size of the sample. Some researchers suggested the 50% reduction in the initial stiffness of the sample as the point where fatigue failure occurs (Kanaan, Ozer & Al-Qadi, 2014; Arega, Bhasin & de Kesel, 2013). Rowe (1993) and Rowe and Boldin (2000) suggested that the fatigue failure occurs when the dissipated energy per loading cycle changes. According to Reese (1997), a good indication for the fatigue failure criterion is when the phase angle versus time curve shows a peak, followed by a rapid decrease of phase angle. Another approach to characterize the fatigue life of asphalt mixtures is based on the viscoelastic continuum damage (VECD) theory, and a 50% reduction of the pseudostiffness, C, has been considered as a reasonable fatigue failure criterion (Park, Kim & Schapery, 1996; Lee, 1996; Lee & Kim, 1998a; Lee, Daniel & Kim, 2000; Daniel & Kim, 2002; Palvadi, 2011; Palvadi, Bhasin & Little, 2012).

In the continuum damage mechanics, the microstructural changes of the material are the basis of the theory. A damaged body is represented as a homogeneous continuum and the microstructural changes are quantified by internal state variables, (*S*), that reflect the state of damage of the material (Schapery, 1984). The theory was first developed to elastic materials and later extended to account for damage of viscoelastic materials, by elastic-viscoelastic correspondence principles, which transform physical variables in pseudo variables, eliminating time-dependence effects (Schapery, 1990). A mechanistic fatigue prediction model based on the VECD was developed by Lee et al. (2000) for the controlled strain mode of loading, and it was later adapted by Daniel and Kim (2002) for various cyclic strain amplitudes and frequencies and different monotonic rates. The results of the studies indicate that a single characteristic curve *C vs. S* describes the changes of the material integrity as damage grows, independent of the loading conditions.

Authors like Palvadi (2011), Palvadi et al. (2012), Karki, Li and Bhasin (2015b) and Karki, Bhasin and Underwood (2016) developed studies based on the VECD theory to investigate the fatigue life of asphalt mixtures and observed the similarity of the characteristic curves *(C vs. S)* for samples of a given FAM mixture, for both stress and strain controlled modes at different amplitudes. Palvadi (2011) and Palvadi et al. (2012) also proposed a test protocol to evaluate the effects of healing in the performance of asphalt mixtures. In order to investigate the effects of healing, four rest periods (5, 10, 20 and 40 minutes) were introduced during the tests when the sample reaches a certain level of stiffness (20, 30 and 40 percent of pseudo stiffness). In this method, one sample was needed for each stiffness level. It was demonstrated that healing is a characteristic material property and a unique healing characteristic function can be obtained for each material. The results showed that healing measured at higher damage levels was around 10 to 20 percent lower than the healing measured at lower damage levels, indicating that a distribution of micro cracks in a body provides a better condition to heal when compared to a distribution of macro cracks.

The characterization of healing procedure was improved by Karki et al. (2015b) and Karki et al. (2016) to a test method that integrates the damage and healing tests and utilize a single FAM sample. The single-specimen protocol provided healing characteristics similar to the ones obtained from the previous multi-specimen protocol, suggesting that the healing behavior at higher levels of damage is not affected by a history of healing at

lower levels of damage. The authors became the first to utilize the simplified viscoelastic continuum damage (S-VECD) theory to characterize damage on FAM mixtures.

2.2.4. FAM containing RAP mixtures

A traditional protocol to evaluate the performance of reclaimed asphalt pavement (RAP) and recycled asphalt shingles (RAS) consists of rheological testing of the binder extracted and recovered from the mixture (Peterson et al., 2000; Sondag, Chadbourn & Drescher, 2002). However, some issues are related to the extraction method, like the alteration of the rheological properties of the extracted binder due to chemical solvents (Ma et al., 2011) or the increase of the binder stiffness after extraction (Burr et al., 1991). In order to overcome these problems, an alternative to investigate the mechanical characteristics of RAP without binder extraction is the employment of the DMA technique to characterize FAM mixtures.

He et al. (2016) developed a procedure for preparing and testing FAM samples. The method is comprised of the following steps: (i) prepare a full-graded asphalt mixture at optimum binder content with virgin material according to AASHTO R 35; (ii) short-term age the loose asphalt mix in accordance with AASHTO R 35; (iii) sieve the loose asphalt mix using sieve 2.36 mm (#8); (iv) determine the binder content of the fine mixture either by extraction test (AASHTO T 164) or by ignition oven test (AASHTO T 308); v) sieve the RAP/RAS material at sieve 2.36 mm (#8); (vi) determine the binder content and gradation of the fine RAP/RAS particles; (vii) determine the material quantities for the RAP/RAS mixtures (virgin binder content, virgin aggregates and RAP/RAS quantities); viii) prepare the RAP/RAS mixtures; (ix) short-term age the loose RAP/RAS mix according to AASHTO R 35; (x) determine the theoretical maximum specific gravity of the FAM mixture (AASHTO T 209); (xi) compacted the FAM mixture in a Superpave gyratory compactor (AASHTO T 312) to fabricate the samples of 50 mm in height and 150 mm in diameter; (xii) long-term age the specimen, if required for the testing; xiii) extract the 12.5 mm cylindrical FAM samples; (xiv) determine the air voids content; (xv) store the samples.

Nabizadeh (2015) studied the effect of different types of rejuvenating agents and one warm mix asphalt (WMA) additive on mixtures compounded with 65 percent of RAP. A phenomenological regression model and the mechanist fatigue life prediction model based on the VECD theory were utilized to predict the fatigue response of the materials. The results from both phenomenological and mechanistic approaches were compared

with measured fatigue lives, and the comparison presented a good correlation. Furthermore, semi-circular bending tests were performed to compare the results with the ones from the time sweep tests using FAM samples in order to explore a linkage between the two scales. The linkage of AC mixture and FAM was investigated by observing the material response to permanent deformation, fatigue cracking and stiffness. The correlations between the results from the asphalt mixture and its correspondent FAM demonstrate that the FAM phase can provide reasonable information to predict the behavior of the full mixture.

Zhu et al. (2017) evaluated the properties of FAM containing RAS by utilizing the conventional time sweep test and a proposed strain sweep test. The time sweep tests were performed in the controlled-strain mode of loading at 10 Hz and 20°C. The strain sweep tests were conducted also at 10 Hz and 20°C, but the loading strain was increased from 0.002 to 0.006 percent. The comparison of the data indicated that the strain sweep test is more efficient than the time sweep test, once the ranking of the asphalt fatigue life of the mixtures was found to be the same for the conventional time sweep tests and the proposed strain sweep tests, but the required time per test is lower for the strain sweep tests.

2.2.5. Rheological properties

The changes of the rheological properties of the FAM have been investigated by some researchers in an attempt to better understand the effect of the binder content and the air voids on the mixture performance (Underwood & Kim, 2011; Underwood & Kim, 2013; Izadi, 2012; Nabizadeh, 2015; Zhu et al., 2017). Underwood and Kim (2011) and Underwood and Kim (2013) investigated the sensitivity of the dynamic shear modulus, $|G^*|$, of changes in material composition by performing tests on different material scales (binder to full mixture). It was found that the FAM presents sensitivity to volumetric composition similar to that observed for full asphalt mixtures, while the mastic did not present sensitivity of changes in the volume fraction of the filler, up to a given filler fraction (Underwood & Kim, 2011).

The volumetric composition of FAM materials affects the LVE and tensile properties of the material (Underwood & Kim, 2011; Underwood & Kim, 2013). The fatigue cracking characteristics of the FAM specimens were strongly influenced by the binder content (Izadi, 2012). Underwood & Kim (2013) investigated for the changes of the dynamic shear modulus, |G*|, and tensile properties (strength and strain at failure) of FAMs by varying

the asphalt and air void content. The findings showed that for an increase of one percent in the asphalt content it is observed: (i) a 20– 35% decrease in $|G^*|$; (ii) a 4–6% decrease in strength; and iii) a 25– 40% increase in strain tolerance (Underwood & Kim, 2013). For an increase of one percent in the air voids content, it is observed that: (i) the $|G^*|$ value decreases 5–8% for the mixture with a nominal maximum size of aggregate (NMSA) of 9.5 mm and 10–12% for the mixture with NMSA of 19.0 mm; (ii) the strength decreases 10%; and iii) the strain tolerance increases 0–5% (Underwood & Kim, 2013).

Izadi (2012) evaluated the internal microstructure of different FAM mixtures in order to investigate the influence of gradation and binder content on mixture performance. It was observed that the fatigue cracking characteristic of the FAMs were more related to the binder content than to the fine aggregate fraction. The healing characteristics were not significantly different for three FAMs: the control mixture, the mixture containing a percentage of fines higher than the control mixture value, and the mixture with a percentage of binder higher than the control mixture value, indicating that the healing rate is mostly influenced by the type of binder and not significantly influenced by the gradation or binder content, for a same volumetric distribution of the mastic.

Absorption, creep modulus and *m*-value were the properties analyzed by Gong et al. (2016) in order to explore the effect of freeze-thaw cycles on the low-temperature properties of FAM mixtures with different gradation, asphalt content, gyration level and temperature. The bending beam rheometer (BBR) was utilized to perform tests on FAM beams (127 × 12.7 × 6.35 mm). The findings indicated that the variables evaluated (gradation of fine aggregates, optimal asphalt content and FAM compaction level) can be determined by combining the creep stiffness and the *m*-value with the impact of freeze–thaw cycle. The BBR test was considered as an effective tool for investigation of low-temperatures properties, leading to a better control of the cracking potential of the FAM within the asphalt pavement in cold climates.

2.3. Theory of viscoelastic continuum damage – VECD

Fatigue behavior of viscoelastic materials is a complex phenomenon of difficult characterization due to the amount of involved variables. Amplitude and frequency of applied loads, loading history, material properties, temperature variation and healing are some of the factors that influence the fatigue life of a viscoelastic material. The fatigue

process initiates as micro-cracks, that are followed by crack propagation and formation of macro-cracks, until complete failure. One approach to model this behavior is the so called viscoelastic continuum damage theory (VECD), in which it is assumed that a damaged body with a given stiffness is an undamaged body of reduced stiffness, and the cracks are distributed uniformly within the body.

Schapery (1984, 1990) developed the work potential theory, which is based on the methods of thermodynamics of irreversible process, to describe the mechanical behavior of elastic materials with growing damage. The theory characterizes the material using macroscale observations, quantifying the changes of the material microstructure by the use of internal state variables. The elastic model was then extended to describe the mechanical behavior of viscoelastic media, through the use of elastic-viscoelastic correspondence principles, transforming physical variables in pseudo variables, eliminating time-dependence of the material.

Park et al. (1996), Lee (1996) and Lee and Kim (1998a) utilized Shapery's theory to develop a constitutive model that describes the damage evolution process of asphalt concrete under varying materials, loading, and environmental conditions. This constitutive model was simplified by Lee et al. (2000) to a practical fatigue prediction model for asphalt concrete specimens under uniaxial cyclic loading, that was adapted by Kim and Little (2005) for asphalt concrete samples under torsional shear cyclic loading mode without rest periods. The model has been considered capable to provide a reasonable representation of fatigue life of asphalt mixtures.

2.3.1. The work potential theory

According to the thermodynamic theory, a generalized notation to the behavior of an elastic body with changing structure is expressed by means of relationships between generalized forces, Q_j, and independent generalized displacements, q_j, as showed in Equation 2.3, where δq_j is the virtual displacement and $\delta W'$ is the virtual work. For different physical situations, q_j can represent strain, displacement or rotation, and Q_j can be stress, force or moment.

$$\delta W' = Q_j \delta q_j \tag{2.3}$$

For any process of interest, the existence of a *strain energy* function, $W = W(q_j, S_m)$, was assumed, where S_m (m = 1, 2, 3, M) refers to the increase in the value of the internal state variable, S. The relationship between the work done on a body, during the process in which damage occurs, and the strain energy function is expressed by Equation 2.4, where f_m is the *thermodynamic force* (Equation 2.5).

$$dW = \frac{\partial W}{\partial q_j} dq_j + \frac{\partial W}{\partial S_m} dS_m = Q_j dq_j - f_m dS_m \tag{2.4}$$

$$f_m = -\frac{\partial W}{\partial S_m} \tag{2.5}$$

Integrating Equation 2.4 during a time interval t_1–t_2, and assuming that a state function $W_S = W_S(S_m)$ exists such that the *thermodynamic force*, f_m, is given by Equation 2.6, the work to vary the internal state of the material, from a state 1 to a state 2, is expressed by Equation 2.7. The variable $\dot{S}_m$ is the damage evolution rate.

$$f_m = \frac{\partial W_S}{\partial S_m} \quad \text{when} \quad \dot{S}_m \neq 0 \tag{2.6}$$

$$\Delta W_T = W^{(2)} - W^{(1)} + \int_1^2 f_m dS_m \tag{2.7}$$

Solving the integral in Equation 2.7, the work is given by Equation 2.8. Assuming the time $t_1=0$, the total work from $t=0$ to the current time t_2 is given as follows in Equation 2.9.

$$\Delta W_T = W^{(2)} - W^{(1)} + {W_S}^{(2)} - {W_S}^{(1)} \tag{2.8}$$

$$W_T = W + W_S \tag{2.9}$$

The total work input to the elastic body by the forces Q_j is given by Equation 2.10, where j = 1, 2, ..., J, and W_T is the total work done on the body considering that S_m is variable in time.

$$W_T = \int Q_j \, dq_j \tag{2.10}$$

The elements of Schapery's theory, expressed in terms of stress-strain relationships, may be represented as follows in Equation 2.11 and Equation 2.12, where σ_{ij} is the stress tensor, ε_{ij} is the strain tensor, and S_m is the internal state variable.

$$W = W(\varepsilon_{ij}, S_m) \tag{2.11}$$

$$W_T = \int \sigma_{ij} \, d\varepsilon_{ij} \tag{2.12}$$

By considering Equations 2.5 and 2.6, the damage evolution law for elastic media is represented by Equation 2.13, where $W_S = W_S(S_m)$ is the dissipated energy due to damage growth. The right-hand side of the law represents the required force for damage growth, while the left-hand side of the damage evolution law represents the available thermodynamic force to produce damage growth.

$$-\frac{\partial W}{\partial S_m} = \frac{\partial W_S}{\partial S_m} \tag{2.13}$$

2.3.2. Elastic-viscoelastic correspondence principle

As demonstrated by Schapery (1984), using correspondence principles and a new damage evolution law, the elastic continuum damage theory can be extended to describe damage evolution in viscoelastic materials. For elastic materials, the stress-strain relationship is expressed by Hooke's Law (Equation 2.14), where E is the elasticity modulus. For viscoelastic materials, the time dependency has to be considered, and the stress is expressed by a convolution integral (Equation 2.15), where τ is an increment in the value of time, t, and $G(t)$ is the relaxation modulus of the material.

$$\sigma = E\varepsilon \tag{2.14}$$

$$\sigma = \int_0^t G(t-\tau)\frac{d\varepsilon}{d\tau}d\tau \tag{2.15}$$

The artifice proposed to eliminate the time dependent effects was to transform the stress-strain relationships of viscoelastic media into a pseudo domain that corresponds to a hypothetical elastic material, suggesting that the constitutive equation for viscoelastic media (Equation 2.16) is identical to that for elastic media (Equation 2.14). However, the stress and the strain are not necessarily physical quantities, but pseudo variables: pseudostress (σ^R) and pseudostrain (ε^R). According to the correspondence principles, σ^R=σ, where σ is the time dependent stress applied to a viscoelastic material, and the pseudostrain is given by the Equation 2.17, where ε is the time-dependent strain into a viscoelastic material, G*(t)* is the linear viscoelastic relaxation modulus of the material and E^R is the modulus of hypothetical elastic material (Schapery, 1984, 1990).

$$\sigma = E_R\varepsilon^R \tag{2.16}$$

$$\varepsilon^R = \frac{1}{E_R}\int_0^t G(t-\tau)\frac{d\varepsilon}{d\tau}d\tau \tag{2.17}$$

The same equations for the elastic materials are used to solve the viscoelastic cases by considering the elastic-viscoelastic correspondence principles. The pseudo strain energy density function is expressed by Equation 2.18, where the physical strain, ε, is substituted by the pseudo strain, ε^R. The stress-pseudo strain relationship is given by Equation 2.19, where W^R is the pseudo strain energy density (Schapery, 1990).

$$W^R = W^R(\varepsilon^R, S_m) \tag{2.18}$$

$$\sigma = \frac{\partial W^R}{\partial \varepsilon^R} \tag{2.19}$$

For most viscoelastic media, the available force for damage growth and the resistance against the growth are rate-dependent. So, the damage evolution law for elastic materials (Equation 2.11) can not just be transformed into a damage evolution law for viscoelastic materials, by the use of correspondence principles, without further modification. The new damage evolution law for viscoelastic materials is given by Equation 2.20, where $\dot{S}_m$ is the damage evolution rate and α_m is a material-dependent constant (Park & Schapery, 1996).

$$\dot{S}_m = \left(-\frac{\partial W^R}{\partial S_m} \right)^{\alpha_m} \tag{2.20}$$

2.3.3. Viscoelastic continuum damage model

Park et al. (1996) proposed a uniaxial viscoelastic damage model to characterize the behavior of asphalt concrete with time-dependent damage growth, subjected to different strain rates under uniaxial stress. The pseudo strain energy density function is presented in Equation 2.21, where C is a function of the damage parameter S.

$$W^R = \frac{1}{2} C(S)(\varepsilon^R)^2 \tag{2.21}$$

Then, for linear viscoelastic behavior and fixed damage, the stress, σ, can be written as follows in Equation 2.22 and the damage evolution law (Equation 2.20) is specified to the single equation for S, presented in Equation 2.23.

$$\sigma \equiv \frac{\partial W^R}{\partial \varepsilon^R} = C(S)\varepsilon^R \tag{2.22}$$

$$\dot{S} = \left(-\frac{\partial W^R}{\partial S} \right)^{\alpha} \tag{2.23}$$

By substituting Equation 2.21 into Equation 2.23, Park et al. (1996) obtained a relationship between S and a new damage parameter S^*, given by Equation 2.24, where S^* is a function of strain history (Equation 2.25). The variable k is a free constant

considered in their study, such that the maximum values of *S* and *S** are numerically equal. Thus, Equation 2.22 was replaced by Equation 2.26.

$$S^* = k\left[\int_0^S \frac{dS}{(-0.5dC/dS)^\alpha}\right]^{1/(2\alpha)} \tag{2.24}$$

$$S^* \equiv k\left[\int_0^t |\varepsilon^R|^{2\alpha} dt\right]^{1/(2\alpha)} \tag{2.25}$$

$$\sigma = C(S^*)\varepsilon^R \tag{2.26}$$

For a given material, the function *C(S)* and the constant α have to be determined. The function *C(S)* may be obtained from experimental stress-pseudo strain curves and the damage evolution law. However, the evolution law itself requires prior knowledge of *C(S)*, making this procedure inefficient to find *C* and its dependence on *S*. The method proposed by Park et al. (1996) to overcome this problem was to determine a transformed damage variable, $\hat{S}$ (Equation 2.27), that may be obtained from the numerical scheme presented in Equation 2.28, where ε_i^R *(i = 1, 2, 3, N)* denotes pseudo strain levels, $C' \equiv dC/d\hat{S}$ and $\hat{S}(0) = 0$. This method allows to obtain the function $C(\hat{S})$ from experimental stress-pseudo strain curves and then the function *C(S)* can be obtained from Equation 2.27, by replacing the transformed damage variable $\hat{S}$ for the original damage variable, *S*.

$$\hat{S} \equiv \frac{1}{(1+1/\alpha)} S^{(1+1/\alpha)} \tag{2.27}$$

$$\hat{S}(\varepsilon_{i+1}^R) = \hat{S}(\varepsilon_i^R) + \frac{C(\varepsilon_{i+1}^R) - C(\varepsilon_i^R)}{\Delta\hat{S}} \tag{2.28}$$

The constant α is related to the material's creep or relaxation properties. According to Schapery (1975), depending on the characteristics of the failure zone on a crack tip, $\alpha = (1 + 1/m)$ if the material's fracture energy and failure stress are constant, or $\alpha = 1/m$ if the fracture process zone size and the material's fracture energy are constant, where $m = logD(t)/log(t)$ or $m = -logE(t)/log(t)$. Park et al. (1996) utilized the relationship $\alpha = (1 +$

1/m), assuming that the damage in the sample is closely related to the growth of micro-cracks. The constant α was obtained by a method of successive approximations until the model better fits with the experimental observations.

Lee (1996) and Lee and Kim (1998a) also proposed a solution to the damage evolution law by studying the mechanical behavior of asphalt concrete. They conducted uniaxial tensile cyclic loading tests, with different loading amplitudes, under controlled-strain and controlled-stress modes of loading. First, they observed a decrease in the slope of each $\sigma - \varepsilon^R$ cycle as the number of loading increases (Figure 2.3), and they found necessary to define the parameter called secant pseudo stiffness, S^R, to represent this change in the slope of stress-pseudo strain loops (Equation 2.29), where ε_m^R is the peak pseudo strain in each stress-pseudo strain cycle and σ_m is the stress that corresponds to ε_m^R.

Figure 2.2 – Stress-Pseudo Strain Behavior and Pseudostiffness Changes In: (a) Controlled-Strain Mode; (b) Controlled-Stress Mode

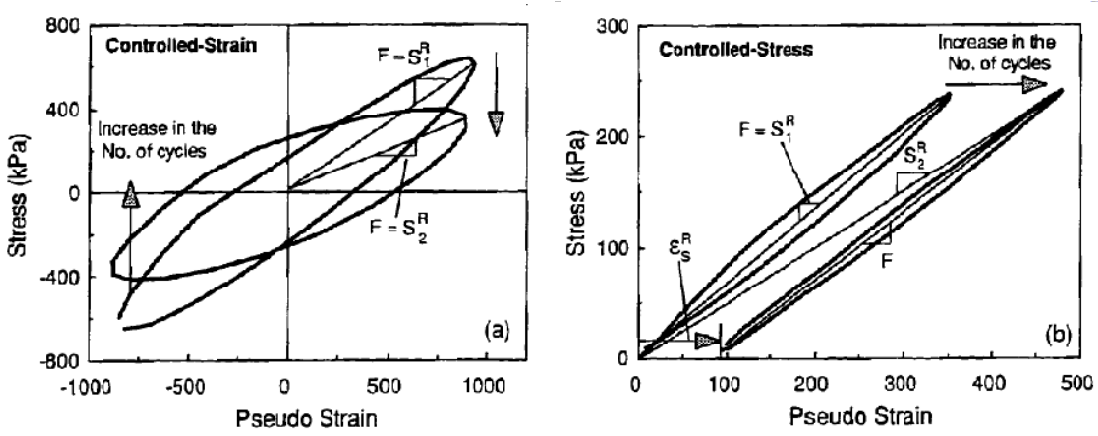

Source: LEE (1996)

$$S^R = \frac{\sigma_m}{\varepsilon_m^R} \tag{2.29}$$

To minimize the sample-to-sample variabilities, the pseudo stiffness was divided by the initial pseudo stiffness, *I*, resulting in the normalized pseudo stiffness, *C*, that is represented by Equation 2.30.

$$C = \frac{S^R}{I} \tag{2.30}$$

By considering Equation 2.29 and Equation 2.30, the constitutive equation for viscoelastic materials with growing damage is expressed by Equation 2.31. The normalized pseudo stiffness, $C(S_m)$, is a function of the internal state variables, S_m, and represents the microstructural changes of the body.

$$\sigma = IC(S_m)\varepsilon_m^R \tag{2.31}$$

The researchers assumed an internal state variable, S_1, to determine the change in pseudo stiffness due to growing damage and the work function (W^R) for viscoelastic materials is given by Equation 2.32, where $C_1(S_1)$ is a function that represents S^R.

$$W^R = \frac{I}{2} C_1(S_1)(\varepsilon_m^R)^2 \tag{2.32}$$

Despite the material function C_1 can be found by the use of experimental data and the damage evolution law (Equation 2.20), this procedure is not convenient to find C_1 and its dependence on S_1, because the evolution law requires prior knowledge of $C_1(S_1)$. The method presented to overcome this problem was to utilize a chain rule (Equation 2.33) to eliminate the S on the right-hand of the evolution law, and, through mathematical substitutions (Equation 2.34), the numerical approximation given by Equation 2.35 was obtained. The function $C_1(S_1)$ may be obtained by cross plotting the C values, obtained from Equation 2.31, against the S values, obtained from Equation 2.35, and by performing a regression on the data (Equation 2.36), where C_{10}, C_{11}, and C_{12} are the regression coefficients.

$$\frac{dC}{dS} = \frac{dC}{dt}\frac{dt}{dS} \tag{2.33}$$

$$\frac{dS}{dt} = \left[-\frac{I}{2}\frac{dC}{dS}(\varepsilon^R)^2\right]^{\alpha/(1+\alpha)} \tag{2.34}$$

$$S \equiv \sum_{i=1}^{N} \left[\frac{I}{2}(\varepsilon^R)^2(C_{i-1} - C_i)\right]^{\alpha/(1+\alpha)} (t_i - t_{i-1})^{1/(1+\alpha)} \quad (2.35)$$

$$C_1(S_1) = C_{10} - C_{11}(S_1)^{C_{12}} \quad (2.36)$$

For the material parameter α, Lee and Kim (1998b) observed that $\alpha = (1 + 1/m)$ is adequate for controlled strain mode of loading, while $\alpha = 1/m$ is a better assumption for controlled stress mode of loading. These observations suggest that the material's fracture energy and failure stress are constant under controlled strain mode, whereas the material's fracture energy and the fracture process zone size are constant controlled stress mode.

2.3.4. Mechanistic fatigue life prediction model

Fatigue cracking is a common and very complex mode of failure in flexible pavements. The repetitive traffic loads and the variation of the binder properties along time cause a reduction in the structural capacity of the asphalt layer. On the field, this phenomenon can be observed by cracking in the surface layer, however, in the laboratory, fatigue failure characterization is quite difficult and often rather arbitrary due to the amount of involved variables and the difficulty in reproducing in the laboratory the conditions observed in the field. There are two main approaches to characterize the material fatigue behavior in the laboratory: the phenomenological approach and the mechanistic. The phenomenological models relate the stress or strain on the sample with the number of cycles to failure. This approach is relatively simple. However, it does not account for the complexity of the fatigue phenomenon. On the other hand, mechanistic approach accounts for how damage evolves throughout the fatigue life at different load and environmental conditions, leading to a better estimation of the fatigue behavior of asphalt concrete mixtures.

A mechanistic fatigue life prediction model, which is derived from the original VECD model, is described in Equations 2.37 to 2.39. The model estimate the number of cycles required to degrade the material, N_f, to a certain pseudo-stiffness level, C, or to reach a certain amount of damage, S_f, at an arbitrary frequency, f, and controlled pseudo strain

amplitude, ε^R. The parameters C_1 and C_2 are obtained from Equation 2.36 (Lee et al., 2000; Kim & Little, 2005).

$$N_f \equiv A(\varepsilon^R)^{-B} \tag{2.37}$$

$$A = f\left\{\frac{1}{2}C_1C_2\right\}^{\alpha}\{1+\alpha(1-C_2)\}^{-1}S_f^{[1+\alpha(1-C_2)]} \tag{2.38}$$

$$B = 2\alpha \tag{2.39}$$

Kim and Little (2005) performed torsional shear cyclic tests, on different asphalt mixtures, and compared the measured fatigue lives of the materials tested with the predicted values calculated from the prediction fatigue model (Equations 2.37 to 2.39). They concluded that the model parameters might provide a reasonable representation of the fatigue response.

2.4. Linear viscoelasticity

The behavior of elastic materials is not time dependent, i. e., the response to a constant load is a constant deformation and a complete recover when the load is removed. The stiffness of these materials is denoted by the relationship between stress and strain, the Young's Modulus, E. On the other hand, viscous materials present a flow resistance or a resistance to be deformed and the whole energy is dissipated. Stress is dependent on the rate of strain and this relationship is denoted as viscosity, η. Viscoelastic materials combine the elastic and viscous behaviors, and its properties depend on temperature and rate of loading. At low temperatures or at high rates of loading, viscoelastic materials have a behavior that tends more to elastic, whereas, at high temperatures or long times of loading, their behavior tends more to viscous.

Two types of testing are performed on viscoelastic materials: creep and relaxation. In a creep test, the accumulation of strain is observed as a constant load is applied to the material over time. The creep compliance, J, is obtained by dividing the strain by the stress. In a relaxation test, the material suffers a deformation that is maintained constant by relaxing the stress. The stress function, $G(t)$, to keep the strain constant, is referred to

as relaxation modulus. In the dynamic test the stress or strain is varied cyclically along time and the response at different frequencies is measured (Vincent, 2012).

Oscillatory tests can be performed to characterize the linear viscoelastic response of the asphalt mixtures. The frequency sweep can be carried out in order to obtain *G** values at different frequencies. A Prone series model, $G(t)=G_0+G_1t^{-m}$, is adjusted to the obtained data and a Laplace transform is applied to transform data from the frequency domain, *G* = f(w)*, to the time domain, *G = f(t)*. The model is adjusted to data in order to obtain the material parameter *m*, where *m = - logG(t)/log(t),*. G_0 and G_1 are materials constants and *G(t)* is the relaxation modulus.

3. MATERIALS AND METHOD

This chapter is divided in three sections and describes in detail: i) the materials and procedures utilized to fabricate the samples of FAM mixtures; ii) the test procedure to measure the linear viscoelastic properties and the damage properties of the FAM mixtures; and iii) the method utilized to analyze the data obtained from the rheological tests.

3.1. Mineral aggregates

3.1.1. Virgin mineral aggregates

One source of new mineral aggregate was used in the production of the FAM mixtures: a basalt rock obtained from Bandeirantes Quarry, located in the City of São Carlos, State of São Paulo. The characterization of the new mineral aggregate was carried out according to the standard procedures from DNIT (Departamento Nacional de Infraestrutura de Transportes – National Department of Transportation Infrastructure) and ASTM (American Society for Testing and Materials): i) gradation (DNER-ME 083/98); ii) absorption and specific gravity of the fine aggregate (ASTM C128-15) and specific gravity of filler (DNER-ME 084/95). Table 3.1 presents the results obtained from the characterization of the mineral aggregate.

Table 3.1. Characteristics of the mineral aggregate

Properties	Results
Absorption	0.6 %
Adhesion	Unsatisfactory
Specific gravity	2.957

3.1.2. Reclaimed asphalt pavements (RAP)

One source of RAP of an unidentified origin was used. The supplier informed that the mineral aggregate used in the construction of the asphalt layer is basalt and that the asphalt binder is PG 88-XX. The results of the test performed in order to classify the performance grade of the RAP binder are presented in Table 3.2 and Table 3.3.

Table 3.2. $G^*/\sin\delta$ values for the RAP binder

Temperature (°C)	Sample 1	Sample 2	Variability
52	233.10	250.12	-7.0
58	104.96	107.40	-2.3
64	47.59	47.37	0.5
70	20.56	21.15	-2.9
76	9.48	9.67	-1.9
82	4.46	4.54	-1.7
88	2.18	2.23	-2.0

Table 3.3. Performance grade of the RAP binder

Sample 1	Sample 2	Final
87,96	88,07	88

3.1.3. Aggregate gradation

For this study, the material passing sieve #10 was selected to produce the FAM samples. The FAM gradation distribution was established by adopting the DNIT specification (DNIT 031/2004-ES). A dense curve located at the center of the range C of the specification was chosen, because it is a typical dense mixture used for the road construction in Brazil. The portion of aggregates passing the sieves below sieve #10 was determined by Equation 3.1, in which #ii refers to the sieves below sieve #10. Table 3.4 and Figure 3.1 present the FAM and HMA gradation distribution.

$$\frac{\text{mass of aggregate passing sieve \#ii in full mixture}}{\text{mass of aggregate passing sieve \#10 in full mixture}} \times 100 \qquad (3.1)$$

Table 3.4. Mineral aggregate gradation for the FAM and HMA mixtures

Sieve number	Opening size (mm)	FAM	HMA
		Percentage by mass passing (%)	
3/4"	19.1	–	100
1/2"	12.7	–	90
3/8"	9.52	–	80
nº 4	4.76	–	58
nº 10	2.00	100	36
nº 40	0.42	47	17
nº 80	0.18	28	10
nº 200	0.075	17	6

Figure 3.1. Aggregate gradation for the FAM and HMA mixtures

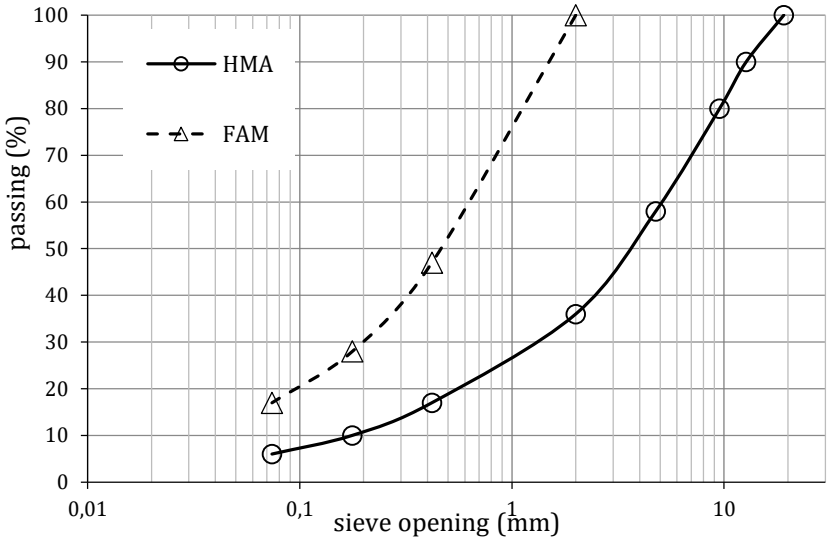

3.2. Asphalt binders

Two asphalt binders were used in order to correct the asphalt content of the RAP mixture and to produce the FAM mixtures: an asphalt binder of low consistency (PG 58-XX provided by Betunel Tecnologia em Asfaltos, and one of intermediate consistency (PG 64-XX), provided by Petrobras (Replan Refinery). Table 3.5 presents the PG classification and the respective percentage of weight loss measured for the two asphalt binders, and Table 3.6 presents the values of the multiple stress creep recovery test (MSCR).

Table 3.5. PG classification and weight loss

asphalt binder	weight loss (%)
PG 58-XX	0,0832
PG 64-XX	0,1094

Table 3.6. Non-recoverable creep compliance (J_{nr})

Asphalt binder	J_{nr} 100 (kPa^{-1})		J_{nr} 3200 (kPa^{-1})	
	64°C	70°C	64°C	70°C
PG 58-XX	6,85	15,20	7,40	16,45
PG 64-XX	6,88	15,77	7,88	17,74

The mixing and compaction temperatures for the two asphalt binders were defined based on viscosity curves obtained after performing tests in the Brookfield viscometer model DVII–PRO. The tests were performed with spindle n°21 and followed the

procedures described in the standard ASTM D 4402M-15. Table 3.7 presents the parameters used during the tests, Table 3.8 presents the rotational viscosities, and Table 3.9 presents the mixing and compaction temperatures for the two asphalt binders used in the preparation of the studied FAM samples.

Table 3.7. Parameter used in the viscosity test

Temperature (ºC)	Rotation (rpm)	Shear rate (1/s)
135	20	19
143	40	37
150	60	56
163	80	74
177	100	93

Table 3.8. Rotational viscosity of the virgin binders

Temperature (°C)	PG 58	PG 64
135	0.57	0.36
143	0.39	0.24
150	0.29	0.18
163	0.18	0.11
177	0.11	0.07

Table 3.9. Mixing and compaction temperatures used in the preparation of the FAMs

Asphalt binder	Mixing (°C)	Compaction (°C)
PG 64	152	140
PG 58	166	152

3.3. Rejuvenating agents

Rejuvenating agents can be added to the mixture, once they act to restore the performance-related properties of the RAP asphalt binder (Carpenter and Wolosick, 1980). The colloidal structure and the chemical components of the aged binder are restored by means of a diffusion process, leading to a reduced viscosity and stiffness, and an increased ductility (Terrel & Epps, 1989; Shen et al., 2005; Brownidge, 2010). When the rejuvenator is selected adequately, the properties of HMA mixtures using RAP are generally satisfactory (Little et al., 1981; Epps et al., 1980). Studies reported the positive effect of the use of rejuvenators, especially on the resistance of the HMA cracking

formation (Shen et al., 2007a,b; Asli et al., 2012; Silva et al., 2012; Hajj et al., 2013; Hill et al., 2013; Mogawer et al., 2013; Zaumanis et al., 2013; Im et al., 2014, Yu et al., 2014; Zaumanis et al., 2014b).

Some studies verified that a shale oil distillate fraction, when used as a recycling agent for aged asphalt, provided results comparable to those with a petroleum-derived commercial recycling agent (Plancher & Peterson, 1982). In this study, different proportions (50% and 100%) of shale oil residue (AR-5) were added to the mixtures in order to evaluate its effect on the fatigue performance. The shale oil residue was first added to the RAP, in order to promote its diffusion into the RAP binder.

3.4. FAM mixtures

3.4.1. FAM design method and preparation of the mixtures

The RAP binder content was defined by extraction and recovery (AASHTO T 164) of the aged binder from the fine portion of RAP (particles lower than 2.00 mm). The binder content was compared to the binder content estimated by means of the specific surface method (Arrambide & Duriez, 1959) to cover all fine aggregates contained in the FAM. The difference between the RAP binder content and the required binder content calculated by means of the specific surface was compensated by adding a complementary proportion of virgin asphalt binder. The RAP binder content was found to be equal to 7.1% and an extra amount of virgin binder was added to all FAMs in order to reach the required binder content of 8%, except for FAM 1, which was prepared with 100 percent of RAP.

Table 3.10 presents detailed information about the composition of the FAMs and also the calculation for correction of the binder content. For FAM 7, i.e., prepared with 20% of RAP and 80% of new aggregates, a percentage of 6.4 of virgin binder is necessary to cover the 80% of new aggregates, by considering an asphalt binder content of 8.0% (8.00x0.8=6.4), and 0.18 percent of virgin binder is necessary to cover the 20% of RAP, considering a residual asphalt binder of 7.1% ([8.00-7.10]x0.20=0.18). The same rationale was applied to the other FAMs: taking FAM 11 as an example, 0.18% refers to 0.09% of virgin binder and 0.09% of rejuvenating agent.

Table 3.10. Composition of the FAMs

designation	PG 58-xx (%)	PG 64-xx (%)	agent (%)	observation
FAM 1	-	-	-	100% RAP
FAM 2	-	8.00	-	new aggregate and binder
FAM 7	-	0.18+6.40=6.58	-	20/80 – 100/0[1]
FAM 8	-	0.36+4,8=5.16	-	40/60 – 100/0
FAM 9	0.18+6.40=6.58	-	-	20/80 – 100/0
FAM 10	0.36+4,8=5.16	-	-	40/60 – 100/0
FAM 11	-	0.09/6.40	0.09	20/80 – 50/50
FAM 12		0.00/6.40	0.18	20/80 – 0/100
FAM 13		0.18/4.80	0.18	40/60 – 50/50
FAM 14		0.00/4.80	0.36	40/60 – 0/100

[1]Proportions: RAP/new aggregate – virgin asphalt/agent

3.4.2. Compaction method

According to the procedure presented by Zollinger (2005), FAM specimens of 100 mm in diameter were compacted in the Superpave Gyratory Compactor (SGC), with a pressure of 600 ± 18 kPa and a gyration angle of 1.25 ± 0.02°. In order to obtain a more homogeneous air voids distribution, both edges of the specimens were trimmed off. This step is important to ensure an uniform air voids distribution over the sample, and to avoid the presence of large air voids contents at the top and bottom of SGC specimens, as reported by Masad et al. (2002).

The compaction was interrupted when the number of gyrations was equal to 100, that is the same criterion used in the compaction of HMA mixtures. It was adopted because a higher number of gyrations can result in border effect (higher air voids at the border and lower air voids at the center of the specimen) (Masad et al., 1999). The cylindrical FAM samples of 40 mm in height and 12 mm in diameter were extracted from the CGS specimens (Figure 3.2), utilizing a diamond drill coupled to a drilling machine.

3.4.3. Sample preparation

The samples edges were sanded in order to avoid the application of additional stress or strain that might be caused by possible effects of eccentricity. After the sanding process, the dust particles were removed and two metal caps were glued to the edges of the sample using an instant adhesive. Finally, the sample was attached to the axial clamps of the

equipment by the glued caps (Figure 3.3) and summited to a conditioning process (30 minutes at 25°C).

Figure 3.2. Cylindrical FAM samples extracted from CGS specimens

3.5. Tests in the DSR

The tests on the FAM samples were performed in a dynamic shear rheometer (DSR) model Discovery Hybrid Rheometer (DHR – 2) from TA Instruments (Figure 3.3). Two tests were carried out in order to obtain the linear viscoelastic (LVE) properties of the materials: an amplitude sweep, to define the LVE range for each material, and a fingerprint test, to define the damage evolution rate parameter (α) for each sample. The damage properties of the FAM mixtures, namely pseudostiffness (C) and damage accumulation (S), were mesured by performing time sweep tests under controlled stress. These test protocols and the procedure of analysis are described in detail in the next sections.

Figure 3.3. FAM samples attached to the DSR

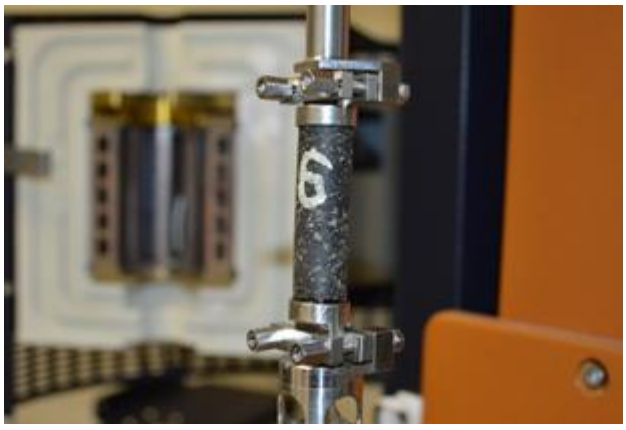

Figure 3.4. Dynamic Shear Rheometer - DSR

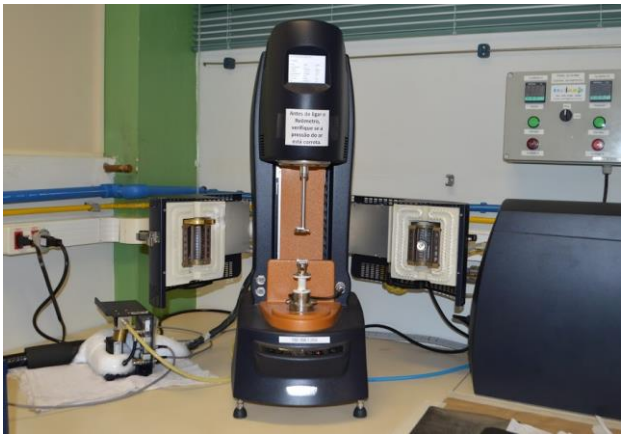

3.5.1. Linear-viscoelastic range

In order to determine the linear-viscoelastic (LVE) range of each material, an oscillatory stress sweep test was performed, with the stress varying from 5 to 450 kPa, at 25°C and 1 Hz. The linear viscoelasticity region was defined as the range of stress under which the materials present a deviation of 10% of their initial stiffness. Such stresses were obtained to perform the fingerprint tests, so that the fingerprint tests do not cause damage to the samples. An example for the FAM 9, prepared with 20% of RAP and the softer binder (PG 58-16), is presented in Figure 3.5.

Figure 3.5. Determination of the LVE range for the FAM 9

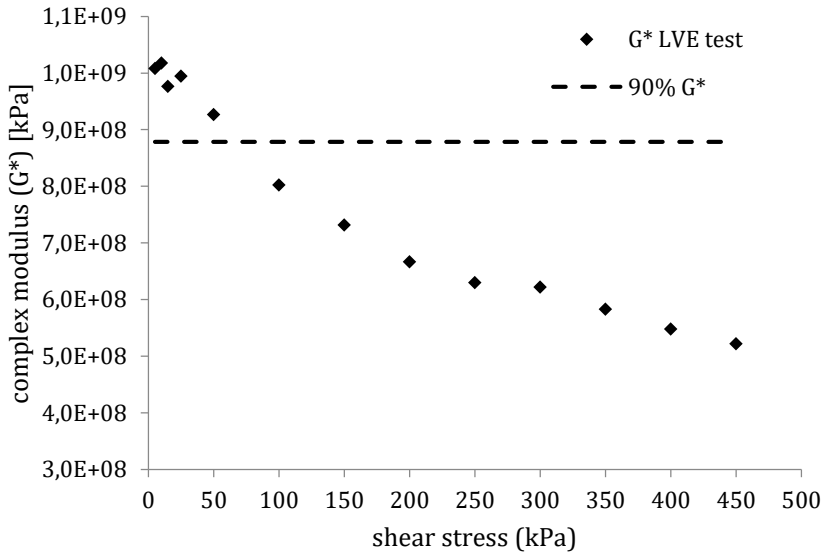

A drop of 10% of the initial G* (0,9*1,01e9=9,07e8) is achieved for a stress level of 70 kPa. It was observed that 15 kPa is a stress within the LVE range that would be

adequate to test all FAMs. One sample of each material was used for the LVE range tests, which was discarded after the test.

3.5.2. Fingerprint test – linear-viscoelastic properties

The second step was the measurement of the linear-viscoelastic properties by performing a fingerprint test. The test allows to obtain the values of G^* and δ of the materials, at different frequencies, in order to calculate the relaxation rate m of the materials. The parameter m is related to the slope of the relaxation modulus curve, which is defined by the response of the material during the loading period. A stress within the LVE range (15 kPa) was applied, in order to avoid the induction of damage to the samples, once the same sample is used in the damage tests.

The level of damage induced to the sample during the fingerprint test was minimized by taking the following steps: i) adoption of a reduced number of frequencies; ii) introduction of a rest period of 5 minutes between one frequency and another; and iii) adoption of a minimum number of loading applications at each frequency. The frequencies used in the fingerprint, in Hz, were the following: 30, 26, 22, 18, 14, 10, 6, 4, 2, 1, 0.5, 0.2, 0.1, 0.05 and 0.01 and cycles of 15 kPa were applied in each frequency.

The relaxation modulus values ($G[t]$) were predicted using the data from the frequency sweep. First, the storage modulus (G') was calculated for each frequency, according to Equation 3.2.

$$G'(\omega) = |G^*(\omega)| cos\delta(\omega) \tag{3.2}$$

A Prony series is a mathematical expression of the generalized Maxell model, which represents the behavior of a viscoelastic material. The Prony series representation of storage modulus as a function of frequency (Christensen, 1982) is presented in Equation 3.3, where G_e is the equilibrium modulus, G_i is the elastic modulus, ρ_i is the relaxation time, ω is the angular frequency and n is the number of elements of the Prony series.

$$G'(\omega) = G_e + \sum_{i=1}^{n} \frac{G_i \omega^2 \rho_i^2}{\omega^2 \rho_i^2 + 1} \tag{3.3}$$

The next step was to fit the Prony series (Equation 3.3) to the experimental data, *G'* versus ω curve, in order to find the parameters G_e, G_i and ρ_i. Figure 3.6 illustrates an example of a four-elements Prony series fitted to the G' data of a fingerprint test.

Figure 3.6. Fitting of a Prony series to G' vs ω data

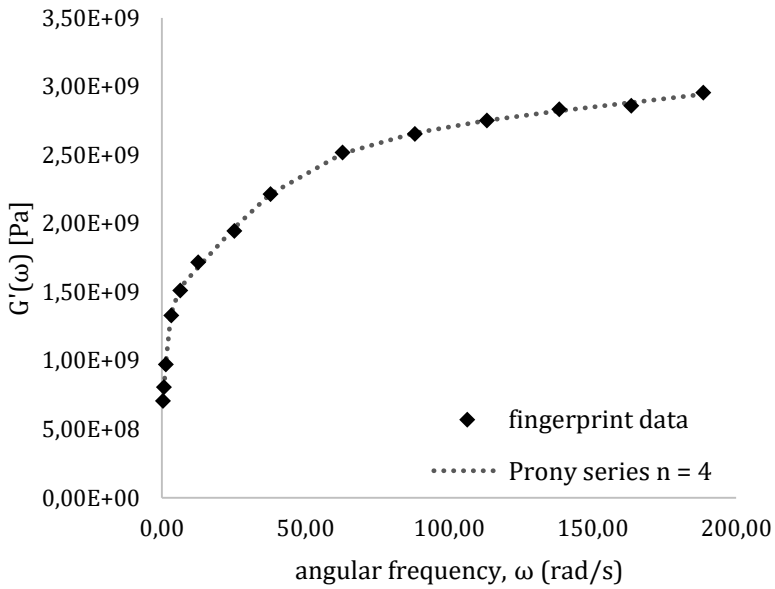

Static relaxation modulus as a function of time can be calculated by Equation 3.4. Equation 3.4 considers the same Prony series material parameters, G_e, G_i and ρ_i, which were determined from linear viscoelastic dynamic frequency sweep testing (Kim & Little, 2005). The *G(t)* values are plotted versus time, and a power law (Equation 3.43) is fitted to the *G(t) vs time* curve, logarithmically scaled, in order to find the parameter m (*m = -logG[t]/log[t]* [Schapery, 1975]). Figure 3.7 presents an example of a power law curve fitted to the relaxation modulus vs time curve.

$$G(t) = G_e + \sum_{i=1}^{n} G_i e^{-\frac{t}{\rho_i}} \tag{3.440}$$

$$G = G_0 + G_1 t^{-m} \tag{3.5}$$

Figure 3.7. Curve G(t)predicted vs time and adjust of the power law model

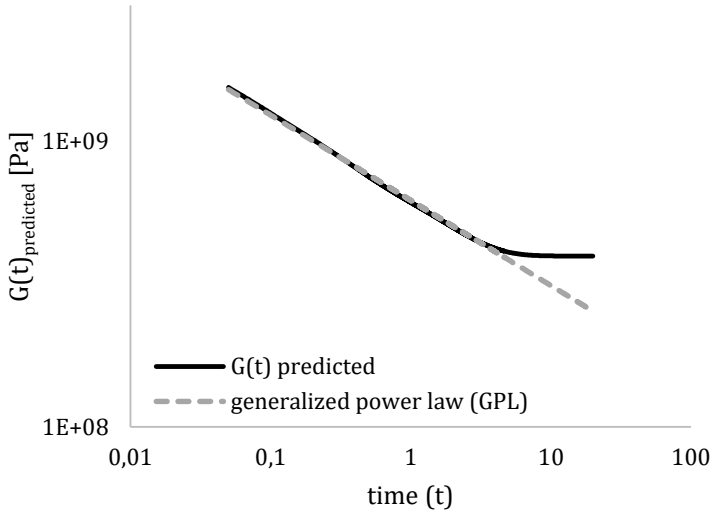

The damage evolution rate, α, can be calculated based on the *m* value obtained from Equation 3.5. According to Schapery (1990) and Park, Kim and Schapery (1996), $\alpha = (1 + 1/m)$, for materials with constant fracture energy and constant fracture stress, and $\alpha = 1/m$, for materials with constant fracture energy and fracture process zone. It has observed that $\alpha = (1 + 1/m)$ is an adequate assumption for controlled strain mode of loading, while $\alpha = 1/m$ is a better assumption for controlled stress mode of loading (Lee & Kim, 1998b; Daniel & Kim, 2002; Karki, 2014). Once the damage tests during this study were performed under controlled stress, the damage evolution rate was taken as $\alpha = 1/m$.

3.5.3. Damage tests

The damage test is a conventional time sweep test, in which a load is continuously applied to the sample until the failure of the material occurs. The tests were performed under controlled stress. The stress applied to the samples was calculated according to the following steps: i) the average of the G^* values at 1 Hz obtained from the fingerprint test, which is the complex modulus within the linear-viscoelastic region, G^*_{LVE}, was calculated; ii) from the linear-viscoelastic range test, the stress that corresponds to a $0{,}9G^*_{LVE}$ value was identified, and a stress level higher than this identified stress was selected to the damage test. This procedure was chosen because each FAM has different stiffness, and the stress level capable to produce damage on the sample is different for each FAM. Furthermore, a high stress level applied to FAMs with low stiffness could cause rupture of the sample, without producing growing damage.

The damage procedure was adapted from the procedure utilized by Karki (2014). First, the damage tests were conducted without the introduction of rest periods, once the effect of healing was not evaluated. Another adaptation of the Karki's procedure is the long duration of the tests and the high volume of data generated during the test. In order to reduce the test duration, the frequency chosen for the tests was 1 Hz, instead of 10 Hz as adopted by Karki (2014). This frequency was adopted because the lower the frequency the lower the stiffness of the material, and the lower the stiffness the lower the number of cycles to reach a certain level of damage, reducing the duration of the test.

3.6. Procedure of analysis

3.6.1. Damage analysis

Based on the VECD theory, shear stress, shear strain and complex modulus from the damage tests were transformed into their pseudo counterparts. The pseudostiffness, C_k, for each cycle of loading, k, was calculated by Equation 3.6, in which G_k^* is the complex modulus at each cycle, I is the sample-to-sample variation in the initial stiffness and $|G^*_{LVE}|$ is the complex modulus obtained from the fingerprint test at a frequency of 1 Hz. In order to plot the *C vs. S* curve with an initial value that is the same for all material, the parameter I was implemented in the pseudostiffness equation, so that all the C vs. S curves start from a C value equal to 1.

$$C_k = \frac{G_k^*}{I|G_{LVE}^*|} \tag{3.6}$$

The correction parameter I was added to the equation in order to minimize: i) the inherent variability of the material, i.e., at the same conditions but at different moments, a sample may present slightly different behavior; ii) the loading history effect that may be caused by the loading application during the fingerprint test; iii) the damage accumulated by the sample during the fingerprint test, i. e., although the fingerprint test is carried out at a low stress, within the linear-viscoelastic range, the material can suffer damage if the number of cycles is high, even under low stresses.

The next step was to rank the C values from the highest to the lowest, once that the C value can be higher at cycle k than at cycle k-*1*. This can occur due to small temperature

variations during the test, which affect the stiffness of the material, or due to the resolution of the equipment. Moreover, the calculation of the accumulate damage (*S*) values requires the ordination of the *C* values.

For a certain number of loading cycles (*N*), the accumulate damage (*S*) was calculated according to Equation 3.7, in which $S_{u,0}$ is the internal state variable at the beginning of load cycles, and Δt_k is the time interval of each cycle.

$$S \equiv S_{u,0} + \sum_{k=1}^{N} \left[\frac{I}{2}(\varepsilon^R)^2(C_{i-1} - C_i)\right]^{\alpha/(1+\alpha)} (t_i - t_{i-1})^{1/(1+\alpha)} \quad (3.7)$$

3.6.2. Prediction of fatigue life

The characteristic curves, *C(S)*, for each material were constructed, but they do not permit a direct comparison of the materials. On the other hand, such curves are able to provide enough information to construct fatigue curves, according to the fatigue model developed by Kim & Little (2005). The fatigue model (Equation 3.9) permits the prediction of the number of axle load repetitions (N_f) required to degrade the material to a certain level of damage (S_f). Two level of damage were chosen, correspondent to a reduction of pseudo stiffness to 50 and 30%, in order to estimate the parameter A of the fatigue model (Equation 3.10). The parameter B is calculated using the damage evolution rate obtained in the fingerprint test (Equation 3.11). The fatigue model provides the estimate of the fatigue life of the materials at any strain imposed by traffic loads to the pavement. The parameters C_0, C_1 and C_2 were obtained by fitting a power law model (Equation 3.8) to the *C vs. S* curve.

$$\mathrm{C}(S)=C_0\text{-}C_1(S)^{C_2} \quad (3.8)$$

$$N_f \equiv A(\varepsilon^R)^{-B} \quad (3.9)$$

$$A = f\left\{\frac{1}{2}C_1C_2\right\}^{\alpha}\{1+\alpha(1-C_2)\}^{-1}S_f^{[1+\alpha(1-C_2)]} \quad (3.10)$$

$$B = 2\alpha \quad (3.11)$$

4. RESULTS

This section presents the results obtained from the tests performed, and the analysis of the mixtures with basis on the fatigue response obtained by means of the mechanistic fatigue prediction model based on the VECD theory.

4.1. Characterization of the samples

The characterization of the samples is presented in Appendix A, which contains the linear viscoelastic properties obtained from the fingerprint tests, a summary of the initial and final conditions of the damage tests and the reasons why the data from a few tests were not considered in the analysis. In some cases, the applied load was relatively low to cause damage on the specimen, so the test was aborted. In other cases, the material state was influenced by variations in the test temperature and such results were also left out of the analysis.

4.2. Linear viscoelastic properties

Table 4.1 presents the viscoelastic properties of the materials, including G^*_{LVE}, phase angle and strain. The air voids of the samples are also presented for reference. Figure 4.1 and 4.2 show graphical comparisons of the results of G^*_{LVE} of the mixtures prepared with 20% and 40% RAP, respectively. The average results of G^*_{LVE} of the samples indicate that the FAM prepared with 100% of RAP is the stiffest material and the FAM prepared with virgin mineral aggregate and virgin binder is the less stiff material. The FAMs prepared with 20 and 40% of RAP present intermediate G^*_{LVE} values between the stiffness observed for the FAMs 1 and 2. For all the cases, the FAMs prepared with 40% of RAP presented stiffness values higher than the FAMs prepared with 20% of RAP. The RAP material is naturally stiffer than a mixture prepared with only new material and the mixing of such hard material with new materials turns the final composite into a material stiffer than the FAM prepared with only new materials.

Table 4.1 and Figures 4.1 and 4.2 also show that the use of a lower PG grade reduced slightly the stiffness of the samples, as compared to the PG 64, and this is valid for the two RAP contents. By comparing the FAM 11 and 12, it is possible to notice that the use of only

oil, as compared to the use of asphalt and oil, did not produce any effect on stiffness, but, on the other hand, the use of only oil, in the case of FAMs 13 and 14, resulted in a lower stiffness. By comparing FAMs 7, 9 and 11, all prepared with 20% of RAP, it is evident that the use of a softer binder is capable of reducing the stiffness, as compared to the stiffness of the FAM prepared with the PG 64 binder, but the substitution of 50% of oil for 50% of a PG 64 binder resulted in a stiffness higher than the FAM prepared only with the PG 64 binder. The same observation is valid for the FAMs prepared with 40% of RAP (FAMs 8, 10 and 13). It was believed that the oil would be capable of reducing the stiffness in all cases, but the opposite results were observed in some comparisons, and they are probably due to the low diffusion of the oil into the old binder.

Table 4.11. Viscoelastic properties of the materials

MATERIAL	SAMPLE	AIR VOIDS (%)	G^*_{LVE} (Pa)	G^*_{LVE} average (Pa)	VARIABILITY (%)[4]	δ (degree)	γ (μstrain)
FAM01: 100% RAP	3	3.9	5.12E+09	5.12E+09	-	12	4
FAM02: N.A.[1]+PG64	2	1.2	5.05E+08	5.08E+08	1.25	40	30
	4	1.3	5.12E+08			39	29
FAM07: 20%RAP+PG64	7	1.2	1.00E+09	8.54E+08	34.25	29	15
	9	1.2	7.08E+08			27	21
FAM08: 40%RAP+PG64	6	2.3	1.36E+09	1.54E+09	23.14	14	11
	7	2.5	1.72E+09			19	9
FAM09: 20%RAP+PG58	3	1.0	7.40E+08	7.95E+08	13.73	31	20
	5	0.9	8.49E+08			35	18
FAM10: 40%RAP+PG58	4	0.8	1.32E+09	1.29E+09	5.59	22	10
	6	0.7	1.25E+09			21	11
FAM11: 20%RAP+50/50(V.B.[2]/R.A.[3])	1	4.1	1.04E+09	9.83E+08	11.43	25	14
	4	3.3	9.27E+08			26	16
FAM12: 20%RAP+0/100(V.B./R.A)	9	4.0	1.42E+09	1.21E+09	35.58	26	11
	12	4.0	9.91E+08			24	15
FAM13: 40%RAP+50/50(V.B./R.A)	7	4.8	1.89E+09	1.84E+09	5.95	22	8
	13	7.2	1.78E+09			24	8
FAM14: 40%RAP+0/100(V.B./R.A)	2	7.2	1.24E+09	1.56E+09	40.10	14	12
	6	7.3	1.87E+09			17	8

[1]: N.A. - NEW AGGRAGETES; [2]: V.B. - VIRGIN BINDER: PG-64; [3]: R.A. - REJUVENATING AGENT; [4]: DIFFERENCE BETWEEN VALUES DIVIDED BY AVERAGE

Figure 4.1. Comparison of G^*_{LVE} of the mixtures containing 20% of RAP

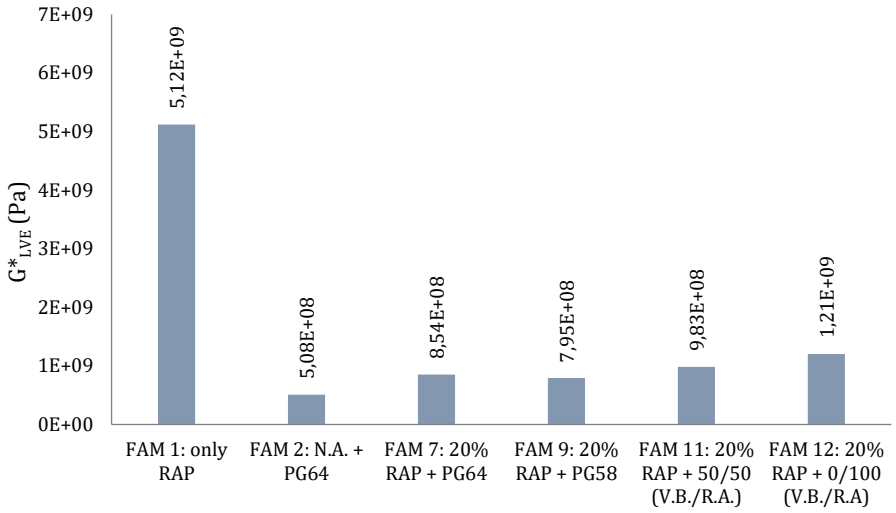

Figure 4.2. Comparison of G^* of the mixtures containing 40% of RAP

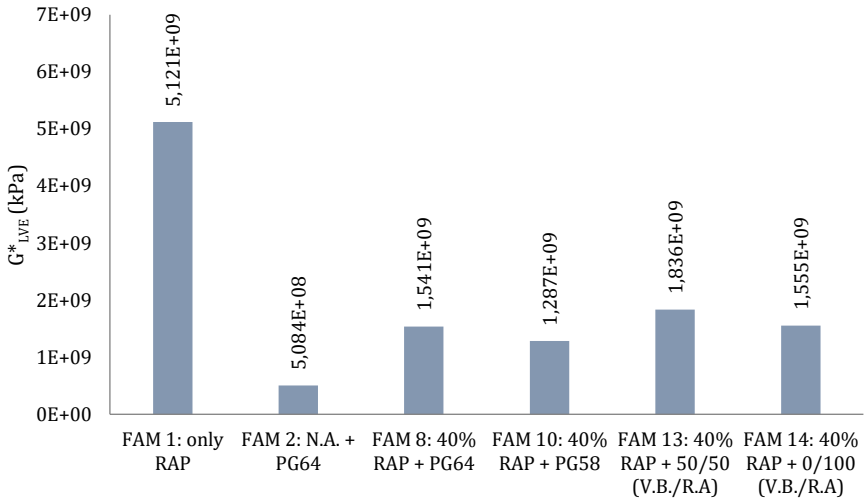

4.3. Relaxation properties and damage evolution rate

Table 4.2 presents the parameter *m*, given by the slope of the relaxation curves and the damage evolution rate (α=1/*m*) of the materials. Figure 4.3 and 4.4 show graphical comparisons of the relaxation rates of the mixtures prepared with 20% and 40% RAP, respectively. The air voids of the samples are presented again for reference. The average results of the relaxation rate of the samples indicate that the FAM prepared with 100% of RAP is the worst material in terms of relaxation and the FAM prepared with new mineral aggregate and new binder is the best one. The FAMs prepared with 20 and 40% of RAP present intermediate relaxation rates between the values observed for the FAMs 1 and 2.

For all the cases, the FAM prepared with 40% of RAP presented lower relaxations rates as compared to the FAM prepared with 20% of RAP. The RAP material is naturally less capable of relaxing stresses, because of the presence of the aged binder, as compared to a mixture prepared with only new material, and the mixing of such aged material with new materials turns the final composite into a material with a lower relaxation rate, as compared to the FAM prepared with only new materials.

Table 4.12. Relaxation properties and damage evolution rate of the materials

MATERIAL	SAMPLE	AIR VOIDS (%)	m	m (average)	VARIABILITY (%)[4]	α	α (average)
FAM01: 100% RAP	3	3.9	0.141	0.141	-	7.104	7.104
FAM02: N.A.[1]+PG64	2	1.2	0.547	0.545	0.65	1.828	1.834
	4	1.3	0.544			1.840	
FAM07: 20%RAP+PG64	7	1.2	0.351	0.354	1.53	2.850	2.828
	9	1.2	0.356			2.807	
FAM08: 40%RAP+PG64	7	2.0	0.206	0.194	13.13	4.844	5.184
	6	2.3	0.181			5.524	
FAM09: 20%RAP+PG58	5	0.9	0.415	0.408	3.28	2.408	2.449
	3	1.0	0.402			2.489	
FAM10: 40%RAP+PG58	4	0.8	0.231	0.232	1.25	4.330	4.303
	6	0.7	0.234			4.276	
FAM11: 20%RAP+50/50(V.B.[2]/R.A.[3])	1	4.1	0.351	0.378	14.62	2.851	2.657
	4	3.3	0.406			2.462	
FAM12: 20%RAP+0/100(V.B./R.A)	9	4.0	0.299	0.308	6.39	3.350	3.246
	12	4.0	0.318			3.142	
FAM13: 40%RAP+50/50(V.B./R.A)	7	4.8	0.273	0.281	5.48	3.661	3.564
	13	7.2	0.289			3.466	
FAM14: 40%RAP+0/100(V.B./R.A)	2	7.2	0.175	0.187	13.23	5.730	5.375
	6	7.3	0.199			5.019	

[1]: N.A. - NEW AGGRAGETES; [2]: V.B. - VIRGIN BINDER; [3]: R.A. - REJUVENATING AGENT; [4]: DIFFERENCE BETWEEN VALUES DIVIDED BY AVERAGE

Table 4.2 and Figures 4.3 and 4.4 also show that the use of a lower PG grade increased slightly the relaxation rate of the samples, as compared to the PG 64, and this is valid for the two RAP contents. By comparing FAMs 11 and 12 and FAMs 13 and 14, it is possible to notice that the use of only oil, as compared to the use of asphalt and oil, decreased the relaxation rate of the samples. By comparing FAMs 7, 9 and 11, all with 20% of RAP, it is evident that the use of a softer binder is capable of increasing the relaxation rate, as compared to the relaxation rate of the FAM prepared with the PG 64 binder, and

the substitution of 50% of oil for 50% of a PG 64 binder resulted in a relaxation rate intermediate between the ones obtained for the FAMs prepared with the PG 64 binder and the PG 58 binder. By comparing FAMs 8, 10 and 13, all with 40% of RAP, it is evident that the use of a softer binder is capable of increasing the relaxation rate, as compared to the relaxation rate of the FAM prepared with the PG 64 binder, and the substitution of 50% of oil for 50% of a PG 64 binder resulted in a relaxation rate higher than the ones obtained for the FAMs prepared with the PG 64 binder and the PG 58 binder.

Figure 4.3. Comparison of *m* values of the mixtures containing 20% of RAP

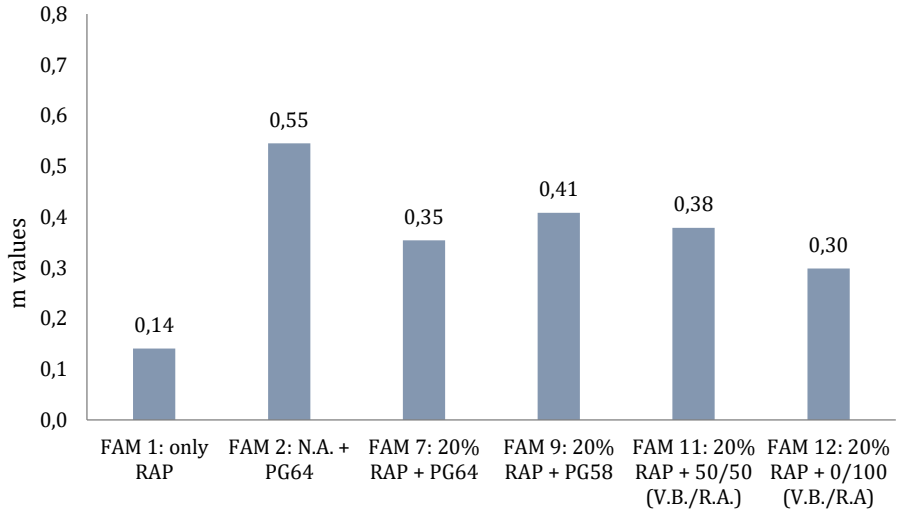

Figure 4.4. Comparison of *m* values of the mixtures containing 40% of RAP

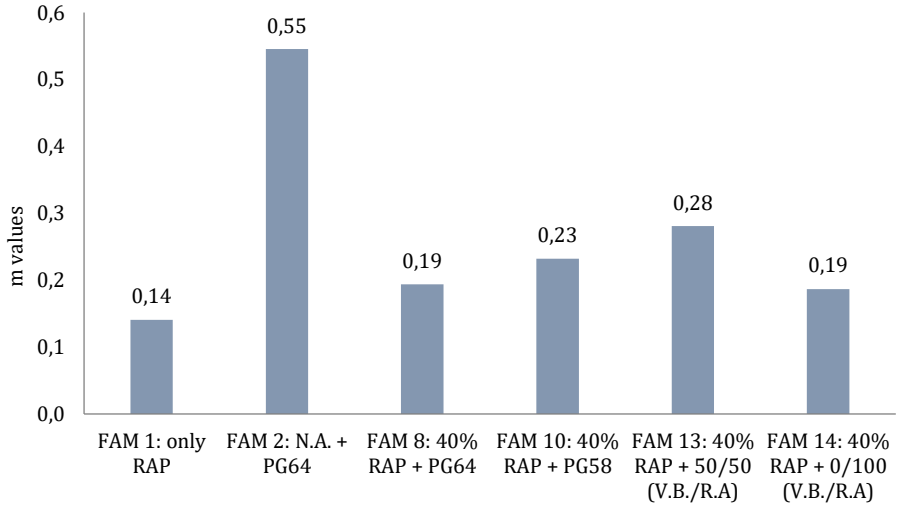

The results obtained for FAM 11 reinforce the evidence of the low diffusion rates of the oil into the aged binder, but, on the other hand, there are also evidences of a good

diffusion rate, as shown by FAM 13 in terms of relaxation rate. The worst option seems to be the use of only oil (FAMs 12 and 14), once that the relaxation rates obtained for such materials are lower than the ones obtained for the FAMs prepared with the PG 64 binder with no oil. This is another important evidence of the low diffusion rate of the oil into the aged binder.

Figure 4.5 and 4.6 show graphical comparisons of the damage evolution rates of the mixtures prepared with 20% and 40% RAP, respectively. The average results of the damage evolution rate of the samples indicate that the FAM prepared with 100% of RAP is the material with the highest rate of damage accumulation and the FAM prepared with new mineral aggregate and new binder is the material with the lowest rate. The FAMs prepared with 20 and 40% of RAP present intermediate damage evolution rates between the values observed for the FAMs 1 and 2. For all the cases, the FAM prepared with 20% of RAP presented lower damage evolution rates as compared to the FAM prepared with 40% of RAP. The RAP material is naturally more prone to damage accumulation, because of the presence of the aged binder, as compared to a mixture prepared with only new material, and the mixing of such aged material with new materials turns the final composite into a material with a higher damage evolution rate, as compared to the FAM prepared with only new materials. Table 4.2 and Figures 4.5 and 4.6 also show that the use of a lower PG grade reduced the damage evolution rate of the materials, as compared to the PG 64, and this is valid for the two RAP contents. By comparing the FAM 11 and 12, it is possible to notice that the use of only oil, as compared to the use of asphalt and oil, was incapable of decreasing the damage evolution rate of the materials. The same is valid for the FAM produced with 40% of RAP (FAMs 13 and 14). By comparing FAMs 7, 9 and 11, it is evident that the use of a softer binder is capable of decreasing the damage evolution rate, as compared to the stiffness of the FAM prepared with the PG 64 binder, but the substitution of 50% of oil for 50% of a PG 64 binder resulted in a damage evolution rate that is intermediate between the results obtained for the FAM prepared with the PG 58 binder and the PG 64 binder. The same observation is valid for the FAMs 8 and 10, in the case of the use of a softer binder, but FAM 13, in opposition to what was observed for FAM 11, presented a damage evolution rate lower than the FAM prepared with the soft binder. As mentioned previously for the m values, the results of α values obtained for FAM 11 also reinforce the evidence of the low diffusion rates of the oil into the aged binder, but, on the other hand, there are also evidences of a good diffusion rate, as shown by FAM

13 in terms of damage evolution rate. The worst option seems to be the use of only oil (FAMs 12 and 14), once that the damage evolution rates obtained for such materials are higher than the ones obtained for the FAMs prepared with the PG 64 binder with no oil. As mentioned before, this is another important evidence of the low diffusion rate of the oil into the aged binder.

Figure 4.5. Comparison of α values of the mixtures containing 20% of RAP

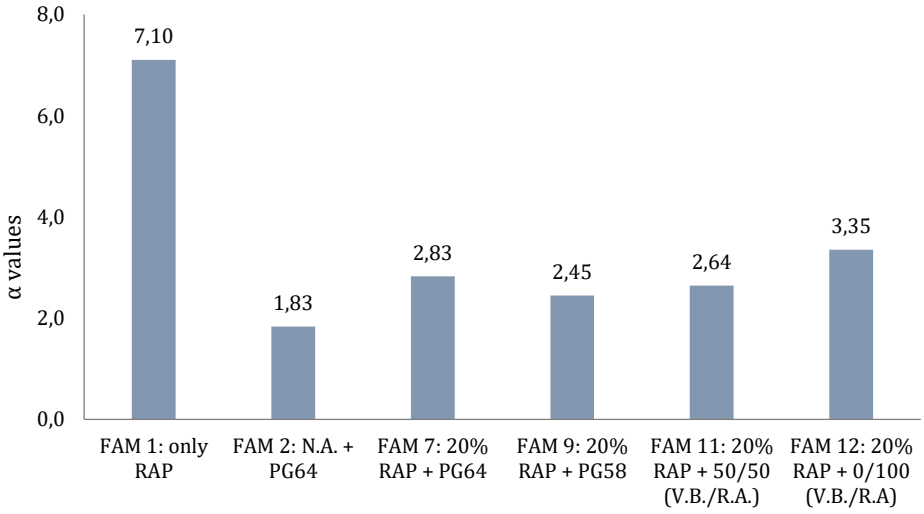

Figure 4.6. Comparison of α values of the mixtures containing 40% of RAP

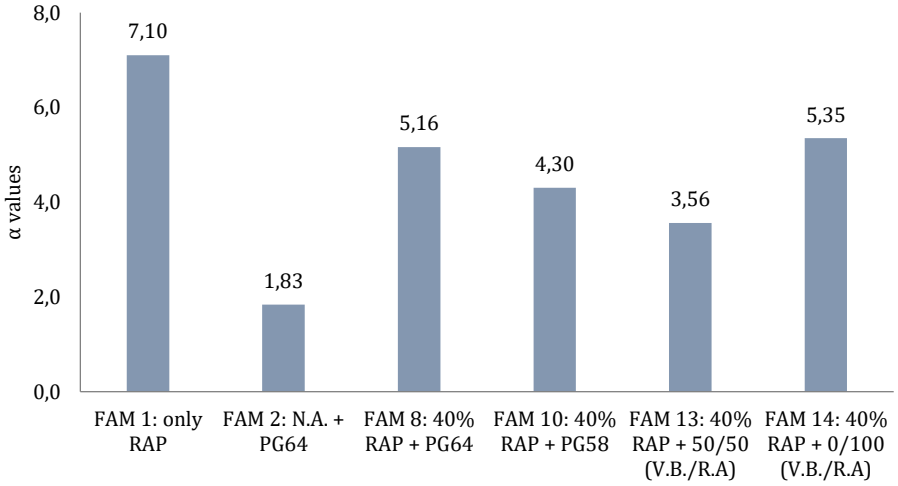

The overall results of relaxation rate and damage accumulation rate show that the harder the material (in terms of G^*_{LVE} values) the lower the relaxation rate and higher the damage accumulation rate. This is a direct effect of the presence of RAP. In other words, the aged binder compromises the relaxation rates and increases the damage evolution

rate due to its higher stiffness. The use of a softer binder is capable of increasing the relaxation rates and consequently reducing the damage evolution rate, as compared to a FAM prepared with a PG 64 binder. On the other hand, the effect of substituting 50% of the PG 64 binder by oil had a divergent effect: a positive effect when 40% of RAP was used and a negative effect when 20% of RAP was used.

4.4. Characteristics curves – *CxS*

The characteristic curves of the materials were constructed by means of the VECD model proposed by Lee and Kim (1998). The heterogeneity in the material properties for two samples of the same material may result in different characteristic curves. In order to overcome this issue and to predict an accurate damage behavior of the mixtures, the average of the sample properties was considered in the model. It was observed that, by considering the average of the properties, a unique characteristic curve for each material can represent its damage behavior.

FAM 1 (100% of RAP) is a mixture with a high stiffness that requires a high level of stress to damage it. Although a few samples were tested, just one has provided consistent results. For this reason, the characteristic curve of FAM 1 was constructed with basis on the viscoelastic properties and the damage test of only one sample. Figure 4.7 presents the *CxS* curve for FAM 1.

Figure 4.7. *CxS* curves: (a) FAM 1 – only RAP; and (b) FAM 2 – only virgin aggregates and virgin binder

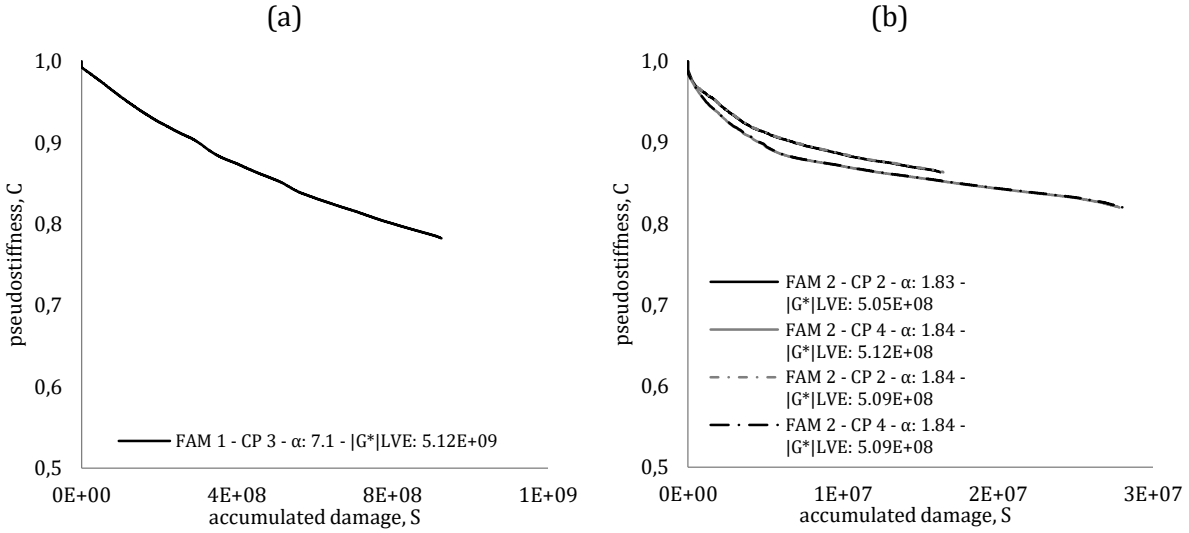

For all the other mixtures, the average of the data from two samples was considered. Figures 4.8 to 4.11 present the individual *CxS* curves, and the adjustment of the curves by considering the average properties.

Figure 4.8. Original and adjusted *CxS* curves, by considering the average of the properties: (a) FAM 7 – 20% RAP + PG 64; and (b) FAM 8 – 40% RAP + PG 64

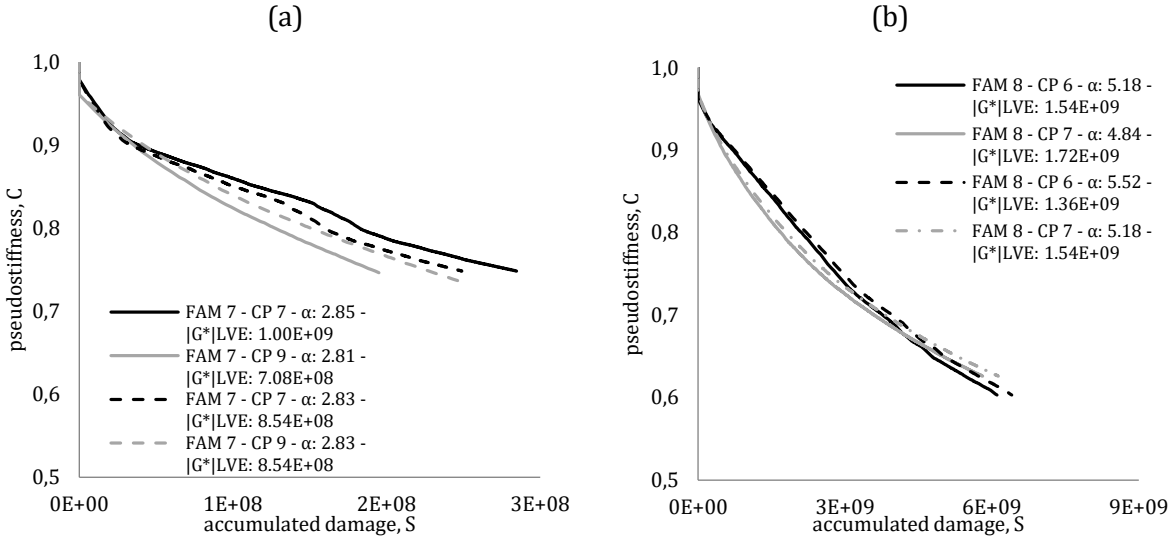

Figure 4.9. Original and adjusted *CxS* curves: (a) FAM 09 – 20% RAP + PG 58; and (b) FAM 10 – 40% RAP + PG 58

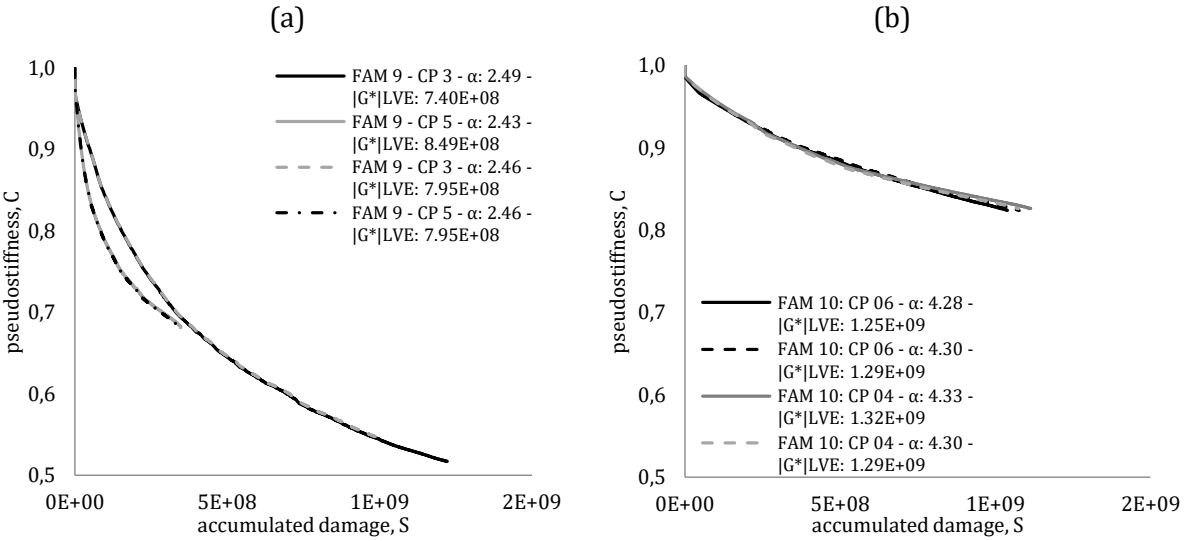

Figure 4.10. Original and adjusted *CxS* curves: (a) FAM 11 – 20% RAP + 50/50 (binder/agent); and (b) FAM 12 – 20% RAP + 0/100 (binder/agent)

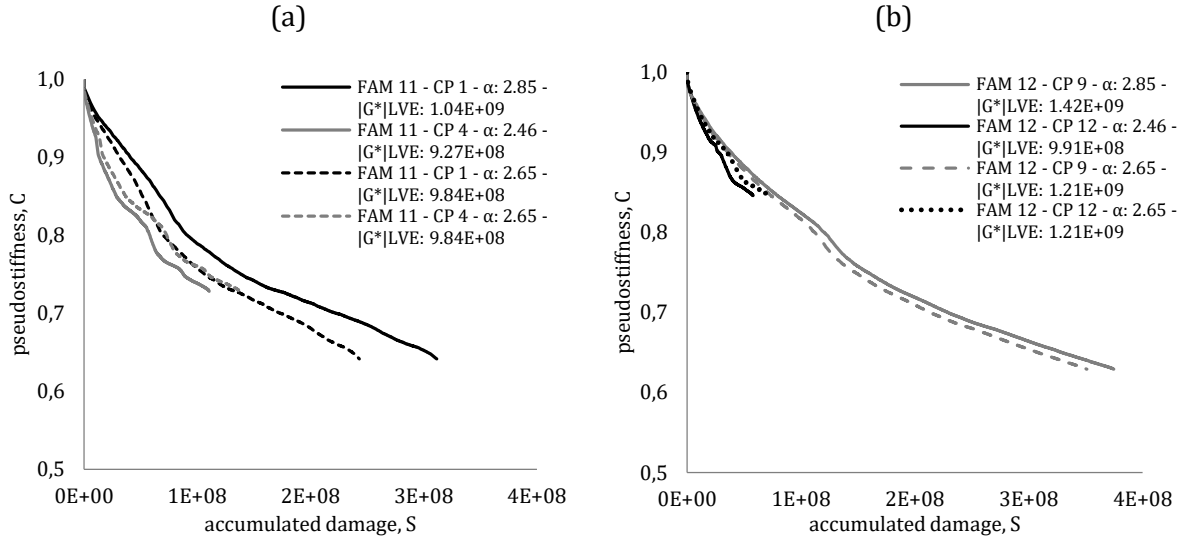

Figure 4.11. Original and adjusted *CxS* curves: (a) FAM 13 – 40% RAP + 50/50 (binder/agent); and (b) FAM 14 – 40% RAP + 0/100 (binder/agent)

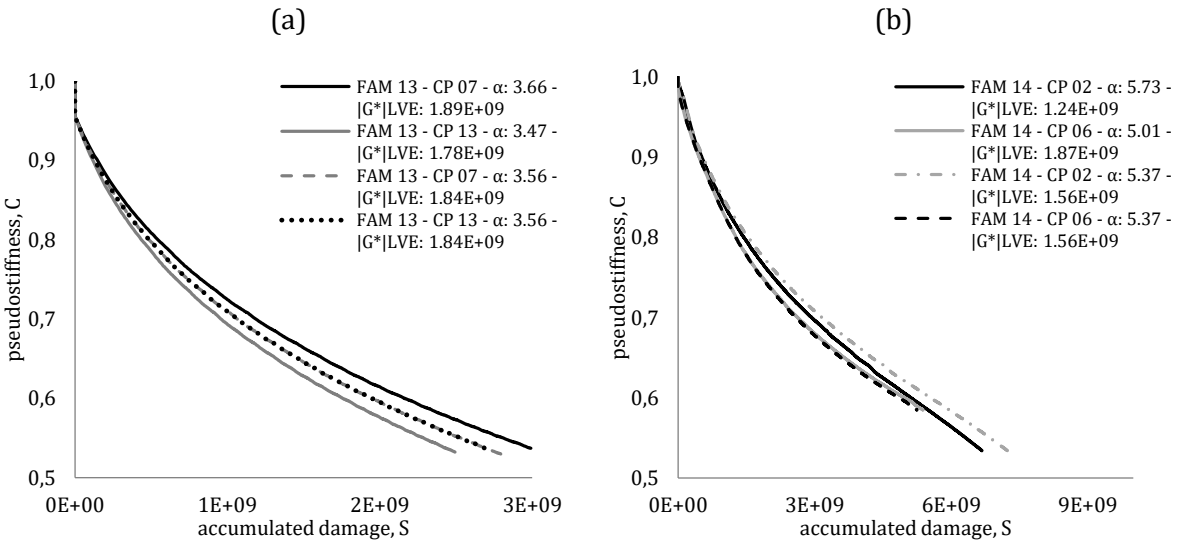

According to Lee and Kim (1998), each material presents a single characteristic curve that represents its damage behavior. Based on this premise, the adjustment of the CxS curves was considered in order to construct the fatigue curves for the FAMs. Figure 4.12 presents the final *CxS* curves of all FAMs.

Figure 4.12. Adjusted *CxS* curves of all FAMs

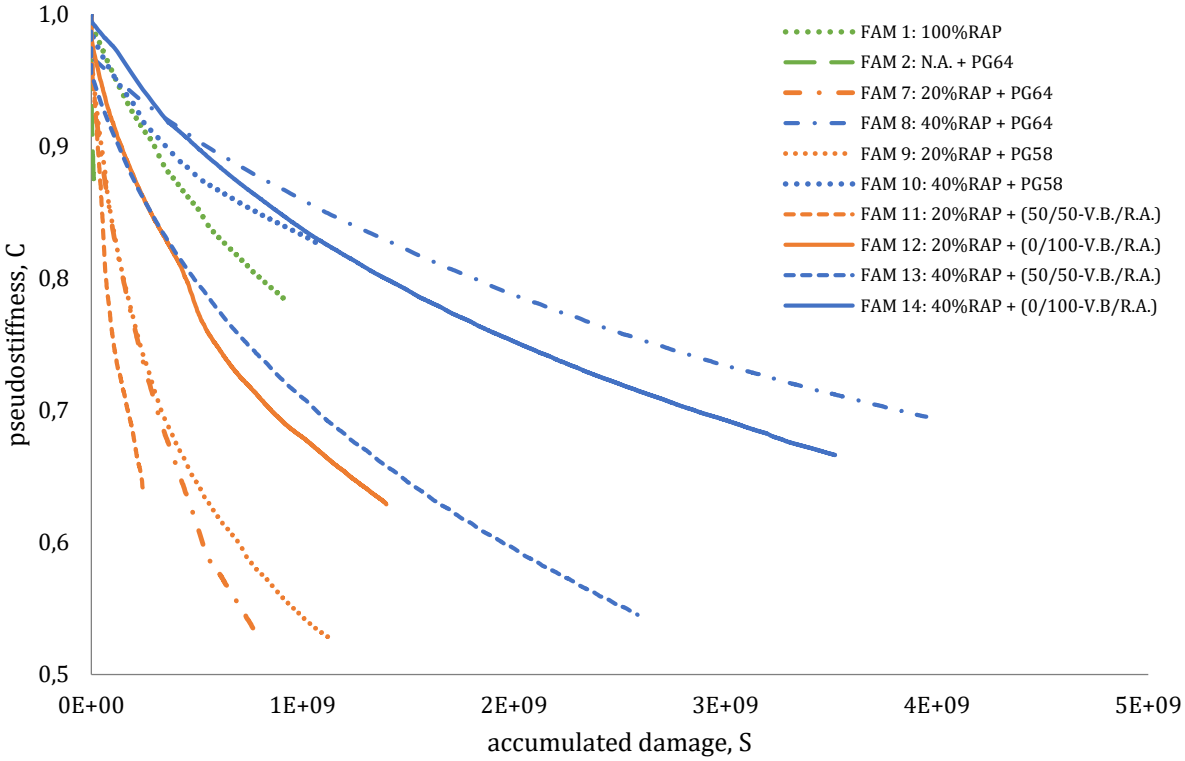

4.5. Fatigue models

The fatigue life of the materials, N_f, was predicted by considering the mechanistic fatigue prediction model developed by Lee et al. (2000) and Kim and Little (2005). The fatigue models were adjusted for a 50% reduction in the pseudostiffness of the FAMs. The parameter A of the fatigue model is correlated to the initial complex modulus (when the material still did not suffer damage) and to the material integrity variation as a function of the accumulated damage (*CxS* curve). The parameter B refers to the damage evolution rate of the material. The parameters A and B of the fatigue models are presented in Table 4.3.

FAM 1 presents the highest values of A and B, what is a reflection of the highest initial stiffness and the lowest relaxation rate of this material. Because of that, such material is more prone to fatigue cracking than all the others. On the other hand, FAM 2 presents the lowest values of A and B, what is a reflection of the lowest initial stiffness and the highest relaxation rate of this material. Because of that, such material presents one of

the best fatigue performance. Graphical comparison of the A values is not practical, once that the values are extremely high and different.

Table 4.13. Parameters A and B of the fatigue model

material	sample	air voids (%)	A	A (average)	variability (%)[4]	B	B (average)	variability (%)[4]
FAM01: 100% RAP	3	3.9	1.75E+83	1.75E+83	-	14.21	14.21	-
FAM02: N.A.[1]+PG64	2	1.2	9.03E+26	5.00E+26	161	3.66	3.67	0.66
	4	1.3	9.64E+25			3.68		
FAM07: 20%RAP+PG64	7	1.2	1.95E+37	1.01E+37	186	5.70	5.66	1.53
	9	1.2	7.11E+35			5.61		
FAM08: 40%RAP+PG64	6	2.3	2.42E+69	1.21E+69	200	11.05	10.37	13.13
	7	2.5	4.63E+61			9.69		
FAM09: 20%RAP+PG58	3	1.0	1.35E+34	1.28E+34	10.3	4.98	4.92	2.36
	5	0.9	1.21E+34			4.86		
FAM10: 40%RAP+PG58	3	1.0	5.17E+57	2.63E+57	191	8.66	8.63	0.62
	12	0.9	1.09E+56			8.61		
FAM11: 20%RAP +50/50(V.B.[2]/R.A.[3])	1	4.1	1.48E+36	7.39E+35	200	5.70	5.31	14.72
	4	3.3	6.30E+31			4.92		
FAM12: 20%RAP +0/100(V.B./R.A)	9	4	1.24E+41	6.20E+40	200	6.70	6.49	6.40
	12	4	1.18E+38			6.28		
FAM13: 40%RAP +50/50(V.B./R.A)	7	4.8	2.81E+47	1.41E+47	199	7.32	7.13	5.48
	13	7.2	1.06E+45			6.93		
FAM14: 40%RAP +0/100(V.B./R.A)	2	7.2	1.53E+71	7.66E+70	200	11.46	10.75	13.22
	6	7.3	6.51E+63			10.04		

[1]: N.A. - NEW AGGRAGETES; [2]: V.B. - VIRGIN BINDER; [3]: R.A. - REJUVENATING AGENT; [4]: DIFFERENCE BETWEEN VALUES DIVIDED BY AVERAGE

Figures 4.13 and 4.14 show a comparison of the results for the parameters B of the FAMs prepared with 20 and 40% of RAP, respectively. Once that the A values are related to the stiffness, such correlations will be taken into account, and once that the B values are related to the m and α values, such correlations will be taken into account.

For the FAMs prepared with 20% of RAP, the use of the softer binder reduced the A value of FAM 9 (prepared with the PG 58 binder) compared to FAM 7 (prepared with the PG 64 binder), and such results are compatible with the reduction of stiffness observed for FAM 9 compared to FAM 7. The use of only oil instead of 50% of binder + 50% of oil led to an increase in the A value of FAM 12 compared to FAM 11, but in terms of stiffness, such reduction was not observed, once that the stiffness of both FAMs is similar. For the FAMs prepared with 40% of RAP, the use of the softer binder reduced the A value of FAM

10 (prepared with the PG 58 binder) compared to FAM 8 (prepared with the PG 64 binder), and such results are compatible with the reduction of stiffness observed for FAM 10 compared to FAM 8. The use of only oil instead of 50% of binder + 50% of oil led to an increase in the A values of FAM 14 compared to FAM 13, but in terms of stiffness, an opposite result was observed, once that the stiffness of FAM 14 is lower than the one obtained for FAM 13. By comparing the A values of the FAMs prepared with 20 and 40% of RAP, it is clearly visible that the increase in the RAP amount increases the A values, as a consequence of the addition of the aged binder.

Figure 4.13. Comparison of the B values of the FAMs prepared with 20% of RAP

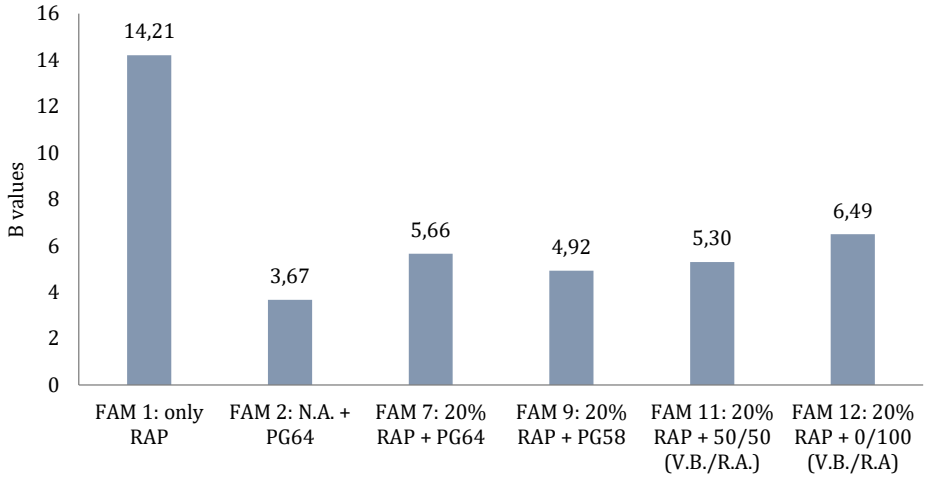

Figure 4.14. Comparison of the B values of the FAMs prepared with 40% of RAP

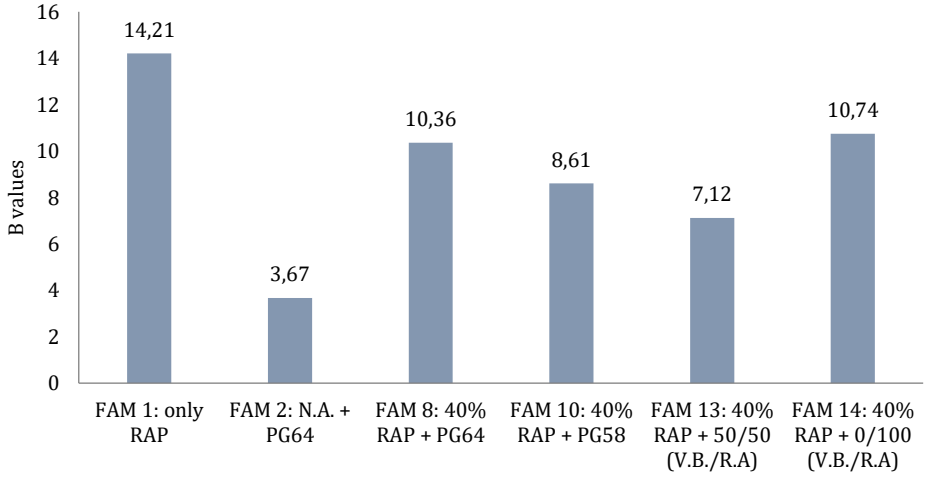

The same trends observed for the relaxation rates are observed for the B values, once that they are linear combinations. For the FAMs prepared with 20% of RAP, the use

of the softer binder reduced the B value of FAM 9 (prepared with the PG 58 binder) compared to FAM 7 (prepared with the PG 64 binder). The use of only oil instead of 50% of binder + 50% of oil led to an increase in the B value of FAM 12 compared to FAM 11. For the FAMs prepared with 40% of RAP, the use of the softer binder reduced the B value of FAM 10 (prepared with the PG 58 binder) compared to FAM 8 (prepared with the PG 64 binder). The use of only oil instead of 50% of binder + 50% of oil led to an increase in the B values of FAM 14 compared to FAM 13. By comparing the B values of the FAMs prepared with 20 and 40% of RAP, it is clearly visible that the increase in the RAP amount increases the B values, as a consequence of the addition of the aged binder.

When the fatigue curves are constructed, it can be observed that they are slightly different for two samples of the same material, once they are constructed by means of the damage characteristics obtained from the *CxS* curves. As mentioned before, the variability of the viscoelastic properties of the samples leads to CxS curves different of a same material. Such difference can be corrected by the reconstruction of the *CxS* curves based on the average of the viscoelastic properties. Then, after the superposition of the *CxS* curves, the fatigue curves for each sample can be constructed by considering the average of the viscoelastic characteristics. The fatigue curves by considering the original characteristics and the average characteristics, are presented in Figures 4.15 to 4.20.

Figure 4.15. Fatigue curves based on original data and based on the average of viscoelastic properties: (a) FAM 1 – only RAP; and (b) FAM 2 – only new aggregates and new binder

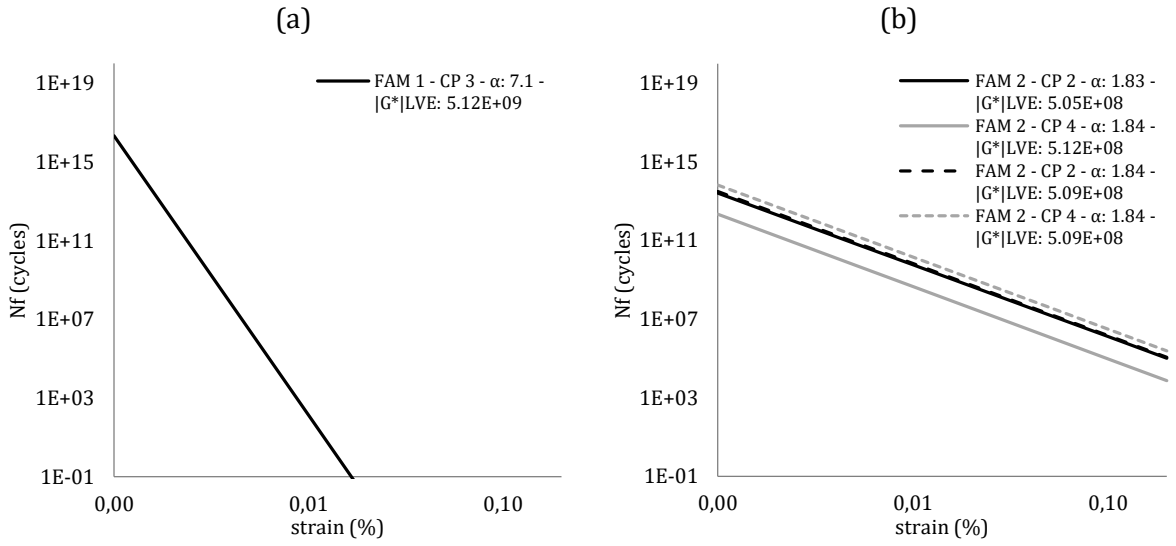

Figure 4.16. Fatigue curves based on original data and based on the average of viscoelastic properties: (a) FAM 7 – 20% RAP + PG 64; and (b) FAM 8 – 40% RAP + PG 64

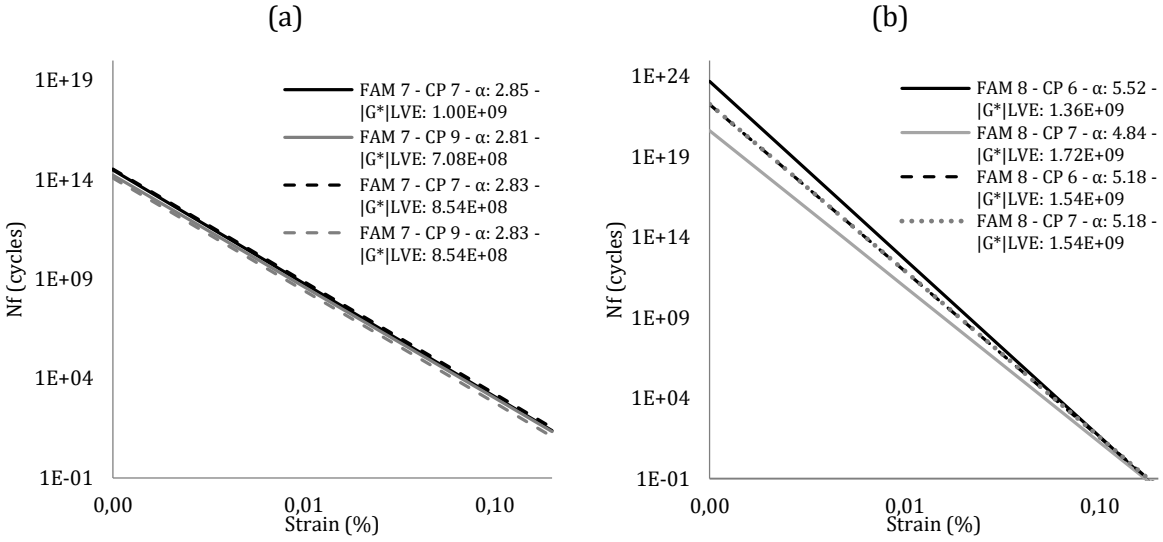

Figure 4.17. Fatigue curves based on original data and based on the average of viscoelastic properties: (a) FAM 9 – 20% RAP + PG 58; and (b) FAM 10 – 40% RAP + PG 58

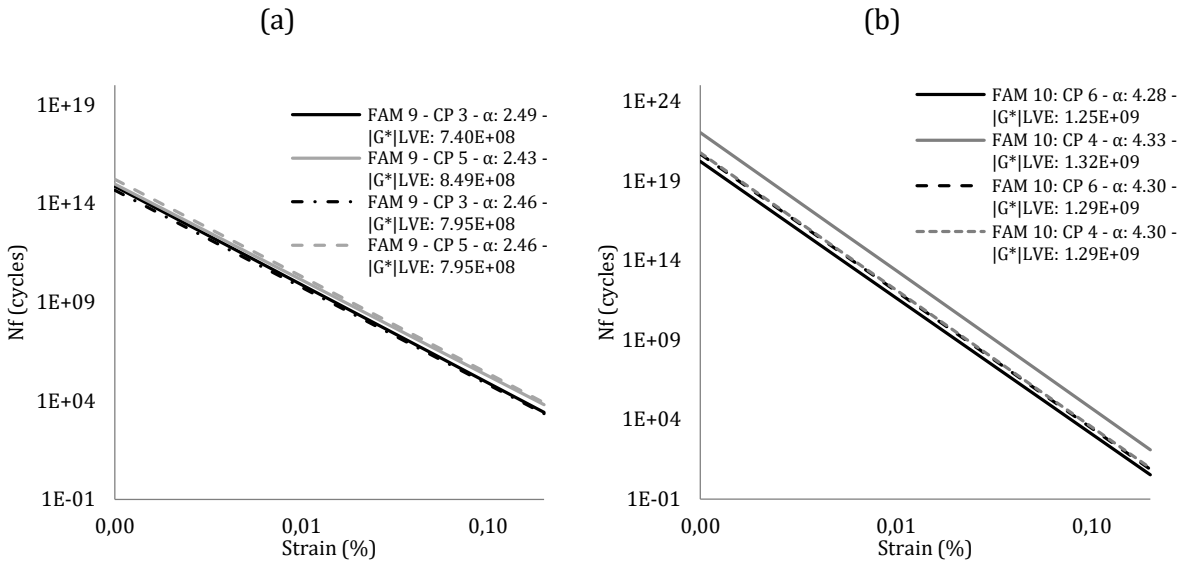

Figure 4.18. Fatigue curves based on original data and based on the average of viscoelastic properties: (a) FAM 11 – 20% RAP + 50/50 (binder/agent); and (b) FAM 12 – 20% RAP + 0/100 (binder/agent)

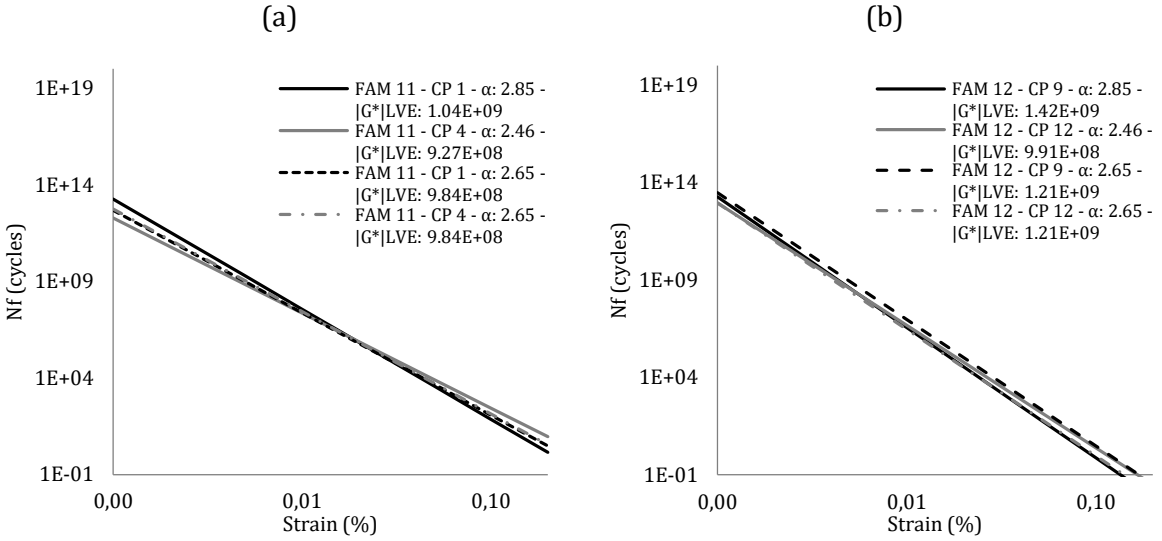

Figure 4.19. Fatigue curves based on original data and based on the average of viscoelastic properties: (a) FAM 13 – 40% RAP + 50/50 (binder/agent); and (b) FAM 14 – 40% RAP + 0/100 (binder/agent)

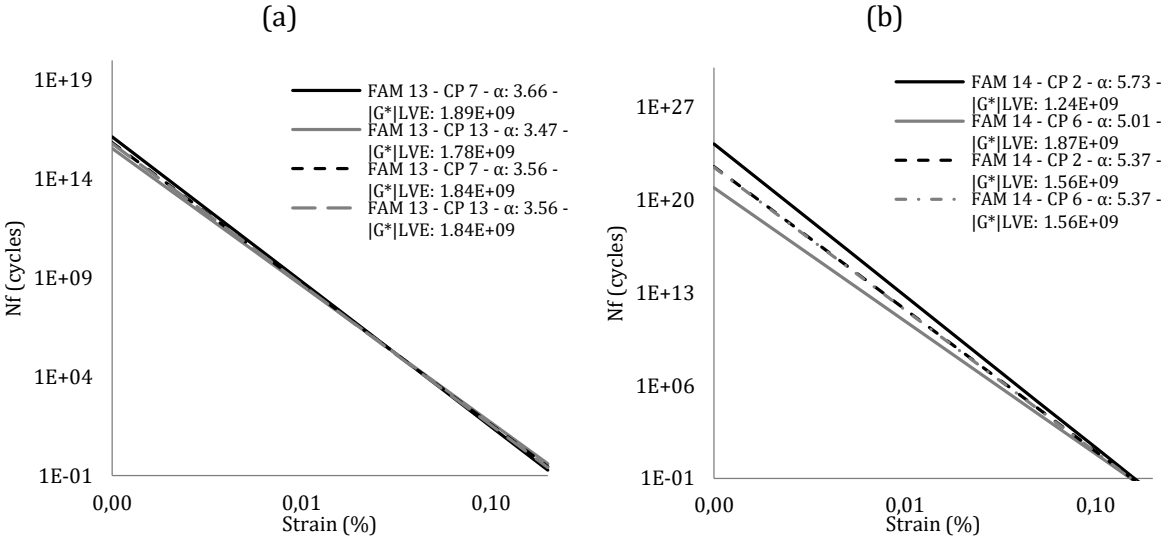

4.6. Comparison of the fatigue lives of the FAMs at different strain levels

By observing the fatigue curves of the FAMs (Figure 4.20), it is possible to see that the materials behave differently at different strain levels, and because of that, two strain levels were adopted in this analysis (0.005% and 0.050%), in order to estimate the numbers of axle load repetitions to failure (N_f). The comparisons were made for specific

groups of FAMs, in order to isolate some effects on the fatigue performance of the materials.

Figure 4.20. Fatigue curves of all FAMs

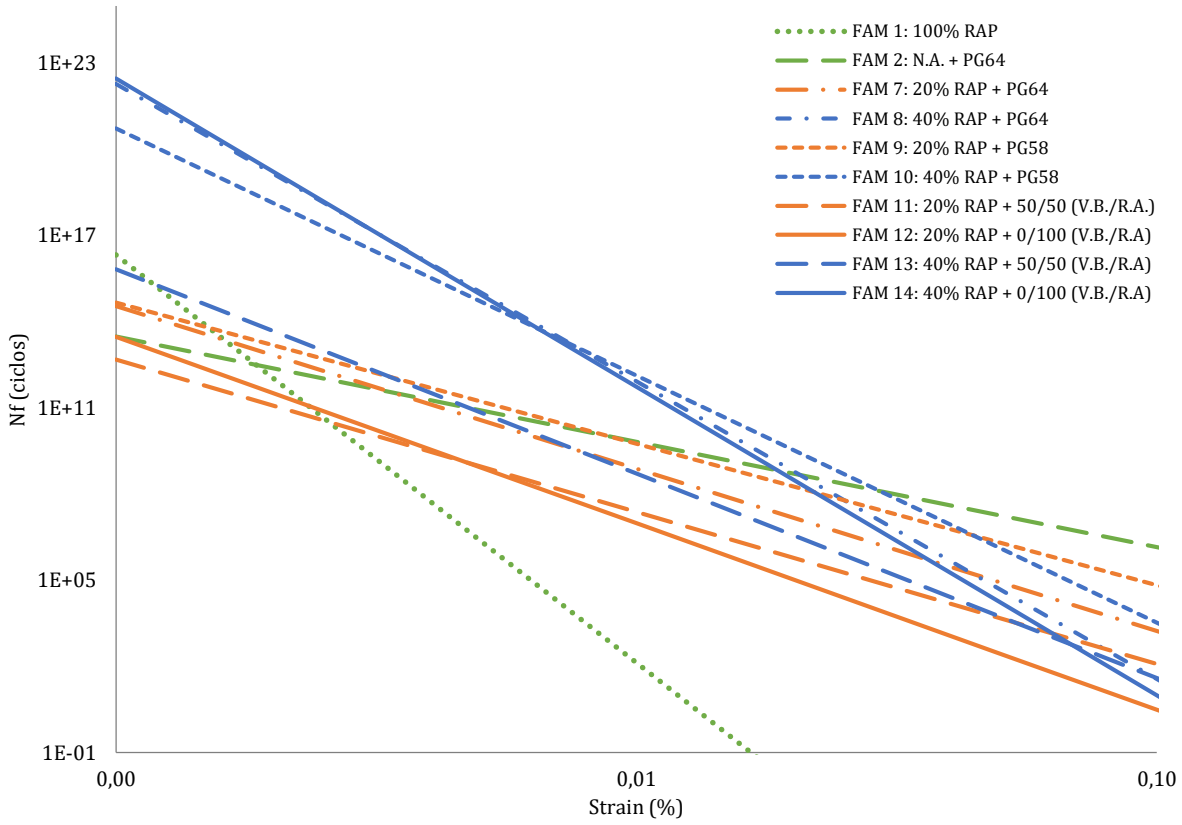

4.6.1. FAM 1 (only RAP) and FAM 2 (only new materials)

FAMs 1 and 2 were compared in order to see which would be the performance of a mixture produced only with RAP, if it would be possible. Table 4.4 presents the viscoelastic properties of the FAMs and the fatigue model parameters A and B, along with the number of cycles to failure (N_f) at two strain levels.

Table 4.14. Characteristics of FAMs 1 and 2

FAM	G^*_{LVE}	m	α	A	B	N_f (0,005%)	N_f (0,050%)
FAM 1: only RAP	5.121E+09	0.14	7.10	1.75E+83	14.21	2.52E+06	1.56E-08
FAM 2: N.A.[1] + PG64	0.509E+09	0.55	1.83	1.22E+27	3.67	8.48E+10	1.82E+07

[1]: N.A. - NEW AGGRAGETES.

FAM 1 presents a very high stiffness and a very low relaxation rate, compared to FAM 2, because of the aged binder. These characteristics result in higher A and B values,

compared to FAM 2. Because of such expressive differences between FAM 1 and 2, the fatigue lives at both strain levels are expressively lower for FAM 1. Figure 4.21 shows the comparisons of the linear viscoelastic properties and Figure 4.22 shows the comparison of the fatigue lives of the FAMs analyzed in this subsection.

Figure 4.21. Graphical comparisons of m, G^*_{LVE} and α values of FAMs 1 and 2

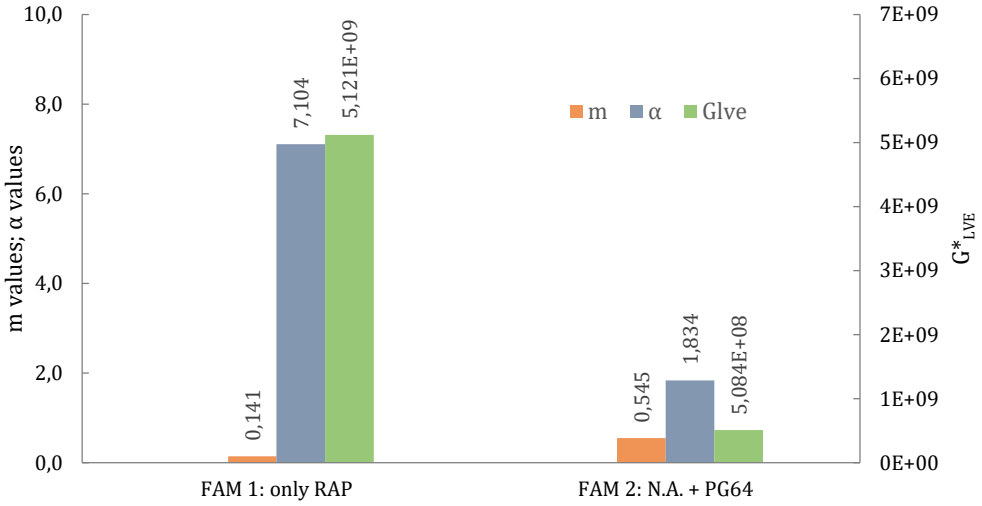

Figure 4.22. Fatigue lives of FAMs 1 and 2

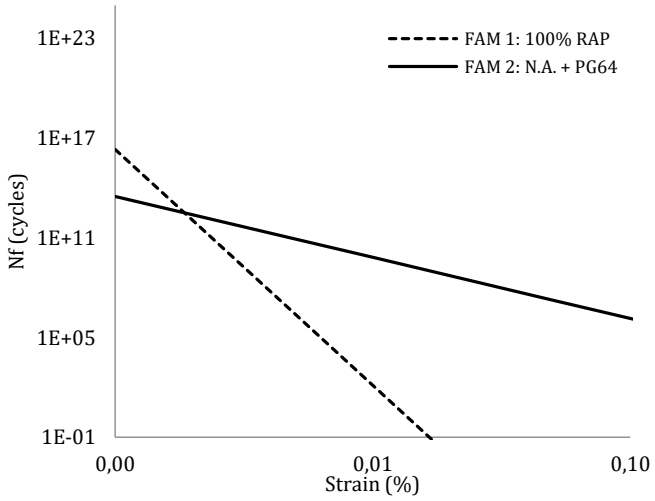

4.6.2. FAM 1 (only RAP), FAM 2 (only new materials) and FAM 7 (20%RAP+PG64)

FAMs 1, 2 and 7 were compared in order to evaluate the effect of the addition of 20% of RAP in the mixture when the binder content is corrected with the addition of a PG64 binder. Table 4.5 presents the viscoelastic properties of the FAMs and the fatigue model parameters A and B, along with the number of cycles to failure (N_f) at two strain levels. FAM 7 presents an intermediate stiffness between FAM 1 and FAM 2, as well as all the other

parameters. The resulting fatigue lives are also intermediate between FAM 1 and 2. Figure 4.23 shows the comparisons of the linear viscoelastic properties and Figure 4.24 shows the comparison of the fatigue lives of the FAMs analyzed in this subsection.

Table 4.15. Characteristics of FAMs 1, 2 and 7

FAM	G^*_{LVE}	m	α	A	B	N_f (0,005%)	N_f (0,050%)
FAM 1: 100% RAP	5.12E+09	0.14	7.10	1.75E+83	14.21	2.52E+06	1.56E-08
FAM 2: N.A.[1] + PG64	5.09E+08	0.55	1.83	1.22E+27	3.67	8.48E+10	1.82E+07
FAM 7: 20% RAP + PG64	8.54E+08	0.35	2.83	6.31E+36	5.66	3.91E+10	8.55E+04

[1]: N.A. - NEW AGGRAGETES.

Figure 4.23. Graphical comparisons of *m*, G^*_{LVE} and *α* values of FAMs 1, 2 and 7

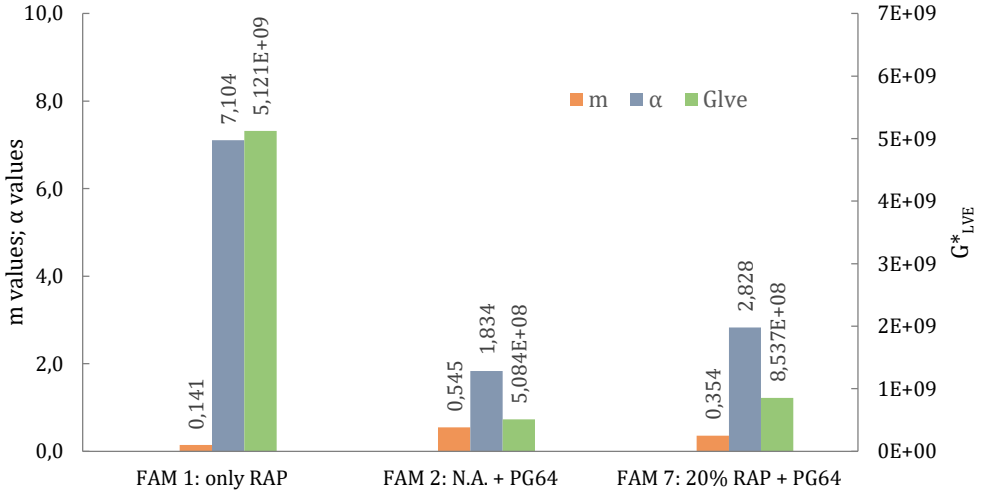

Figure 4.24. Fatigue lives of FAMs 1, 2 and 7

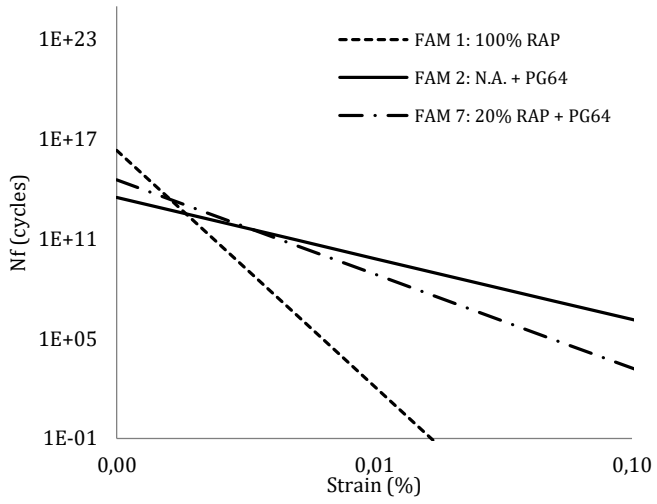

4.6.3. FAM 1 (only RAP), FAM 2 (only new materials) and FAM 8 (40%RAP+PG64)

FAMs 1, 2 and 8 were compared in order to evaluate the effect of the addition of 40% RAP in the mixture when the binder content is corrected with the addition of a PG64 binder. Table 4.6 presents the viscoelastic properties of the FAMs and the fatigue model parameters, A and B, along with the number of cycles to failure (N_f) at two strain levels.

Table 4.16. Characteristics of FAMs 1, 2 and 8

FAM	G^*_{LVE}	m	α	A	B	N_f (0,005%)	N_f (0,050%)
FAM 1: 100% RAP	5.12E+09	0.14	7.10	1.75E+83	14.21	2.52E+06	1.56E-08
FAM 2: N.A.[1] + PG64	5.09E+08	0.55	1.83	1.22E+27	3.67	8.48E+10	1.82E+07
FAM 8: 40% RAP + PG64	1.54E+09	0.19	5.16	4.66E+65	10.36	1.11E+15	4.84E+04

[1]N.A. - NEW AGGRAGETES

Figure 4.25. Graphical comparisons of *m*, G^*_{LVE} and *α* values of FAMs 1, 2 and 8

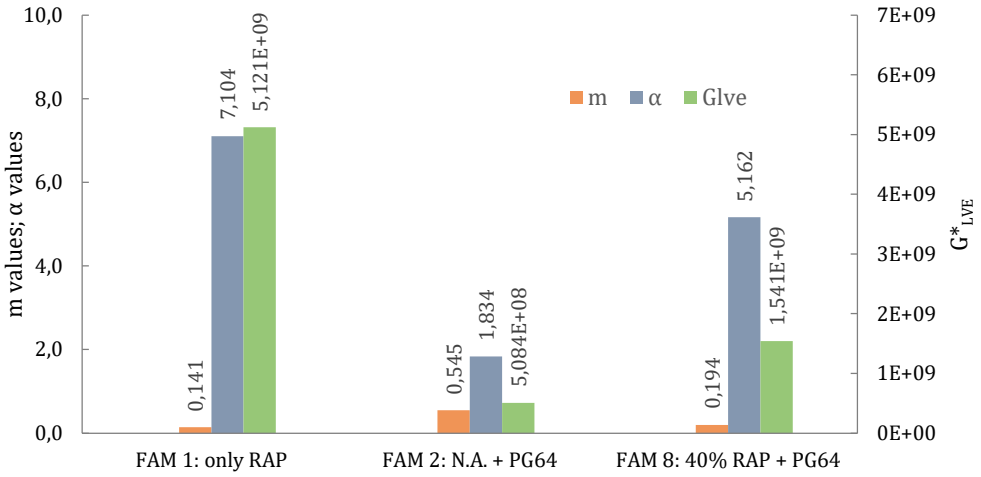

Figure 4.26. Fatigue lives of FAMs 1, 2 and 8

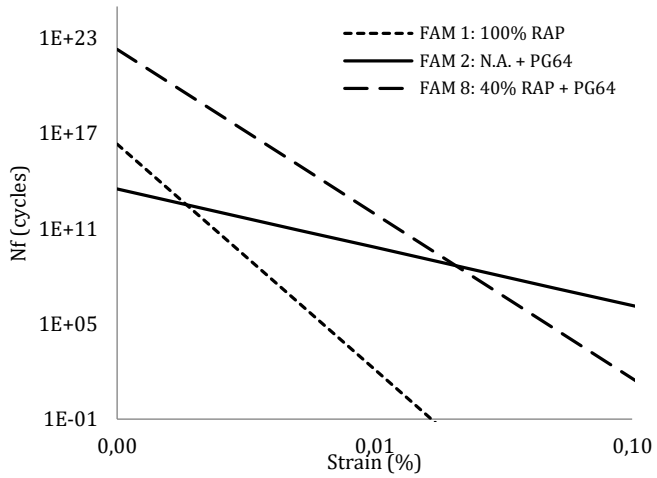

FAM 8 presents an intermediate stiffness between FAM 1 and FAM 2, as well as all the other parameters. At low strain, FAM 8 presented the highest fatigue life. At high strain, the resulting fatigue life is intermediate between FAM 1 and 2.

4.6.4. FAM 1 (only RAP), FAM 2 (only new materials) and FAM 9 (20%RAP+PG58)

FAMs 1, 2 and 9 were compared in order to evaluate the effect of the addition of 20% of RAP in the mixture when the binder content is corrected with the addition of a PG58 binder. Table 4.7 presents the viscoelastic properties of the FAMs and the fatigue model parameters A and B, along with the number of cycles to failure (N_f) at two strain levels. Figure 4.27 shows the comparisons of the linear viscoelastic properties and Figure 4.28 shows the comparison of the fatigue lives of the FAMs analyzed in this subsection.

Table 4.17. Characteristics of FAMs 1, 2 and 9

FAM	G^*_{LVE}	m	α	A	B	N_f (0,005%)	N_f (0,050%)
FAM 1: 100% RAP	5.12E+09	0.14	7.10	1.75E+83	14.21	2.52E+06	1.56E-08
FAM 2: N.A.[1] + PG64	5.09E+08	0.55	1.83	1.22E+27	3.67	8.48E+10	1.82E+07
FAM 9: 20% RAP + PG58	7.95E+08	0.41	2.45	7.21E+33	4.92	1.71E+11	2.05E+06

[1]N.A. - NEW AGGRAGETES

Figure 4.27. Graphical comparisons of m, G^*_{LVE} and α values of FAMs 1, 2, and 9

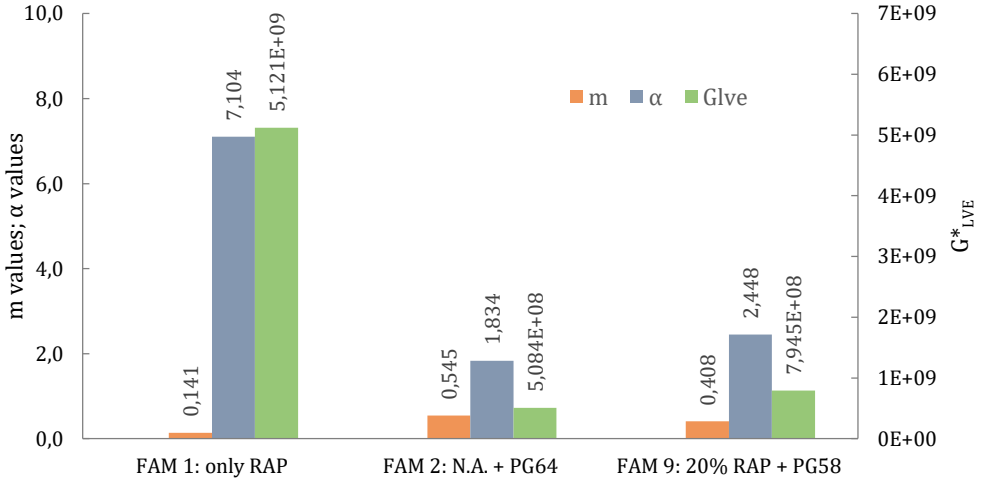

FAM 9 presents an intermediate stiffness between FAM 1 and FAM 2, as well as all the other parameters. At low strain, FAM 9 presented the highest fatigue life. At high strain, the resulting fatigue life is intermediate between FAM 1 and 2.

Figure 4.28. Fatigue lives of FAMs 1, 2, and 9

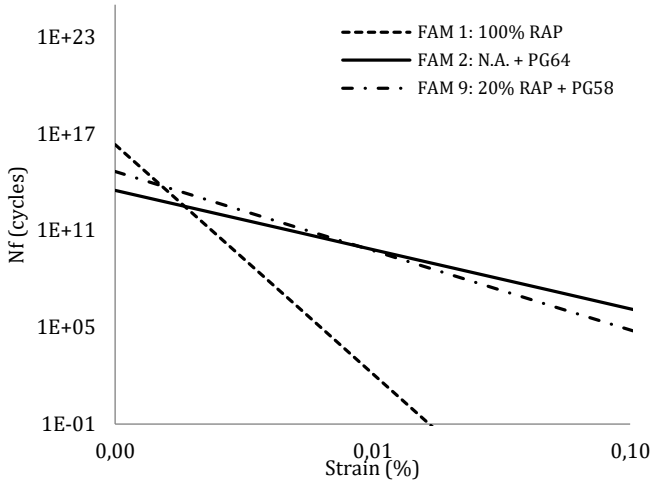

4.6.5. FAM 1 (only RAP), FAM 2 (only new materials) and FAM 10 (40%RAP+PG58)

FAMs 1, 2 and 10 were compared in order to evaluate the effect of the addition of 40% of RAP in the mixture when the binder content is corrected with the addition of a PG58 binder. Table 4.8 presents the viscoelastic properties of the FAMs and the fatigue model parameters A and B, along with the number of cycles to failure (N_f) at two strain levels.

Table 4.18. Characteristics of FAMs 1, 2 and 10

FAM	G^*_{LVE}	m	α	A	B	N_f (0.005%)	N_f (0.050%)
FAM 1: 100% RAP	5.12E+09	0.14	7.10	1.75E+83	14.21	2.52E+06	1.56E-08
FAM 2: N.A.[1] + PG64	5.09E+08	0.55	1.83	1.22E+27	3.67	8.48E+10	1.82E+07
FAM 10: 40% RAP + PG58	1.29E+09	0.23	4.30	1.27E+56	8.61	5.29E+14	1.31E+06

[1]N.A. - NEW AGGRAGETES

Figure 4.29. Graphical comparisons of m, G^*_{LVE} and α values of FAMs 1, 2, and 10

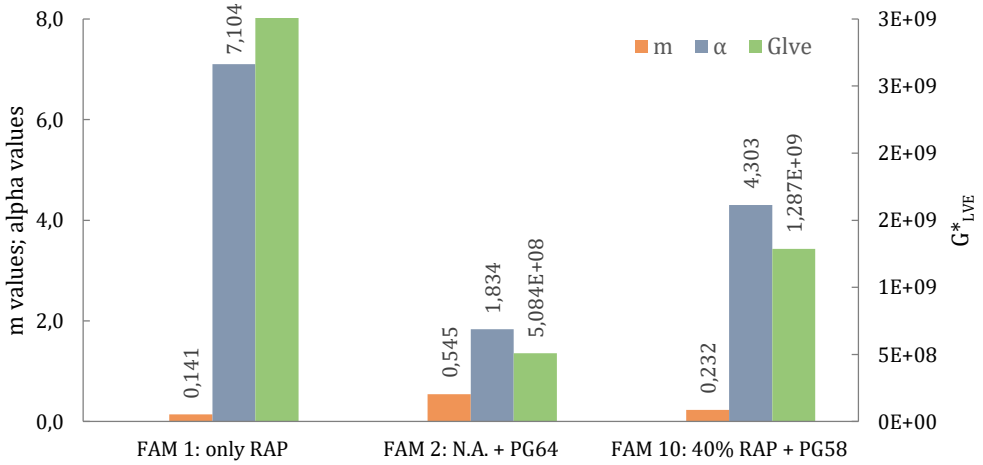

FAM 10 presents an intermediate stiffness between FAM 1 and FAM 2, as well as all the other parameters. At low strain, FAM 10 presented the highest fatigue life. At high strain, the resulting fatigue life is intermediate between FAM 1 and 2.

Figure 4.30. Fatigue lives of FAMs 1, 2, and 10

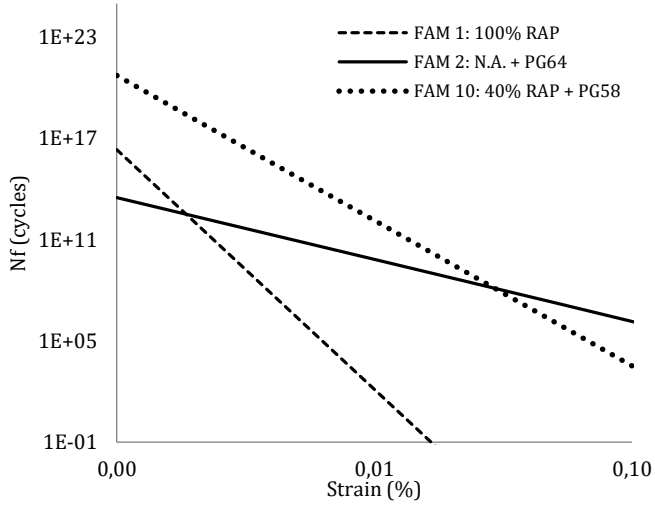

4.6.6. FAM 1 (only RAP), FAM 2 (only new materials) and FAM 11 (20%RAP + 50/50 – PG64/rejuvenator)

FAMs 1, 2 and 11 were compared in order to evaluate the effect of the addition of 50% of oil and 50% of the PG 64 binder to correct the binder content of a mixture prepared with 20% of RAP. Table 4.9 presents the viscoelastic properties of the FAMs and the fatigue model parameters A and B, along with the number of cycles to failure (N_f) at two strain levels. Figure 4.31 shows the comparisons of the linear viscoelastic properties and Figure 4.32 shows the comparison of the fatigue lives of the FAMs analyzed in this subsection. FAM 11 presents an intermediate stiffness between FAM 1 and FAM 2, as well as all the other parameters. The resulting fatigue lives are also intermediate between FAM 1 and 2.

Table 4.19. Characteristics of FAMs 1, 2, and 11

FAM	G^*_{LVE}	m	α	A	B	N_f (0,005%)	N_f (0,050%)
FAM 1: 100% RAP	5.12E+09	0.14	7.10	1.75E+83	14.21	2.52E+06	1.56E-08
FAM 2: N.A.[1] + PG64	5.09E+08	0.55	1.83	1.22E+27	3.67	8.48E+10	1.82E+07
FAM 11: 20% RAP + 50/50 (V.B.[2]/R.A.[3])	9.84E+08	0.38	2.64	7.00E+33	5.30	9.50E+08	4.76E+03

[1]: N.A. – NEW AGGRAGETES; [2]: V.B. – VIRGIN BINDER; [3]: R.A. – REJUVENATING AGENT

Figure 4.31. Graphical comparisons of m, G^*_{LVE} and α values of FAMs 1, 2, and 11

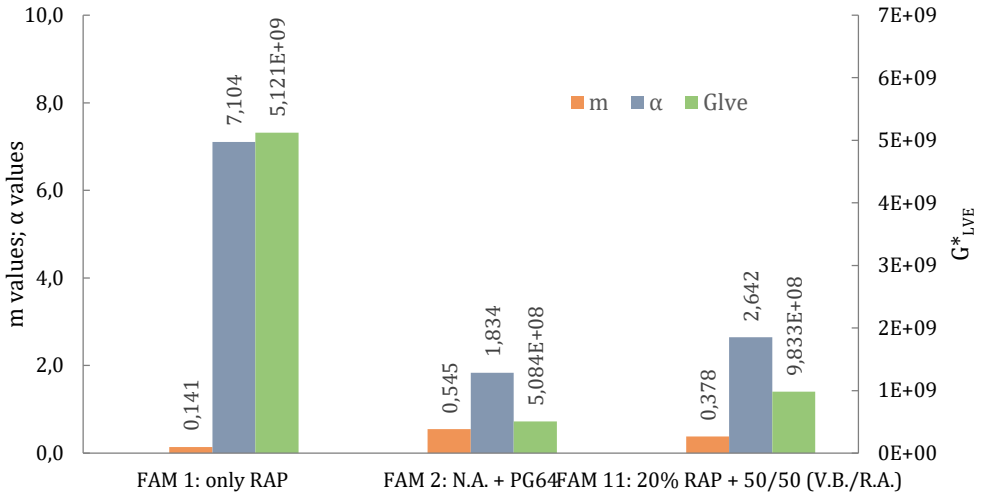

Figure 4.32. Fatigue lives of FAMs 1, 2, and 11

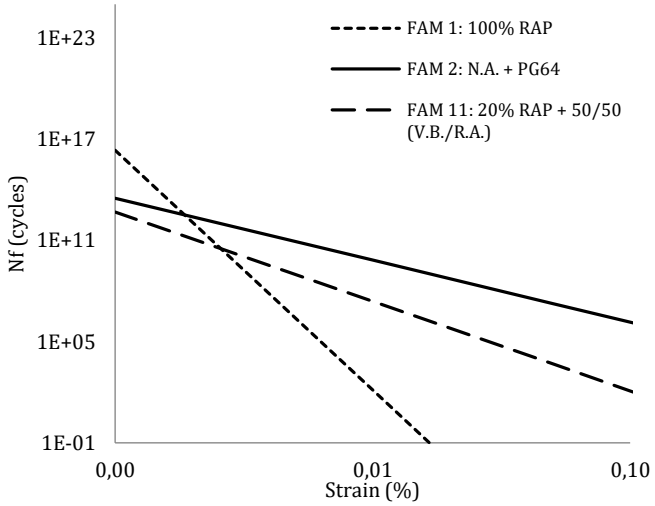

4.6.7. FAM 1 (only RAP), FAM 2 (only new materials) and FAM 12 (20%RAP + 0/100 – PG64/rejuvenator)

FAMs 1, 2 and 12 were compared in order to evaluate the effect of the addition of only oil (no binder) to correct the binder content of a mixture prepared with 20% of RAP. Table 4.10 presents the viscoelastic properties of the FAMs and the fatigue model parameters A and B, along with the number of cycles to failure (N_f) at two strain levels. Figure 4.33 shows the comparisons of the linear viscoelastic properties and Figure 4.34 shows the comparison of the fatigue lives of the FAMs analyzed in this subsection. FAM 12 presents an intermediate stiffness between FAM 1 and FAM 2, as well as all the other parameters. The resulting fatigue lives are also intermediate between FAM 1 and 2.

Table 4.20. Characteristics of FAMs 1, 2, and 12

FAM	G^*_{LVE}	m	α	A	B	N_f (0,005%)	N_f (0,050%)
FAM 1: 100% RAP	5.12E+09	0.14	7.10	1.75E+83	14.21	2.52E+06	1.56E-08
FAM 2: N.A.[1] + PG64	5.09E+08	0.55	1.83	1.22E+27	3.67	8.48E+10	1.82E+07
FAM 12: 20% RAP + 0/100 (V.B.[2]/R.A.[3])	1.21E+09	0.30	3.35	9.38E+39	6.49	8.69E+08	2.80E+02

[1]: N.A. – NEW AGGRAGETES; [2]: V.B. – VIRGIN BINDER; [3]: R.A. – REJUVENATING AGENT

Figure 4.33. Graphical comparisons of *m*, G^*_{LVE} and *α* values of FAMs 1, 2, and 12

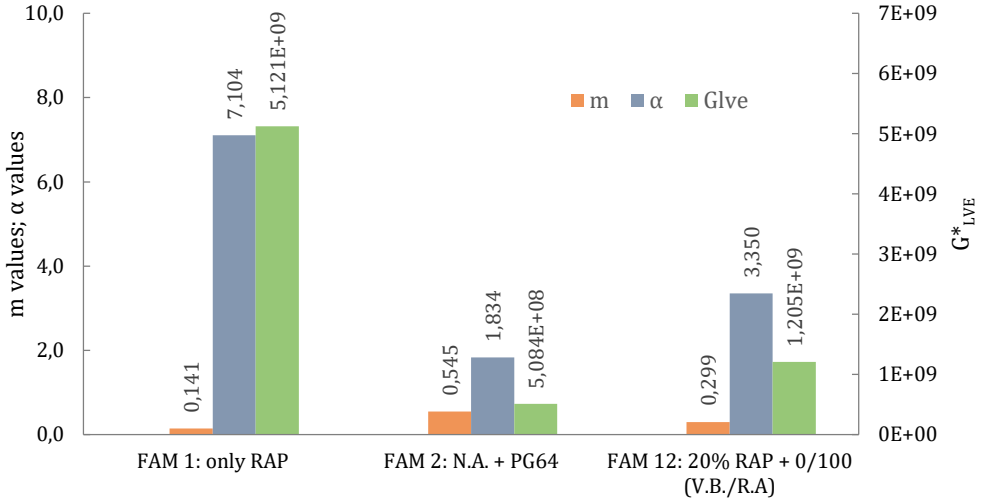

Figure 4.34. Fatigue lives of FAMs 1, 2, and 12

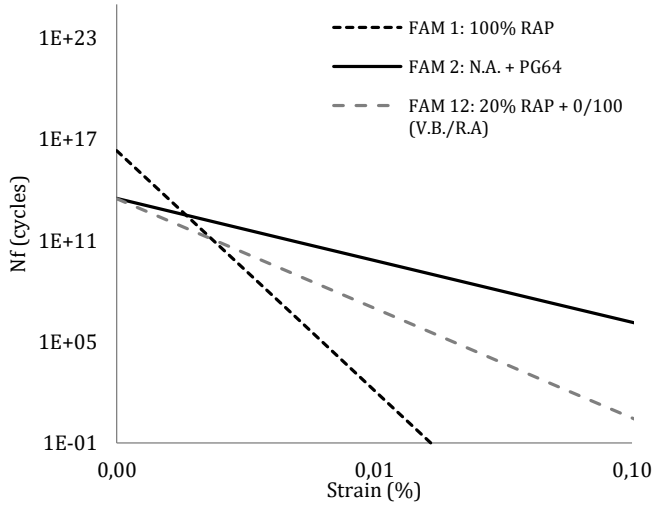

4.6.8. FAM 1 (only RAP), FAM 2 (only new materials) and FAM 13 (40%RAP + 50/50 – PG64/rejuvenator)

FAMs 1, 2 and 13 were compared in order to evaluate the effect of the addition of 50% of rejuvenating agent and 50% of the PG 64 binder to correct the binder content of a mixture prepared with 40 percent of reclaimed asphalt pavement. Table 4.11 presents the viscoelastic properties of the FAMs and the fatigue model parameters A and B, along with the number of cycles to failure (N_f) at two strain levels.

Table 4.21. Characteristics of FAMs 1, 2, and 13

FAM	G^*_{LVE}	m	α	A	B	N_f (0,005%)	N_f (0,050%)
FAM 1: 100% RAP	5.12E+09	0.14	7.10	1.75E+83	14.21	2.52E+06	1.56E-08
FAM 2: N.A.[1] + PG64	5.09E+08	0.55	1.83	1.22E+27	3.67	8.48E+10	1.82E+07
FAM 13: 40% RAP + 50/50 (V.B.[2]/R.A.[3])	1.84E+09	0.28	3.56	1.56E+46	7.12	7.21E+10	5.47E+03

[1]: N.A. – NEW AGGRAGETES; [2]: V.B. – VIRGIN BINDER; [3]: R.A. – REJUVENATING AGENT

Figure 4.35 shows the comparisons of the linear viscoelastic properties. FAM 13 presents an intermediate stiffness between FAM 1 and FAM 2, as well as all the viscoelastic parameters and the fatigue life parameters. The resulting fatigue lives are also intermediate between FAM 1 and 2.

Figure 4.35. Graphical comparisons of m, G^*_{LVE} and α values of FAMs 1, 2, and 13

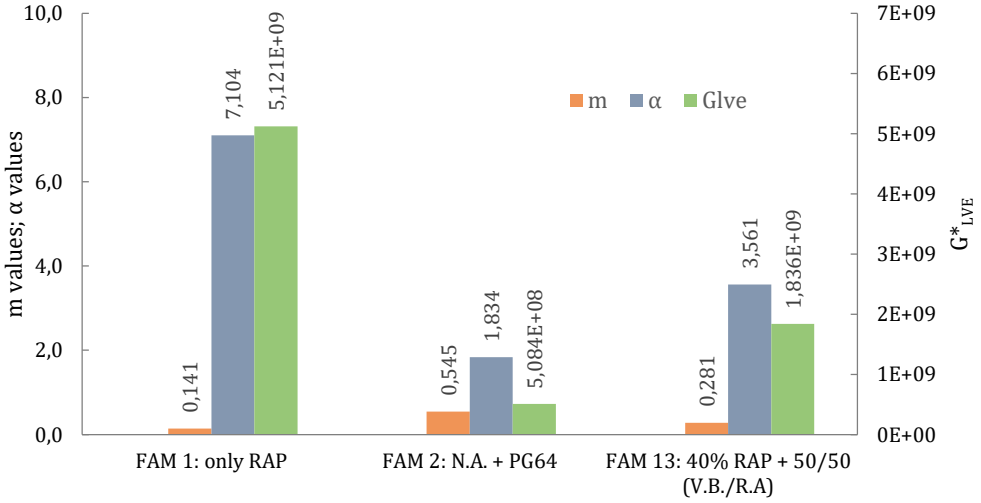

Figure 4.36 shows the graphical comparison of the fatigue lives of the FAMs analyzed in this subsection.

Figure 4.36. Fatigue lives of FAMs 1, 2, and 13

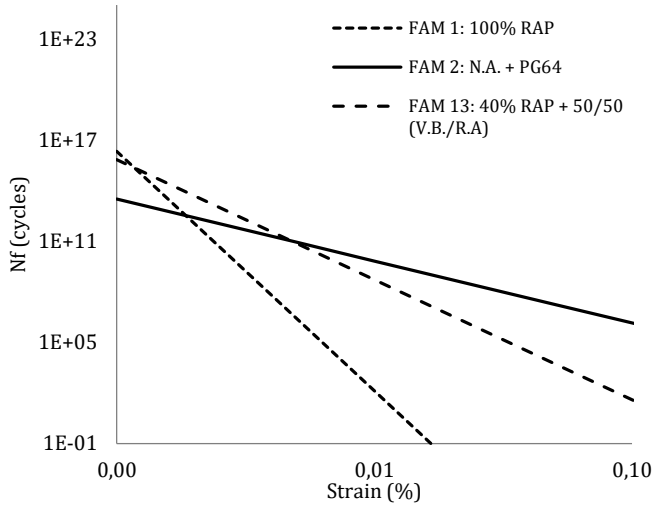

4.6.9. FAM 1 (only RAP), FAM 2 (only new materials) and FAM 14 (40%RAP + 0/100 – PG64/rejuvenator)

FAMs 1, 2 and 14 were compared in order to evaluate the effect of the addition of only oil (no binder) to correct the binder content of a mixture prepared with 40% of RAP. Figure 4.37 shows the comparisons of the linear viscoelastic properties and Figure 4.38 shows the graphical comparison of the fatigue lives of the FAMs analyzed in this subsection.

Figure 4.37. Graphical comparisons of m, G^*_{LVE} and α values of FAMs 1, 2, and 14

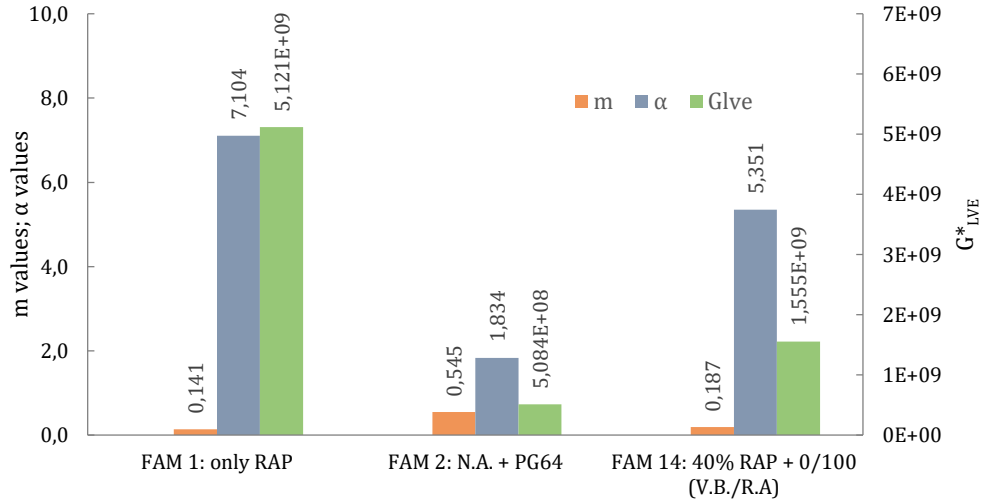

Table 4.12 presents the viscoelastic properties of the FAMs and the fatigue model parameters A and B, along with the number of cycles to failure (N_f) at two strain levels.

FAM 14 presents an intermediate stiffness between FAM 1 and FAM 2, as well as all the viscoelastic parameters and the fatigue life parameters. The resulting fatigue lives are also intermediate between FAM 1 and 2.

Figure 4.38. Fatigue lives of FAMs 1, 2, and 14

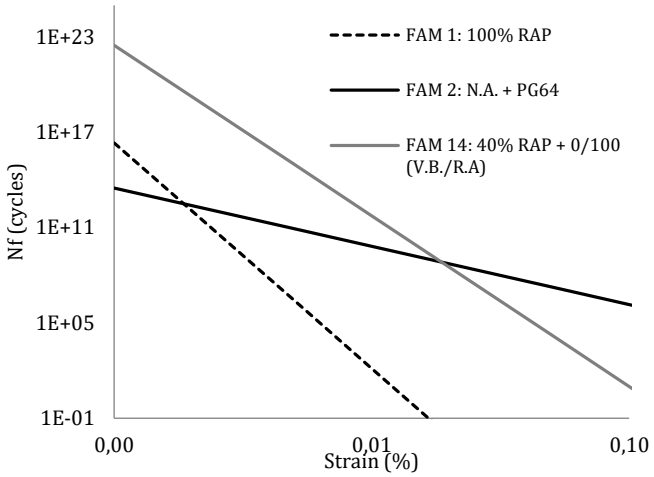

4.6.10. FAM 7 (20%RAP+PG64) and FAM 8 (40%RAP+PG64)

FAMs 7 and 8 were compared in order to evaluate the effect of the addition of different proportions of RAP in the mixture (20% and 40%), when the binder content is corrected with the addition of a PG64 binder. Table 4.13 presents the viscoelastic properties of the FAMs and the fatigue model parameters, A and B, along with the number of cycles to failure (N_f) at two strain levels. The values for FAMs 1 and 2 are also presented for reference.

Table 4.22. Characteristics of FAMs 1, 2, 7 and 8

FAM	G^*_{LVE}	m	α	A	B	N_f (0,005%)	N_f (0,050%)
FAM 1: 100% RAP	5.12E+09	0.14	7.10	1.75E+83	14.21	2.52E+06	1.56E-08
FAM 2: N.A.[1] + PG64	5.09E+08	0.55	1.83	1.22E+27	3.67	8.48E+10	1.82E+07
FAM 7: 20% RAP + PG64	8.54E+08	0.35	2.83	6.31E+36	5.66	3.91E+10	8.55E+04
FAM 8: 40% RAP + PG64	1.54E+09	0.19	5.16	4.66E+65	10.36	1.11E+15	4.84E+04

[1]: N.A. - NEW AGGRAGETES

It can be noted that, at a lower strain level, FAM 8 presents an increase on its fatigue life, when compared to FAM 2, and the fatigue behavior of the FAM 7 is similar to the behavior of FAM 2. For a higher strain level, both FAMs 7 and 8 require a lower number of cycles to failure when they are compared to FAM 2, indicating that the addition of RAP

produced a negative effect on the fatigue life of the mixtures at higher strain levels. Summarizing, the increase in the RAP content from 20 to 40%, when the PG 64 binder is used, increased substantially the fatigue life at low strain levels and reduced it slightly (about 50%) at high strain levels.

Figure 4.39. Graphical comparisons of m, G^*_{LVE} and α values of FAMs 1, 2, 7 and 8

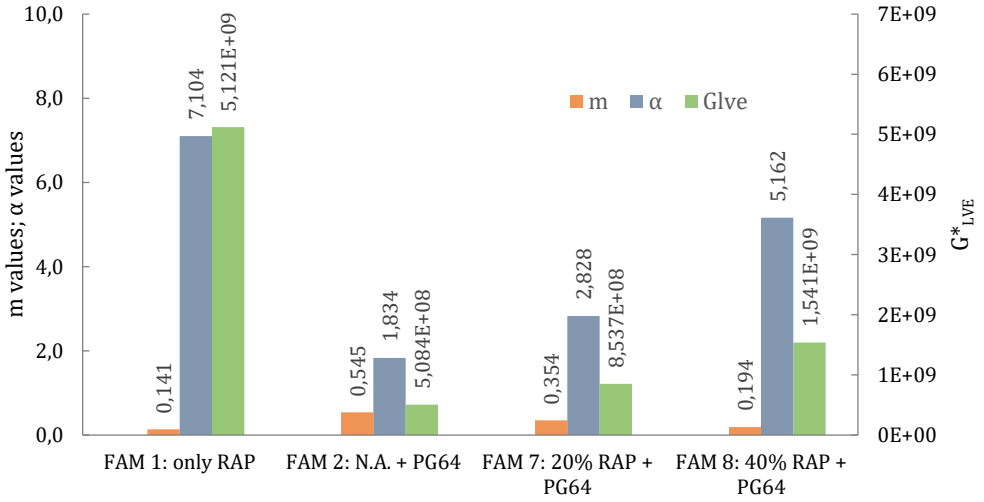

Figure 4.40. Fatigue lives of FAMs 1, 2, 7 and 8

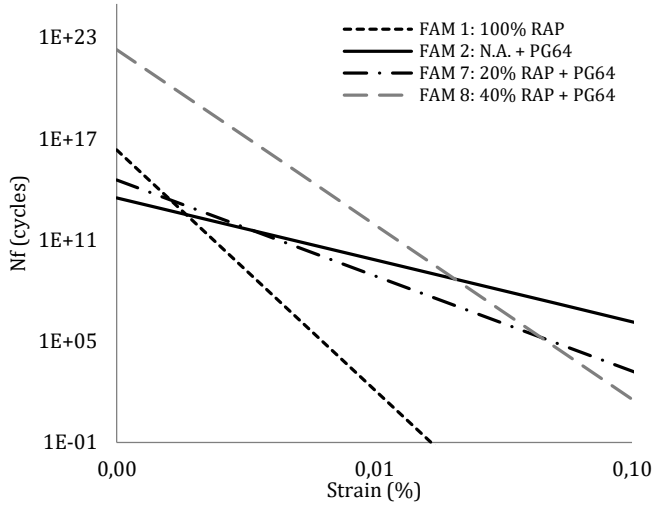

4.6.11. FAM 9 (20%RAP+PG58) and FAM 10 (40%RAP+PG58)

FAMs 9 and 10 were compared in order to evaluate the effect of the addition of different proportions of RAP in the mixture (20% and 40%), when the binder content is corrected with the addition of a PG58 binder. Table 4.14 presents the viscoelastic properties of the FAMs and the fatigue model parameters, A and B, along with the number

of cycles to failure (N_f) at two strain levels. The values for FAMs 1 and 2 are also presented for reference.

Table 4.23. Characteristics of FAMs 1, 2, 9 and 10

FAM	G^*_{LVE}	m	α	A	B	N_f (0,005%)	N_f (0,050%)
FAM 1: 100% RAP	5.12E+09	0.14	7.10	1.75E+83	14.21	2.52E+06	1.56E-08
FAM 2: N.A.[1] + PG64	5.09E+08	0.55	1.83	1.22E+27	3.67	8.48E+10	1.82E+07
FAM 9: 20% RAP + PG58	7.95E+08	0.41	2.45	7.21E+33	4.92	1.71E+11	2.05E+06
FAM 10: 40% RAP + PG58	1.29E+09	0.23	4.30	1.27E+56	8.61	5.29E+14	1.31E+06

[1]: N.A. - NEW AGGRAGETES

Figure 4.41. Graphical comparisons of m, G^*_{LVE} and α values of FAMs 1, 2, 9 and 10

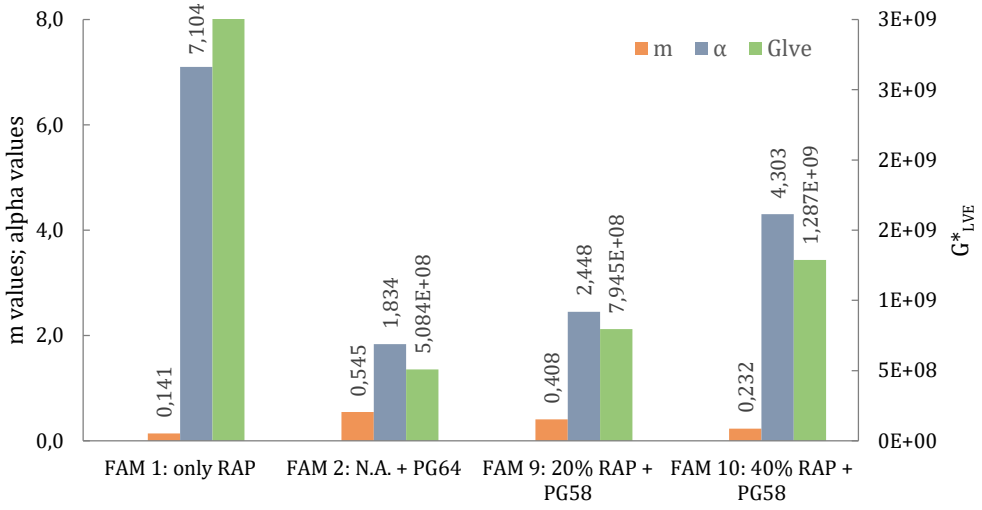

Figure 4.42. Fatigue lives of FAMs 1, 2, 9 and 10

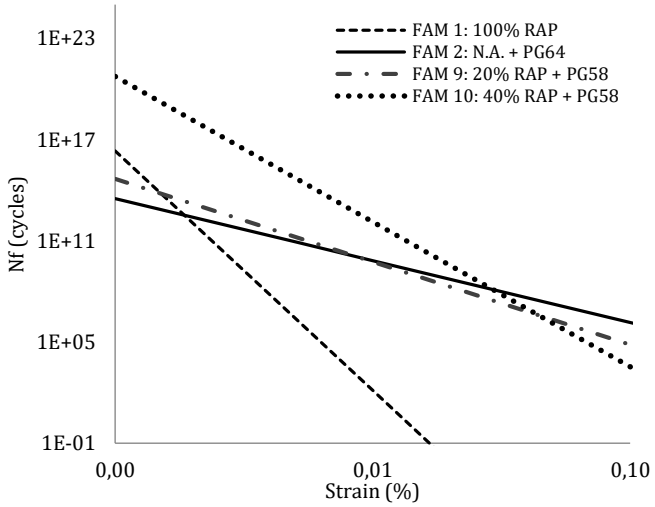

At a lower strain, FAM 9 has a fatigue life two times higher than FAM 2 and FAM 10 presents a fatigue life substantially higher than FAM 2. At a higher strain, FAMs 9 and 10 require a lower number of cycles to failure, when they are compared to FAM 2. Summarizing, the increase in the RAP content from 20 to 40%, when the PG 58 binder is used, increased substantially the fatigue life at low strain levels (two times for FAM 9 and more than 6,000 times for FAM 10) and reduced it expressively (in about 90%) at high strain levels.

4.6.12. FAM 7 (20%RAP+PG64) and FAM 9 (20%RAP+PG58)

FAMs 7 and 9 were compared in order to evaluate the effect of the addition of different binders (PG64 or PG58) to correct the binder content of the mixtures containing 20% RAP. Table 4.15 presents the viscoelastic properties of the FAMs and the fatigue model parameters, A and B, along with the number of cycles to failure (N_f) at two strain levels. The values for FAMs 1 and 2 are also presented for reference.

The type of binder significantly influenced the fatigue life of the mixtures: at low strains, FAM 9 presents a fatigue life 4.4 times higher than FAM 7, and at high strain, the fatigue life is 24 times higher. Compared to FAM 2, FAM 7 presents a lower fatigue life (about 50%) and FAM 9 presents a higher fatigue life (two times), when low strains are taken into account. At higher strain levels, FAM 7 and 9 present much lower fatigue lives as compared to FAM 2 (less than 0.5% for FAM 7 and around 11% for FAM 9). Summarizing, the use of a PG58 in place of a PG64, for a RAP content of 20%, increases the fatigue life both at low and high strain levels, and FAMs 7 and 9, in general terms, present fatigue lives lower than the one presented by FAM 2.

Table 4.24. Characteristics of FAMs 1, 2, 7 and 9

FAM	G^*_{LVE}	m	α	A	B	N_f (0,005%)	N_f (0,050%)
FAM 1: 100% RAP	5.12E+09	0.14	7.10	1.75E+83	14.21	2.52E+06	1.56E-08
FAM 2: N.A.[1] + PG64	5.09E+08	0.55	1.83	1.22E+27	3.67	8.48E+10	1.82E+07
FAM 7: 20% RAP + PG64	8.54E+08	0.35	2.83	6.31E+36	5.66	3.91E+10	8.55E+04
FAM 9: 20% RAP + PG58	7.95E+08	0.41	2.45	7.21E+33	4.92	1.71E+11	2.05E+06

[1]: N.A. - NEW AGGRAGETES

Figure 4.43. Graphical comparisons of *m*, G^*_{LVE} and α values of FAMs 1, 2, 7 and 9

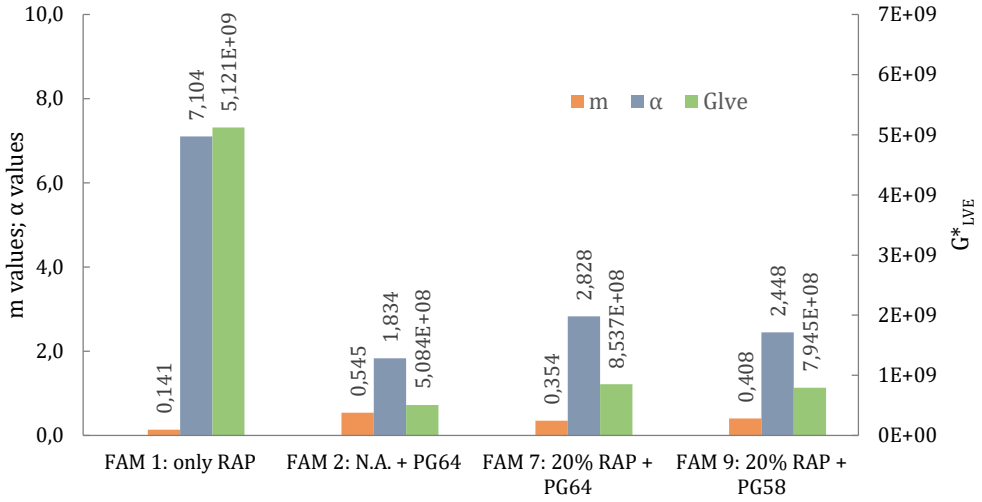

Figure 4.44. Fatigue lives of FAMs 1, 2, 7 and 9

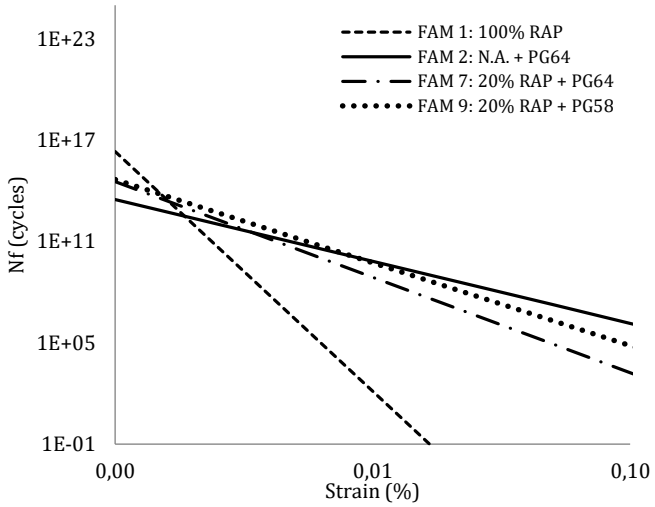

4.6.13. FAM 8 (40%RAP+PG64) and FAM 10 (40%RAP+PG58)

FAMs 8 and 10 were compared in order to evaluate the effect of the addition of a different binder (PG64 or PG58) to correct the binder content of the mixtures containing 40% of RAP. Table 4.16 presents the viscoelastic properties of the FAMs and the fatigue model parameters, A and B, along with the number of cycles to failure (N_f) at two strain levels. The values for FAMs 1 and 2 are also presented for reference.

At a lower level of strain, the FAM 8 and 10 require a higher number of cycles to failure, when they are compared to FAM 2, especially for FAM 8, which presents a significantly increase in its fatigue life. For a higher level of strain, the fatigue lives of the FAMs 8 and 10 presented a decrease, indicating that the addition of 40% of RAP does not improve the fatigue performance, independently of the binder utilized.

The type of binder significantly influenced the fatigue life of the mixtures: at low strains, FAM 8 presents a fatigue life that is roughly 2 times higher than the one estimated for FAM 10, and at high strain, the fatigue life of FAM 10 is 27 times higher than FAM 8. Compared to FAM 2, FAM 8 and 10 present a much higher fatigue life (more than 13 thousand times for FAM 8 and more than 6 thousand times for FAM 10), when low strains are taken into account. At higher strain levels, FAM 8 and 10 present much lower fatigue lives as compared to FAM 2 (less than 0.3% for FAM 8 and around 7% for FAM 10). Summarizing, the use of a PG58 in place of a PG64, for a RAP content of 40%, leads to a reduction of about 50% in the fatigue life of FAM 10 as compared to FAM 8, at low strain levels, and results in an increase of 27 times in the fatigue life of FAM 10 as compared to FAM 8, at high strain levels. When FAMs 8 and 10 are compared to FAM 2, FAMs 8 and 10 present fatigue lives much higher than FAM 2, at low strains, and fatigue lives much lower at high strains.

Table 4.25. Characteristics of FAMs 1, 2, 8 and 10

FAM	G^*_{LVE}	m	α	A	B	N_f (0,005%)	N_f (0,050%)
FAM 1: 100% RAP	5.12E+09	0.14	7.10	1.75E+83	14.21	2.52E+06	1.56E-08
FAM 2: N.A.[1] + PG64	5.09E+08	0.55	1.83	1.22E+27	3.67	8.48E+10	1.82E+07
FAM 8: 40% RAP + PG64	1.54E+09	0.19	5.16	4.66E+65	10.36	1.11E+15	4.84E+04
FAM 10: 40% RAP + PG58	1.29E+09	0.23	4.30	1.27E+56	8.61	5.29E+14	1.31E+06

[1]: N.A. - NEW AGGRAGETES

Figure 4.45. Graphical comparisons of *m*, G^*_{LVE} and *α* values of FAMs 1, 2, 8 and 10

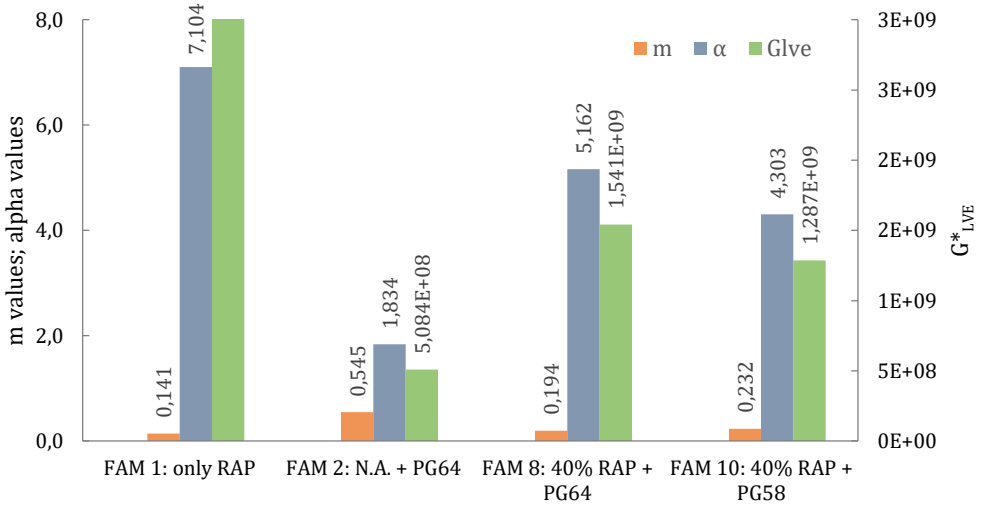

Figure 4.46. Fatigue lives of FAMs 1, 2, 8 and 10

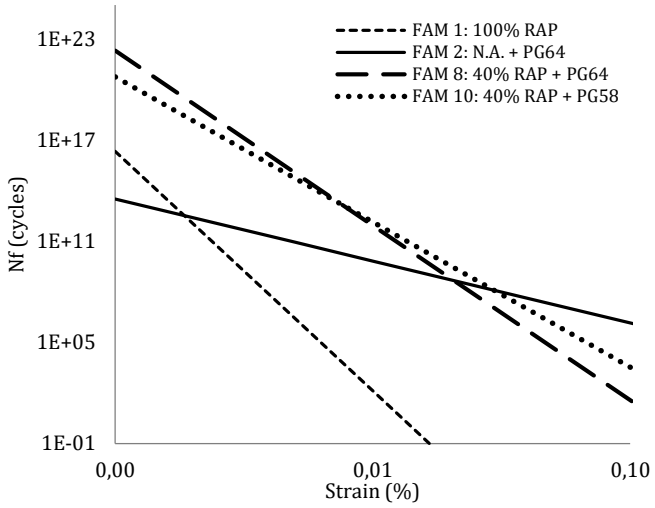

4.6.14. FAM 11 (20%RAP + 50/50 – PG64/rejuvenator) and FAM 12 (20%RAP + 0/100 – PG64/rejuvenator)

FAMs 11 and 12 were compared in order to evaluate the effect of the addition of a different proportion of oil (50% or 100%) to correct the binder content of the mixtures containing 20% of RAP and the PG64 binder. Table 4.17 presents the viscoelastic properties of the FAMs and the fatigue model parameters, A and B, along with the number of cycles to failure (N_f) at two strain levels. The values for FAMs 1 and 2 are also presented for reference.

The use of 100% oil instead of 50/50% ratio of binder/oil to correct the binder content influenced the fatigue life of the mixtures differently at low and high strains: FAM 12 presents a fatigue life that is roughly 10% lower than the one estimated for FAM 11, at low strains, and FAM 12 presents a fatigue life that is roughly 94 percent lower than the one estimated for FAM 11, at high strains. Compared to FAM 2, FAM 11 and 12 present a much lower fatigue life, at both low and high strains: the fatigue lives of FAM 11 and 12 represent about 1 percent of the fatigue life o FAM 2 at low strains and less than 0.1 percent at high strains.

Table 4.26. Characteristics of FAMs 1, 2, 11 and 12

FAM	G^*_{LVE}	m	α	A	B	N_f (0,005%)	N_f (0,050%)
FAM 1: 100% RAP	5.12E+09	0.14	7.10	1.75E+83	14.21	2.52E+06	1.56E-08
FAM 2: N.A.[1] + PG64	5.09E+08	0.55	1.83	1.22E+27	3.67	8.48E+10	1.82E+07
FAM 11: 20% RAP + 50/50 (V.B.[2]/R.A.[3])	9.84E+08	0.38	2.64	7.00E+33	5.30	9.50E+08	4.76E+03
FAM 12: 20% RAP + 0/100 (V.B.[2]/R.A.[3])	1.21E+09	0.30	3.35	9.38E+39	6.49	8.69E+08	2.80E+02

[1]: N.A. – NEW AGGRAGETES; [2]: V.B. – VIRGIN BINDER; [3]: R.A. – REJUVENATING AGENT

Summarizing, the use of only oil instead of a 50/50 percent ratio of binder/oil, when 20% of RAP is used, reduced the fatigue life of the FAM 12 as compared to FAM 11, both at low and high strains. When FAMs 11 and 12 are compared to FAM 2, much lower fatigue lives are obtained, both at low and high strains.

Figure 4.47. Graphical comparisons of m, G^*_{LVE} and α values of FAMs 1, 2, 11 and 12

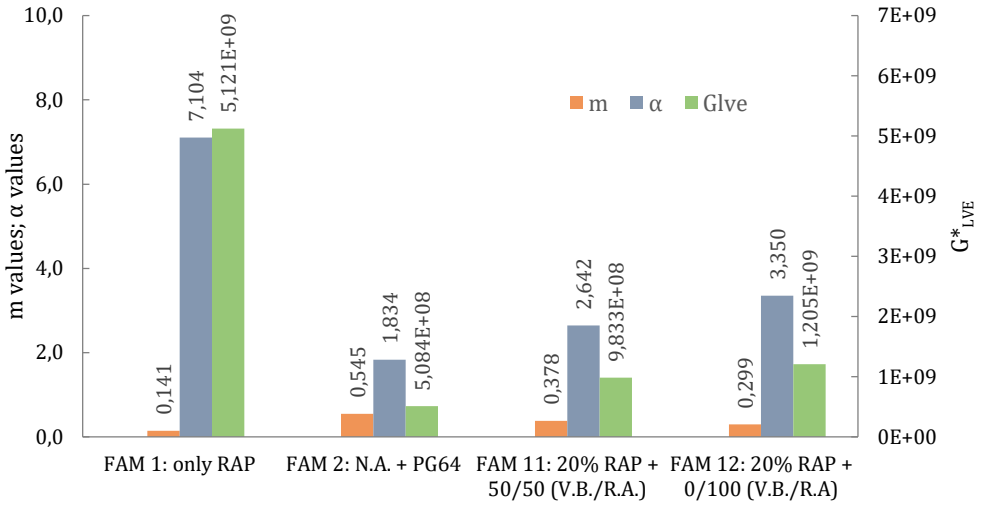

Figure 4.48. Fatigue lives of FAMs 1, 2, 11 and 12

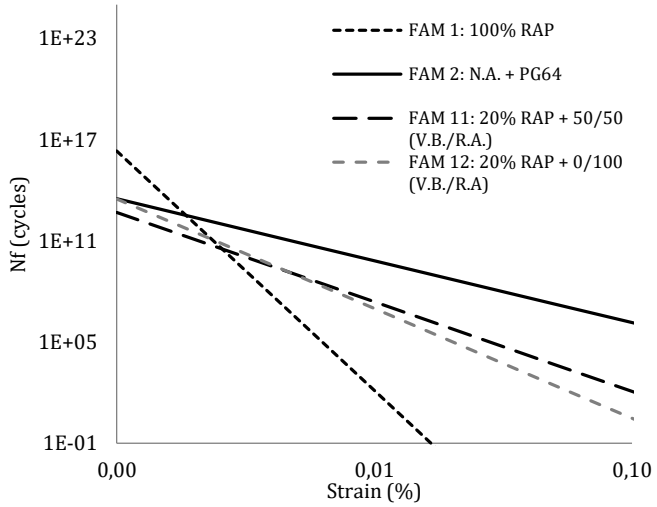

4.6.15. FAM 13 (40%RAP + 50/50 – PG64/rejuvenator) and FAM 14 (40%RAP + 0/100 – PG64/rejuvenator)

FAMs 13 and 14 were compared in order to evaluate the effect of the addition of a different proportion of oil (50% or 100%) to correct the binder content of the mixtures prepared with 40% of RAP and the PG64 binder. Table 4.18 presents the viscoelastic

properties of the FAMs and the fatigue model parameters, A and B, along with the number of cycles to failure (N_f) at two strain levels. The values for FAMs 1 and 2 are also presented for reference.

Table 4.27. Characteristics of FAMs 1, 2, 13 and 14

FAM	G^*_{LVE}	m	α	A	B	N_f (0.005%)	N_f (0.050%)
FAM 1: 100% RAP	5.12E+09	0.14	7.10	1.75E+83	14.21	2.52E+06	1.56E-08
FAM 2: N.A.[1] + PG64	5.09E+08	0.55	1.83	1.22E+27	3.67	8.48E+10	1.82E+07
FAM 13: 40% RAP + 50/50 (V.B.[2]/R.A.[3])	1.84E+09	0.28	3.56	1.56E+46	7.12	7.21E+10	5.47E+03
FAM 14: 40% RAP + 0/100 (V.B./R.A.)	1.56E+09	0.19	5.35	3.25E+67	10.74	9.35E+14	1.70E+04

[1]: N.A. – NEW AGGRAGETES; [2]: V.B. – VIRGIN BINDER; [3]: R.A. – REJUVENATING AGENT

Figure 4.49. Graphical comparisons of m, G^*_{LVE} and α values of FAMs 1, 2, 13 and 14

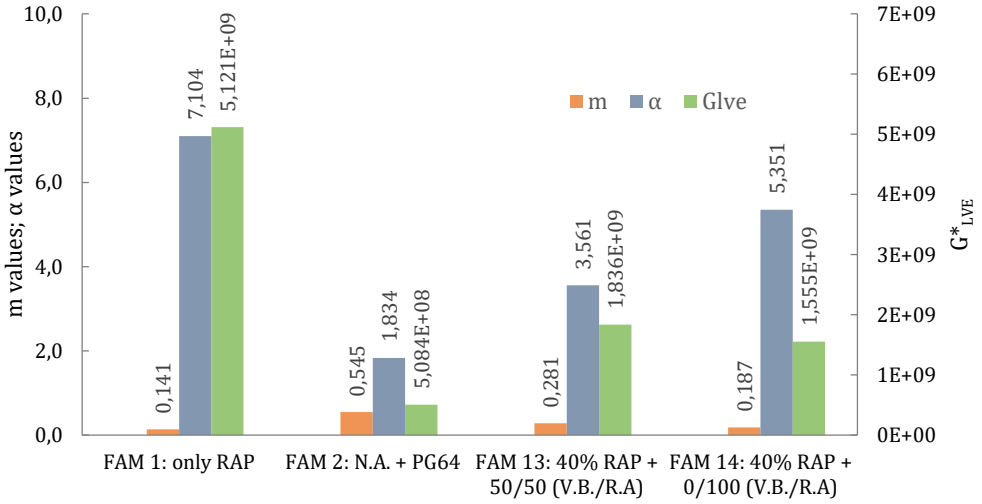

The use of 100% oil instead of 50/50% ratio of binder/oil to correct the binder content was capable of increasing the fatigue lives of the mixtures with different intensities at low and high strains: FAM 14 presents a fatigue life that is 13 thousand times higher than the one estimated for FAM 13, at low strains, and FAM 14 presents a fatigue life that is only 3 times higher than the one estimated for FAM 13, at high strains. Compared to FAM 2, FAM 13 presents a fatigue life slightly lower (85% of the fatigue life of FAM 2), and FAM 14 presents a much higher fatigue life (about 11 thousand times), at low strains. At high strains, FAMs 13 and 14 present much lower fatigue lives than FAM 2 (less than 0.1 percent). Summarizing, the use of only oil instead of a 50/50 percent ratio of binder/oil, when 40% of RAP is used, increased the fatigue life of the FAM 14 as compared to FAM 12, both at low and high strains, with an expressive effect at low strain

(13 thousand times at low strains against 3 times at high strains). When FAMs 11 and 12 are compared to FAM 2, much lower fatigue lives are obtained at low high strains. At low strains, FAM 13 presents a fatigue life slightly lower and FAM 14 presents a fatigue life expressively higher (11 thousand times).

Figure 4.50. Fatigue lives of FAMs 1, 2, 13 and 14

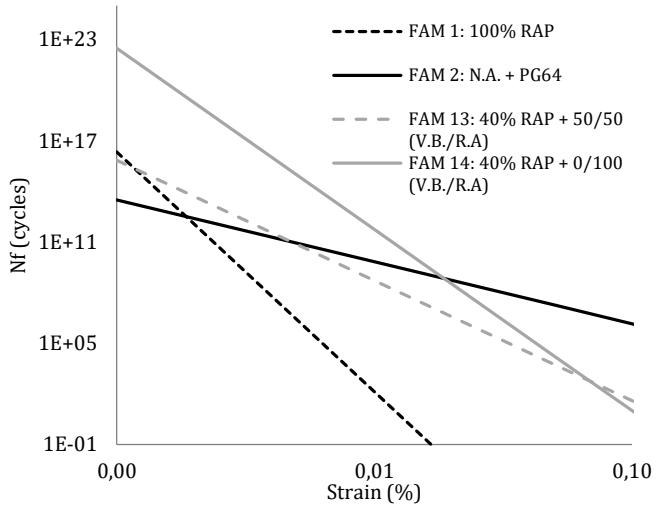

4.6.16. FAM 7 (20%RAP + 100/0 – PG64/rejuvenator), FAM 9 (20%RAP + 100/0 – PG58/rejuvenator), FAM 11 (20%RAP + 50/50 – PG64/rejuvenator) and FAM 12 (20%RAP + 0/100 – PG64/rejuvenator)

FAMs 7, 9, 11 and 12 were compared in order to evaluate which is the best option to correct the binder content of the mixtures containing 20% of RAP: 100% of a PG 64 binder, 100% of a PG 58 binder, 50/50% binder/oil (PG 64), or 100% oil. Table 4.19 presents the viscoelastic properties of the FAMs and the fatigue model parameters, A and B, along with the number of cycles to failure (N_f) at two strain levels.

Table 4.28. Characteristics of FAMs 7, 9, 11 and 12

FAM	G^*_{LVE}	m	α	A	B	N_f (0,005%)	N_f (0,050%)
FAM 7: 20% RAP + PG64	8.54E+08	0.35	2.83	6.31E+36	5.66	3.91E+10	8.55E+04
FAM 9: 20% RAP + PG58	7.95E+08	0.41	2.45	7.21E+33	4.92	1.71E+11	2.05E+06
FAM 11: 20% RAP + 50/50 (V.B.[2]/R.A.[3])	9.84E+08	0.38	2.64	7.00E+33	5.30	9.50E+08	4.76E+03
FAM 12: 20% RAP + 0/100 (V.B.[2]/R.A.[3])	1.21E+09	0.30	3.35	9.38E+39	6.49	8.69E+08	2.80E+02

[1]: N.A. – NEW AGGRAGETES; [2]: V.B. – VIRGIN BINDER; [3]: R.A. – REJUVENATING AGENT

At low strains, the highest fatigue life is generated by the use of 100% of a PG 58 binder, followed by the use of 100% of a PG 64 binder, followed by the use of 50/50 percent binder/oil (PG 64), even though the fatigue life of the FAM prepared with only 100% oil is practically the same of the FAM prepared with 50/50 percent binder/oil (PG 64). Likewise, at high strains, the highest fatigue life is generated by the use of 100% of a PG 58 binder, followed by the use of 100% of a PG 64 binder, followed by the use of 50/50 percent binder/oil (PG 64). The lowest fatigue life is obtained for the FAM prepared with only oil at both strain levels.

Figure 4.51. Graphical comparisons of *m*, G^*_{LVE} and α values of FAMs 7, 9, 11 and 12

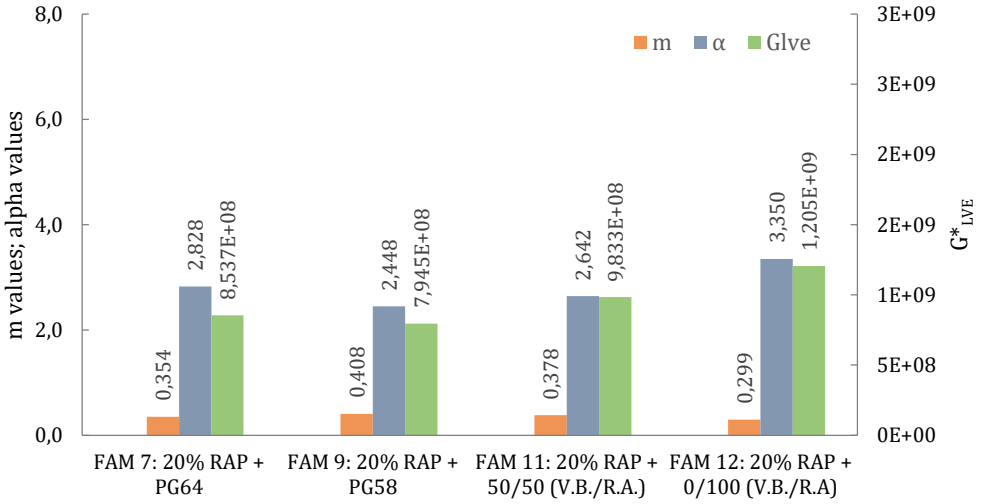

Figure 4.52. Fatigue lives of FAMs 7, 9, 11 and 12

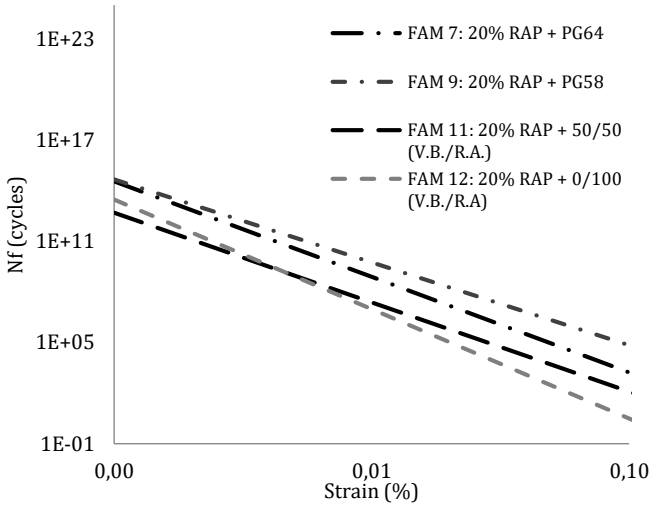

4.6.17. FAM 8 (40%RAP + 100/0 – PG64/rejuvenator), FAM 10 (40%RAP + 100/0 – PG58/rejuvenator), FAM 13 (40%RAP + 50/50 – PG64/rejuvenator) and FAM 14 (40%RAP + 0/100 – PG64/rejuvenator)

FAMs 8, 10, 13 and 14 were compared in order to evaluate which is the best option to correct the binder content of the mixtures containing 40% of RAP: 100% of a PG 64 binder, 100% of a PG 58 binder, 50/50% binder/oil (PG 64), or 100% oil. Table 4.20 presents the viscoelastic properties of the FAMs and the fatigue model parameters, A and B, along with the number of cycles to failure (N_f) at two strain levels.

At low strains, the highest fatigue life is generated by the use of 100% of a PG 64 binder, followed by the use of 100% oil, followed by the use of 100% of a PG 58, with the use of 50/50% binder/oil (PG 64) as the last alternative. At high strains, the highest fatigue life is generated by the use of 100% of a PG 58 binder, followed by the use of 100% of a PG 64 binder, followed by the use of 100% oil, with the use of 50/50% binder/oil (PG 64) as the last alternative.

Table 4.29. Characteristics of FAMs 8, 10, 13 and 14

FAM	G^*_{LVE}	m	α	A	B	N_f (0,005%)	N_f (0,050%)
FAM 8: 40% RAP + PG64	1.54E+09	0.19	5.16	4.66E+65	10.36	1.11E+15	4.84E+04
FAM 10: 40% RAP + PG58	1.29E+09	0.23	4.30	1.27E+56	8.61	5.29E+14	1.31E+06
FAM 13: 40% RAP + 50/50 (V.B.[2]/R.A.[3])	1.84E+09	0.28	3.56	1.56E+46	7.12	7.21E+10	5.47E+03
FAM 14: 40% RAP + 0/100 (V.B./R.A.)	1.56E+09	0.19	5.35	3.25E+67	10.74	9.35E+14	1.70E+04

[1]: N.A. – NEW AGGRAGETES; [2]: V.B. – VIRGIN BINDER; [3]: R.A. – REJUVENATING AGENT

Figure 4.53. Graphical comparisons of m, G^*_{LVE} and α values of FAMs 8, 10, 13 and 14

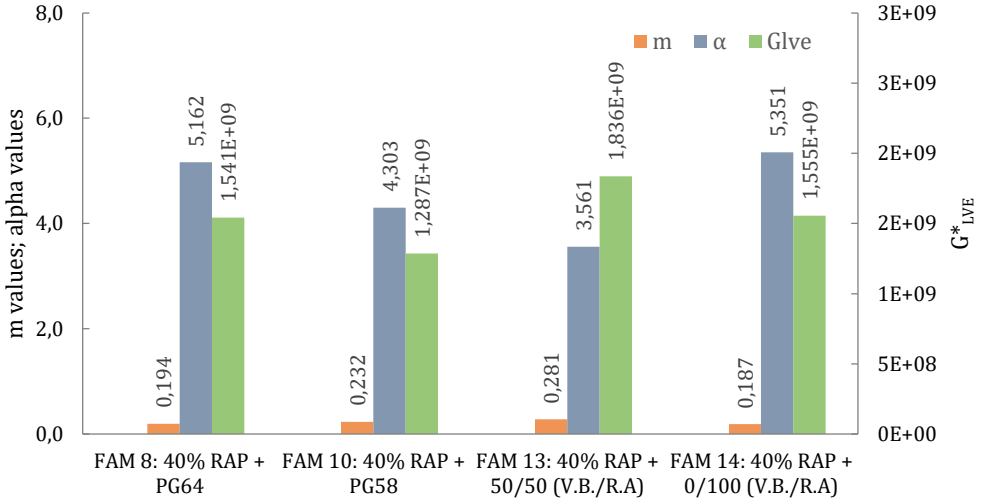

Figure 4.54. Fatigue lives of FAMs 8, 10, 13 and 14

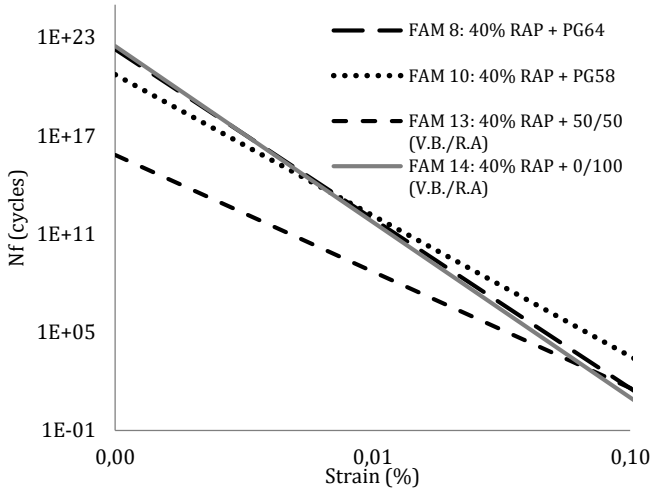

4.6.18. Final rank order

The objective of this section is to order the FAMs in relation to the number of axle-load repetitions that takes the material to failure. Two strain levels where adopted in this analysis, i. e., 0.005 and 0.05%, once that the materials tend to present different responses to low and high strains. This rank order consists in the ascription of a numerical value, between 1 and 10, referring to the classification of the material in a rank of the results of all materials. The numeration was ascribed from the best to the worse materials, in such a way that the best results received lower values and the worse ones received the highest ones. The best results represent the materials whose number of axle load repetitions is higher. The materials were first ranked according to the strain level (0.005 and 0.5 percent). Posteriorly, they were ranked according to the average position for the two strain levels. Two scenarios were taken into account to build this rank order: one in which failure happens after a reduction of pseudo stiffness to 50% of the original one and another one in which failure occurs after a reduction of pseudo stiffness to 30% of the original one. For this analysis, it is assumed that the best results represent the lowest damage evolution rates and the highest fatigue lives.

Figure 4.55 and 4.56 show the rank order of the FAMs for the two strain levels, 0.005 and 0.5 percent, respectively, for a reduction of pseudo stiffness to 50% of the original. Figure 4.57 presents the final rank order for a reduction of pseudo stiffness to 50% of the original, and in this case, the results represent the average rank order for the two strain levels.

Figure 4.55. Rank order of the FAMs for the low strain level (0.005 %) for a reduction to 50% of the original pseudo stiffness

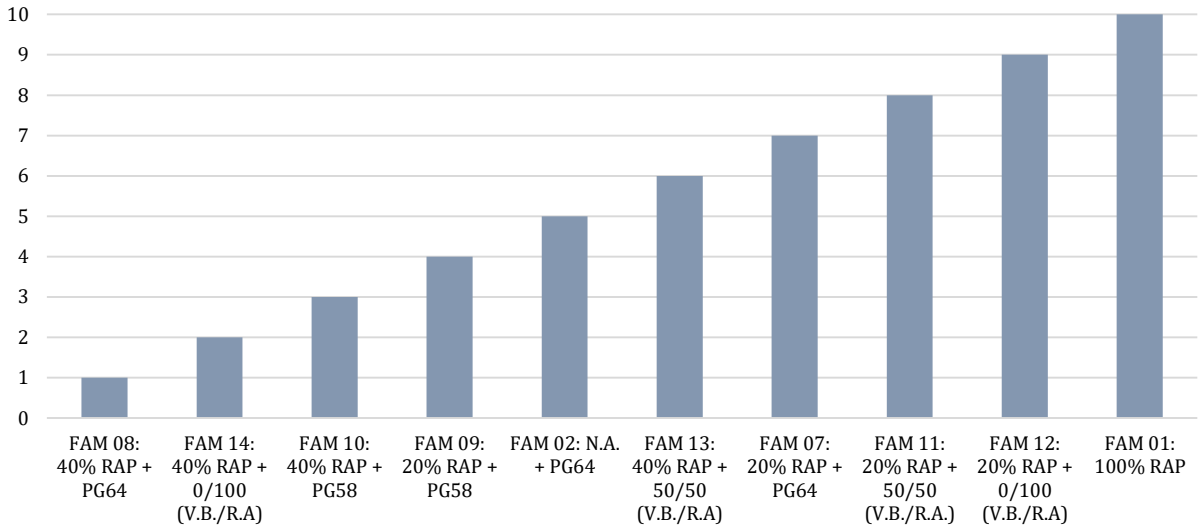

Figure 4.55 shows the rank order of the FAMs for the low strain level (0.005 %) for a reduction to 50% of the original stiffness, with FAM 1 occupying the last position, what means that it presents the lowest fatigue life. On the other hand, FAM 8 presented the highest fatigue life, followed by FAM 14 and FAM 10.

Figure 4.56. Rank order of the FAMs for the high strain level (0.05 %) for a reduction to 50% of the original pseudo stiffness

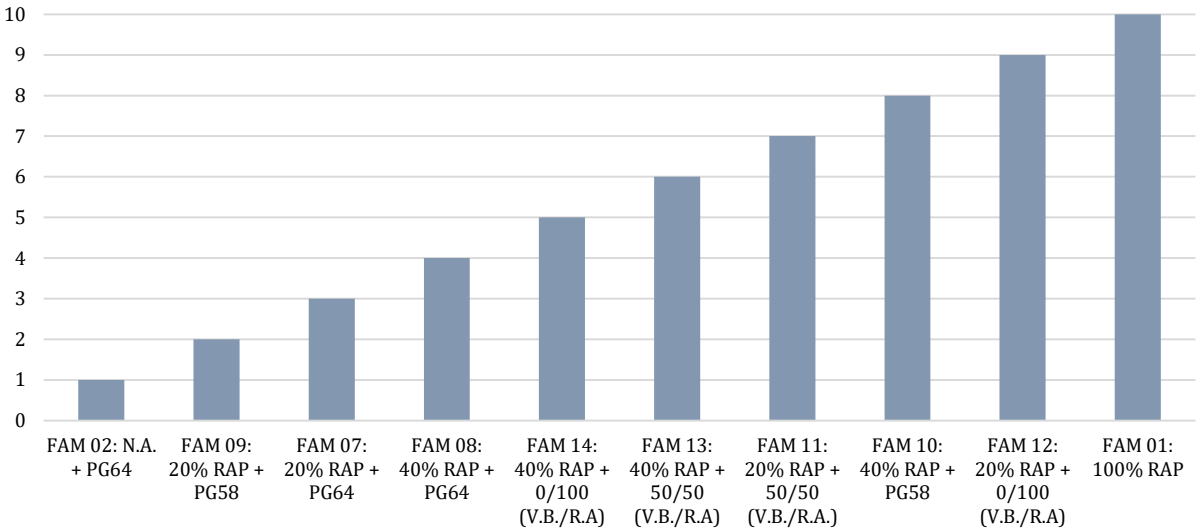

Figure 4.56 shows the rank order of the FAMs for the high strain level (0.05 %) for a reduction to 50% of the original stiffness, with FAM 1 occupying the last position, and FAM 2 occupying the first position, followed by FAM 9 and FAM 7.

Figure 4.58 and 4.59 show the rank order of the FAMs for the two strain levels, for a reduction of pseudo stiffness to 30% of the original. Figure 4.60 presents the final rank order for a reduction of pseudo stiffness to 30% of the original, and in this case, the results represent the average rank order for the two strain levels. Figure 4.57 shows the final rank order of the FAMs for the two strain levels for a reduction to 50% of the original stiffness, with FAM 1 occupying the last position, and FAM 8 occupying the first position, followed by FAM 9 and FAM 2.

Figure 4.57. Rank order of the FAMs for both strain levels (0.005 and 0.05 percent) for a reduction to 50% of the original pseudo stiffness

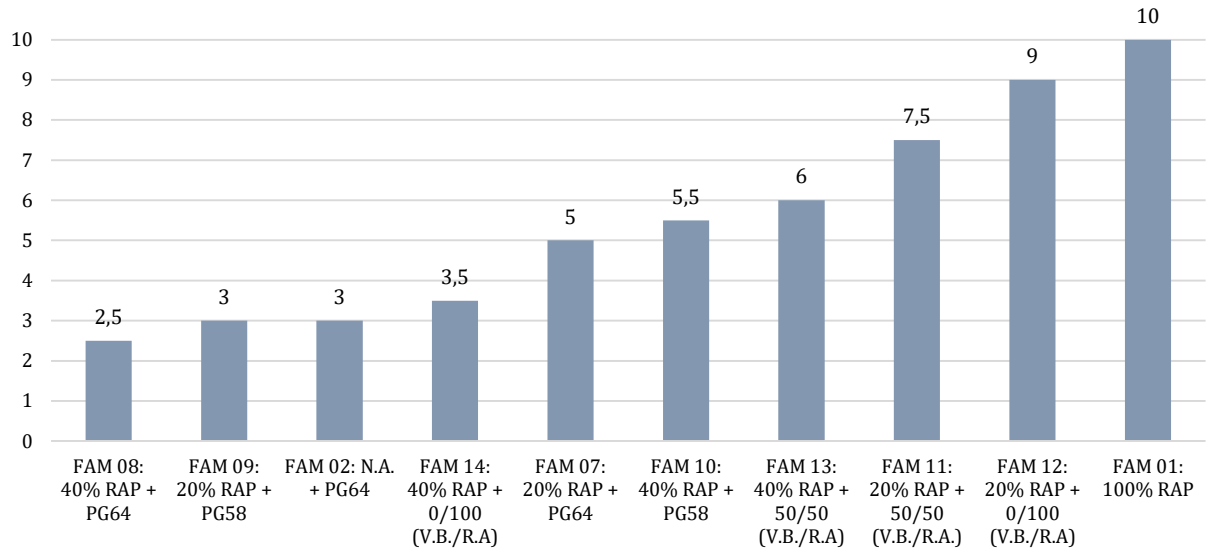

Figure 4.58. Rank order of the FAMs for the low strain level (0.005 %) for a reduction to 30% of the original pseudo stiffness

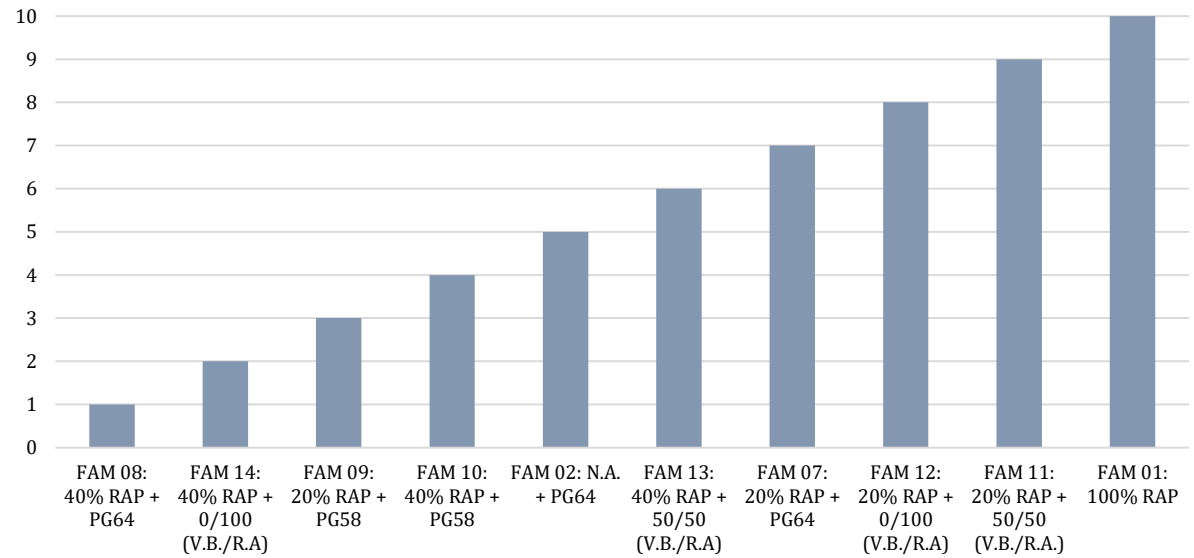

Figure 4.58 shows the rank order of the FAMs for the low strain level (0.005 %) for a reduction to 30% of the original stiffness, with FAM 1 occupying the last position, and FAM 8 occupying the first position, followed by FAM 14 and FAM 9.

Figure 4.59. Rank order of the FAMs for the high strain level (0.05 %) for a reduction to 30% of the original stiffness

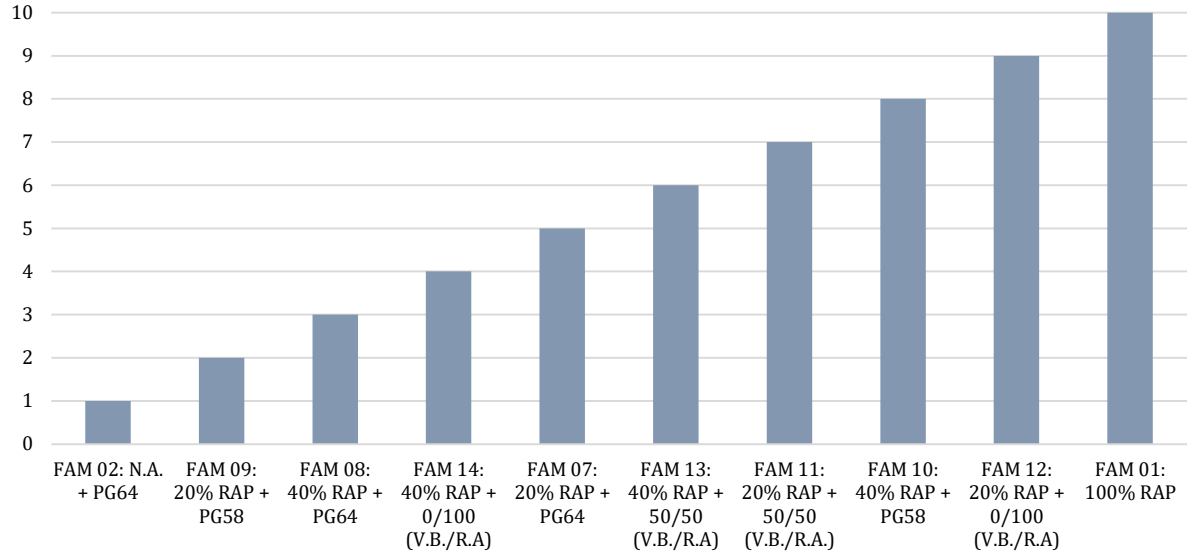

Figure 4.59 shows the rank order of the FAMs for the high strain level (0.5 %) for a reduction to 30% of the original stiffness, with FAM 1 occupying the last position, and FAM 2 occupying the first fatigue life, followed by FAM 9 and FAM 8.

Figure 4.60. Rank order of the FAMs for both strain levels (0.005 and 0.05 percent) for a reduction to 30% of the original pseudo stiffness

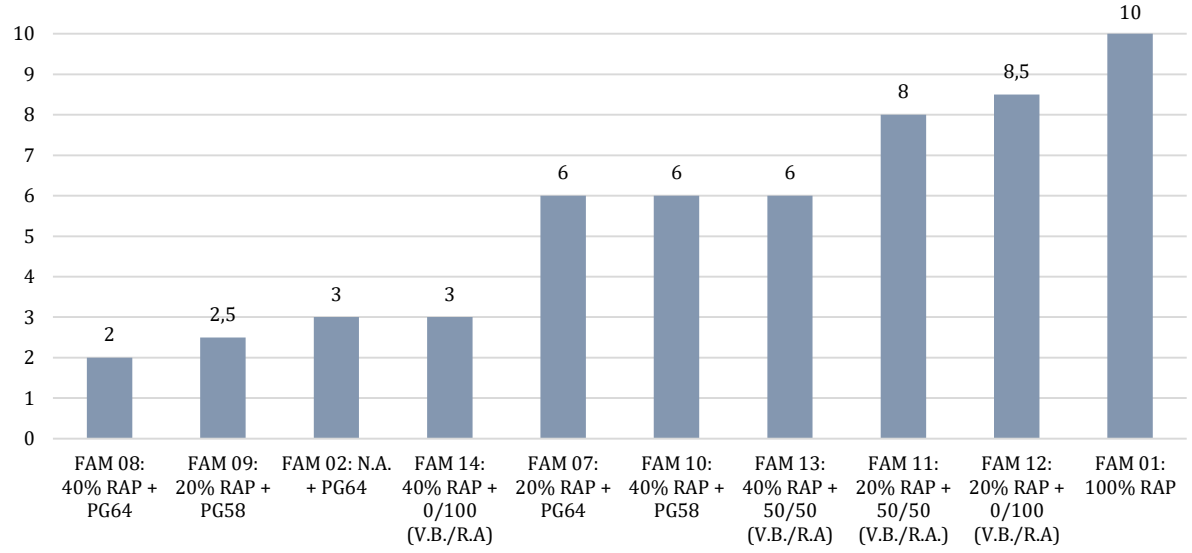

Figure 4.60 shows the final rank order of the FAMs for the two strain levels for a reduction to 30% of the original stiffness, with FAM 1 occupying the last position, and FAM 8 occupying the first position, followed by FAM 9 and FAM 2.

Figure 4.61 shows the final rank order, considering the average rank order for the reductions of pseudo stiffness to 50 and 30% of the initial pseudo stiffness, for low and high strains, with FAM 1 occupying the last position, and FAM 8 occupying the first position, followed by FAM 9 and FAM 2.

Figure 4.61. Final rank order of the FAMs for the average positions for a reduction to 50 and 30% of the original stiffness

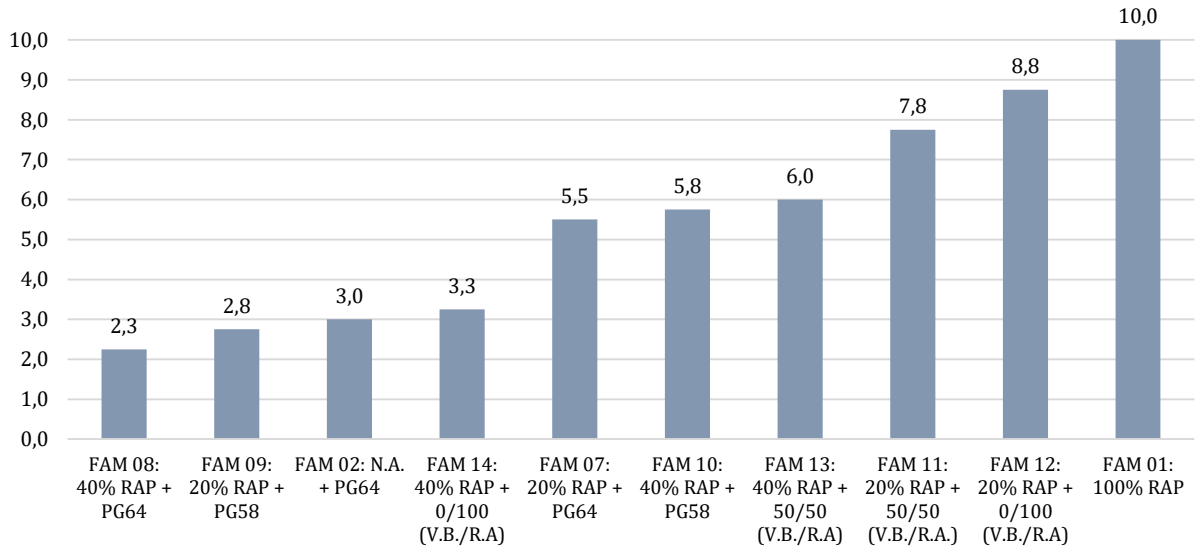

Figures 4.62 and 4.63 show the rank order for the initial stiffness and the damage evolution rate of the FAMs, respectively. It is possible to notice that FAM 1 presents the highest stiffness and the highest damage evolution rate. FAM 2 presents the lowest stiffness, followed by FAM 9 and FAM 7. FAM 2 presents the lowest damage evolution rate, followed by FAM 9 and FAM 11.

Table 4.21 presents the correlations between the results for G^*_{LVE} and N_f at 0.005 and 0.05%, considering a reduction of pseudo stiffness to 50% of the original, along with the correlations between the results for the damage evolution rate and N_f at 0.005 and 0.05%, also considering a reduction of pseudo stiffness to 50% of the original.

Figure 4.62. Rank order of the FAMs for the G^*_{LVE} values

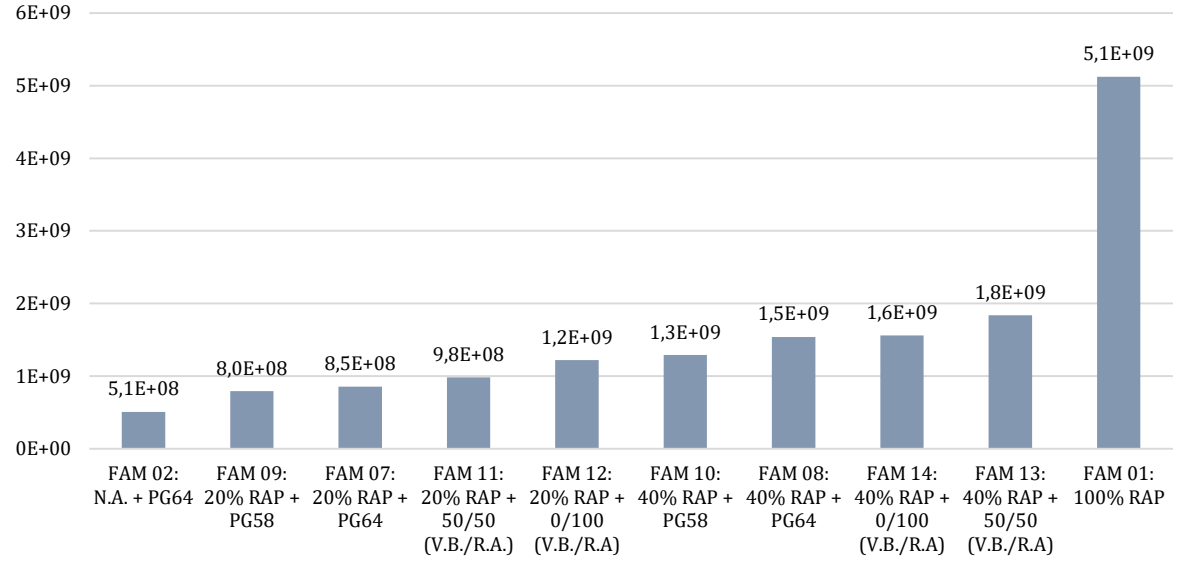

Figure 4.63. Rank order of the FAMs for the α values

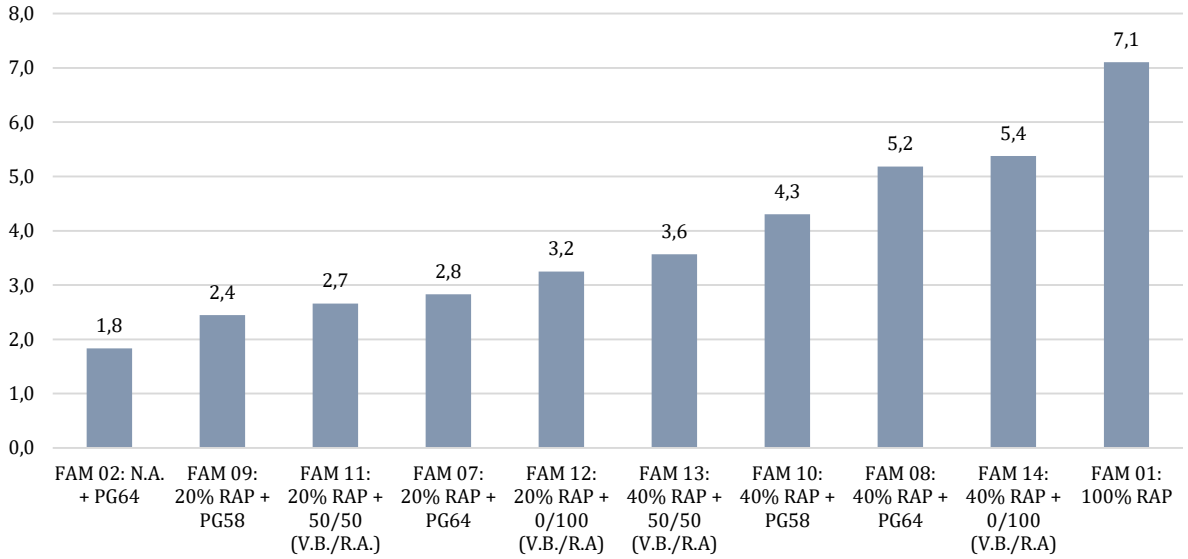

Table 4.30. Correlations between linear viscoelastic properties of the FAMs

properties	correlations
G^*_{LVE} vs α	+0.84
G^*_{LVE} vs N_f at 0.005% strain	-0.04
G^*_{LVE} vs N_f at 0.5% strain	-0.32
α vs N_f at 0.005% strain	+0.49
α vs N_f at 0.5% strain	-0.47

Table 4.25 shows that there is a strong correlation between the initial stiffness of the samples and the damage evolution rate, with the damage evolution rate presenting

higher values at higher material stiffness values. The correlations between the initial stiffness of the samples and the fatigue lives at both strain levels is very poor, but there is some evidence that the trend is the reduction of the fatigue life with the increase in the stiffness. In terms of the damage evolution rate, the correlations are relatively low, with opposite trends depending on the strain level: for low strains, the fatigue life increases with the increase in the damage evolution rate, and for low strains, the fatigue life decreases with the increase in the damage evolution rate.

5. CONCLUSIONS

The objective of this Master's dissertation is to evaluate the effects of the addition of different percentages of Reclaimed Asphalt Pavements (RAP) in the production of new asphalt mixtures on the fatigue performance of fine aggregate matrices (FAMs). This study also evaluated the effects of the use of two binders of different performance grades (PG 64-22 and PG 58-16) and the combination of new binder (PG 64-22) and rejuvenating agent (shale oil residue) at different binder/agent rates (100/0, 50/50 and 0/100). Two reference mixtures were prepared, one with 100 percent RAP and another with 100 percent of new materials (mineral aggregate and asphalt binder), in order to compare their fatigue behavior with those obtained for the FAMs composed with RAP.

The study lays on the hypothesis defended by some researchers that the fatigue cracking starts in discontinuities present in the full asphalt mixtures, such as air voids and micro cracks, and develops under the application of reversible loading over time. Such micro cracks, according to those researchers, develop in two circumstances: (i) after adhesive failure, when the crack occurs in the interface aggregate-mortar, and/or (ii) after cohesive failure, when the crack develops within the mortar. Based on such interpretation of the cracking phenomenon in asphalt mixtures, it is plausible to use the fine aggregate matrices to estimate the fatigue behavior of the full asphalt mixture. This hypothesis is basis for the development of this study, in which the effects of the addition of RAP and the use of different binder/agent ratios on the fatigue behavior of full asphalt mixtures is investigated by means of the study fine aggregate matrices.

5.1. Major findings

The major findings of this investigation are presented below:

- the addition of RAP at the percentages of 20, 40 and 100% had an expressive impact on the viscoelastic properties of the fine aggregates matrices: it increased the linear viscoelastic complex modulus (G^*_{LVE}) and decreased the relaxation rate (m);
- the FAM produced with 100 percent RAP (FAM 1) presented the highest G^*_{LVE} and the lowest relaxation rate; conversely, the FAM produced with 100 percent new materials (FAM 2) presented the lowest G^*_{LVE} and the highest relaxation rate; the

other materials – prepared with 20 and 40% of RAP and different binder/agent ratios – presented G^*_{LVE} and m values between those presented by FAMs 1 and 2; FAM 9 is the second softer materials and FAM 7 is the third softer material; FAM 9 and FAM 11 occupy the second and the third positions in terms of higher relaxation rate;

- the FAMs prepared with 40% of RAP presented higher stiffnesses and lower relaxations rates as compared to the FAMs prepared with 20% of RAP – the RAP material is naturally stiffer than a mixture prepared with only new materials and the mixing of such hard material with new materials turns the final composite into a material stiffer than the FAM prepared with only new materials; such higher stiffness is expressed in terms of lower relaxations rates;
- the use of only a binder of lower performance grade (PG 58) to correct the binder content of the FAMs reduced the stiffness only slightly and increased the relaxation rate of the samples, as compared to the PG64, and this is valid for the two RAP contents;
- the substitution of 50% of oil for 50% of a PG 64 binder resulted in a stiffness higher than the one observed for the FAM prepared only with the PG 64 binder and 20% of RAP; the same observation was made for the FAMs prepared only with the PG 64 binder and 40% of RAP - it is believed that the rejuvenating agent would be capable of reducing the stiffness in all cases, but the opposite results observed in some comparisons are probably due to the low diffusion of the oil into the old binder;
- the substitution of 50% of oil for 50% of a PG 64 binder resulted in a relaxation rate intermediate between the ones obtained for the FAMs prepared with the PG 64 binder and the PG 58 binder, when a RAP content of 20% is considered; for 40% of RAP, the substitution of 50% of oil for 50% of a PG 64 binder resulted in a relaxation rate higher than the ones obtained for the FAMs prepared with the PG 64 binder and the PG 58 binder; it is believed that the rejuvenating agent would be capable of increasing the relaxation rates in all cases, and the higher relaxation rate observed for FAM 13 are evidences of a good diffusion rate, but, on the other hand, the results obtained for FAM 11 reinforce the evidence of the low diffusion rates of the oil into the aged binder;

- the use of only oil to correct the binder contents of the FAMs reduced the stiffness of the samples only when 40% of RAP was used, and it was unable of increasing the relaxation rate of the samples for both RAP contents; the worst alternative is the use of only oil (FAMs 12 and 14), once that the relaxation rates obtained for such materials are lower than the ones obtained for the FAMs prepared with the PG 64 binder with no oil - this is another important evidence of the low diffusion rate of the oil into the aged binder;
- the FAM prepared with 100% of RAP is the material with the highest rate of damage accumulation and the FAM prepared with new mineral aggregate and new binder is the material with the lowest rate; the FAMs prepared with 20 and 40% of RAP present intermediate damage evolution rates between the values observed for the FAMs 1 and 2;
- the FAMs prepared with 20% of RAP presented lower damage evolution rates as compared to the FAMs prepared with 40% of RAP - the RAP material is naturally more prone to damage accumulation, because of the presence of the aged binder, as compared to a mixture prepared with only new material, and the mixing of such aged material with new materials turns the final composite into a material with a higher damage evolution rate;
- the use of a lower PG grade reduced the damage evolution rate of the materials, as compared to the PG 64, and this is valid for the two RAP contents;
- the substitution of 50% of oil for 50% of a PG 64 binder resulted in a damage evolution rate that is intermediate between the results obtained for the FAM prepared with the PG 58 binder and the PG 64 binder, when 20% of RAP is used; the same observation is valid for the FAMs prepared with 40% of RAP, except for FAM 13, which presented a damage evolution rate lower than the FAM prepared with the soft binder;
- the use of only oil, as compared to the use of asphalt and oil, was incapable of decreasing the damage evolution rate of the materials, and the same is valid for the FAM produced with 40% of RAP; the worst alternative is the use of only oil, once that the damage evolution rates obtained for such materials are higher than the ones obtained for the FAMs prepared with the PG 64 binder with no oil;

- FAM 1 presents the highest values of the parameters A and B of the mechanistic fatigue prediction model ($N_f = A.\gamma^{-B}$), what is a reflection of the highest initial stiffness and the lowest relaxation rate of this material – because of that, such material is more prone to fatigue cracking than all the others; conversely, FAM 2 presents the lowest values of A and B, what is a reflection of the lowest initial stiffness and the highest relaxation rate of this material, and because of that, such material presents one of the best fatigue performance; the increase in the RAP amount from 20 to 40% increased the A and B values, as a consequence of the addition of the aged binder;
- for the FAMs prepared with 20 and 40% of RAP, the use of the softer binder reduced the A and B values as compared to the FAMs prepared with the PG 64 binder;
- the use of only oil instead of 50% of binder + 50% of oil led to an increase in the A and B values both for the FAMs prepared with 20 and 40% of RAP;
- the increase in the RAP content from 20 to 40%, when the PG 64 binder is used, increased substantially the fatigue life at low strain levels and reduced it slightly (about 50%) at high strain levels; when the PG 58 binder is used, the fatigue life increases substantially (two times for FAM 9 and more than 6,000 times for FAM 10), at low strain levels, and reduces expressively (in about 90%) at high strain levels;
- the use of a PG58 (FAM 9) replacing the PG64 (FAM 7) resulted in the increase of the fatigue life both at low and high strains, but, in general terms, FAMs 7 and 9 presented fatigue lives lower than the one presented by FAM 2, for a RAP content of 20%; when a RAP content of 40% is adopted, the use of the PG 58 (FAM 10) in substitution to the PG 64 (FAM 8) led to a reduction of about 50% in the fatigue life at low strains, and to an increase of 27 times in the fatigue life at low strains; when compared to FAM 2, FAMs 8 and 10 presented much higher fatigue lives at low strains, and much lower fatigue lives at high strains;
- the use of only oil (FAM 12) instead of a 50/50 percent ratio of binder/agent (FAM 11), when 20% of RAP is used, resulted in the reduction of the fatigue life both at low and high strains; when compared to FAM 2, FAMs 11 and 12 presented much lower fatigue lives both at low and high strains; when 40% of RAP is adopted, the

use of only oil (FAM 14) instead of a 50/50 percent ratio of binder/agent (FAM 13) resulted in the increase of the fatigue life both at low and high strains, with an expressive effect at low strain (13 thousand times at low strains against 3 times at high strains); when compared to FAM 2, FAMs 11 and 12 presented much lower fatigue lives at low high strains, and at low strains, FAM 13 presents a fatigue life slightly lower and FAM 14 presents a fatigue life expressively higher (11 thousand times);

- out of the four alternatives to correct the binder content of the FAMs prepared with 20% of RAP (100% of a PG 64 binder, 100% of a PG 58 binder, 50/50% binder/oil (PG 64), or 100% oil), the following answer are provided: at low strains, the highest fatigue life is generated by the use of 100% of a PG 58 binder, followed by the use of 100% of a PG 64 binder, followed by the use of 50/50 percent binder/oil (PG 64), even though the fatigue life of the FAM prepared with only 100% oil is practically the same of the FAM prepared with 50/50 percent binder/oil (PG 64); likewise, at high strains, the highest fatigue life is generated by the use of 100% of a PG 58 binder, followed by the use of 100% of a PG 64 binder, followed by the use of 50/50 percent binder/oil (PG 64); the lowest fatigue life is obtained for the FAM prepared with only oil at both strain levels;
- a similar evaluation was carried out for the RAP content of 40% and the following answers are provided: at low strains, the highest fatigue life is generated by the use of 100% of a PG 64 binder, followed by the use of 100% oil, followed by the use of 100% of a PG 58, with the use of 50/50% binder/oil (PG 64) as the last alternative; at high strains, the highest fatigue life is generated by the use of 100% of a PG 58 binder, followed by the use of 100% of a PG 64 binder, followed by the use of 100% oil, with the use of 50/50% binder/oil (PG 64) as the last alternative;
- when the materials are ranked in terms of their fatigue lives at low strains (0.005 %) for a reduction to 50% of the original stiffness, FAM 1 occupies the last position, with the lowest fatigue life, and, on the other hand, FAM 8 presents the highest fatigue life, followed by FAM 14 and FAM 10 – in this case, the best FAMs are all produced with 40% of RAP; also at low strains but assuming a reduction to 30% of the original stiffness, FAM 1 presents the lowest fatigue life, and FAM 8 presents the highest one, followed by FAM 14 and FAM 9 – in this case, the first two best FAMs are produced with 40% of RAP;

- when the materials are ranked in terms of their fatigue lives at high strains (0.5 %) for a reduction to 50% of the original stiffness, FAM 1 presents the lowest fatigue life, and FAM 2 presents the highest one, followed by FAM 9 and FAM 7 – FAM 2 produced with 100 percent new materials and the other two produced with 20% of RAP; also at low strains but assuming a reduction to 30% of the original stiffness, FAM 1 presents the lowest fatigue life, and, FAM 2 presents the highest one, followed by FAM 9 (20% of RAP) and FAM 8 (40% of RAP);
- the final rank order of the FAMs for the average positions for a reduction to 50 and 30% of the original pseudo stiffness and for low and high strains showed that FAM 1 presents the lowest fatigue life, and FAM 8 (40% of RAP) presents the highest one, followed by FAM 9 (20% of RAP) and FAM 2;
- the analysis of correlation indicated that there is a strong correlation between the initial stiffness of the samples and the damage evolution rate, with the damage evolution rate presenting higher values at higher material stiffness values; the correlations between the initial stiffness of the samples and the fatigue lives at both strain levels is very poor, but there is some evidence that the trend is the reduction of the fatigue life with the increase in the stiffness; in terms of the damage evolution rate, the correlations are relatively low, with opposite trends depending on the strain level: for low strains, the fatigue life increases with the increase in the damage evolution rate, and for low strains, the fatigue life decreases with the increase in the damage evolution rate.
- it is important to call the reader's attention to the fact that the FAMs present air voids reasonably different, once that the air voids are a significant variable on the fatigue performance of asphalt mixtures. The good performance of FAM 2, 7, 8, 9 and 10 can be partially explained by the lower air voids, once lower air voids represent a lower number of discontinuities in the mixture. On the other hand, experimental results showed that FAMs with similar air voids presented significantly different linear viscoelastic properties and C vs S curves, as can be seen for FAMs 7 and 12. This is an important issue that should be address in future investigations.

5.2. Final remarks

The overall results of relaxation rate and damage accumulation rate show that the harder the material (in terms of G^*_{LVE} values) the lower the relaxation rate and higher the damage accumulation rate. Such increase in stiffness and the consequences on the relaxation rate and the damage evolution rate is a direct effect of the presence of RAP. In other words, the aged binder compromises the relaxation rates of the materials and increases the damage evolution rate due to its higher stiffness. The use of a softer binder is capable of increasing the relaxation rates and consequently reducing the damage evolution rate, as compared to a FAM prepared with a PG 64 binder. On the other hand, the effect of substituting 50% of the PG 64 binder by oil had a divergent effect: a positive effect when 40% of RAP was used and a negative effect when 20% of RAP was used.

In terms of fatigue life predicted by means of the use of the mechanistic fatigue prediction model adjusted with basis on the C vs S curves of the FAMs, two elements are determinant in terms of the number of axle load repetitions that take the material to failure: the stiffness of the material, that determines its damage evolution rate, and the strain level applied to the pavement. The rule observed here is that the stiffer the material, the higher the fatigue life if low strains (low deflection) are present in the pavement. But such rule is reversed when the pavement is subjected to loads that produce high strains: in this case, the harder the material, the lower the fatigue lives. It is clear that the fatigue phenomenon is governed not only by strain level in the pavement, but also by a synergic effect of strain level of the pavement and stiffness level of the material, represented by its damage evolution rate.

The final rank order indicated that the fine aggregate matrix prepared with 40% of RAP and using a PG 64 binder to correct the binder content of the final mixture resulted the best alternative in terms of longer fatigue lives. The second best alternative is the FAM produced with 20% of RAP and a PG 58 binder. These two alternatives provided fatigue lives higher than the conventional alternative of using only new materials to produce the asphalt mixture. It is also important to notice that the alternative of producing a FAM with 40% of RAP and 100% rejuvenating agent to correct the binder content is also good, once that its position in the rank order is very close to the position occupied by FAM 2.

It is also interesting to see that, out of the four FAMs produced with rejuvenating agent, three occupy the last positions in the rank order, what means that they presented

the lowest fatigue lives. This is a clear indication that the shale oil residue did not play its role of rejuvenating the aged binder, probably because of the low diffusion rate of the material into the aged binder. But such difficulty to diffuse into the aged binder can not be attributed only to the possible low diffusion rate, once that the mixing conditions and the time for the diffusion process to occur also influence on the diffusion of the agent into the aged binder. Depending on the chemical characteristics of the new binder and the mixing conditions, the agent can mix first with the new binder instead of mixing with the aged binder – if such phenomenon occurs, no aromatic fractions are available to restore the properties of the aged binder. On the other hand, FAM 14 is an exception to this trend and provides evidence that the rejuvenating agent played its role satisfactorily.

At this moment, it is very important to draw the reader's attention to the fact that all the conclusions made here are based on some assumptions that are always issues of discussion and that can always cast some doubts about the nature of the conclusions. The first one is the assumption that the viscoelastic continuum damage theory is adequate to model the damage evolution characteristics of the samples. The second is that the mechanistic fatigue prediction model adopted here actually represents the fatigue behavior of the asphalt mixture in the field. And the third and probably the most important is the strain levels adopted in the analysis, once that the choice of other strain to perform the same analysis carried out here can lead to distinct results in the material rank.

5.3. Suggestions for future studies

The following suggestions for future studies are presented:

- to evaluate the effect of different rejuvenating agents on the fatigue behavior of FAMs produced with reclaimed asphalt pavements;
- to evaluate the effect of different types of aggregates on the fatigue behavior of FAMs produced with reclaimed asphalt pavements;
- to evaluate the effect of different sources of reclaimed asphalt pavements on the fatigue behavior of FAMs produced with reclaimed asphalt pavements;

- to investigate the chemical interaction of the rejuvenating agent and the aged binder of the RAP mixtures;
- to investigate the influence of air voids of FAM samples prepared with RAP on the fatigue performance.

6. REFERENCES

Al-Qadi, I. L., Aurangzeb, Q., Carpenter, S. H., Pine, W. J., & Trepanier, J. (2012). *Impact of high RAP contents on structural and performance properties of asphalt mixtures*. Research Report 2 FHWA-ICT-12-002. Illinois Department of Transportation. Springfield, IL. 53p.

Ali, A. W., Mehta, Y. A., Nolan, A., Purdy, C., & Bennert, T. (2016). Investigation of the impacts of aging and RAP percentages on effectiveness of asphalt binder rejuvenators. *Construction and Building Materials*. 110, 211–217.

Almeida, L. R., Bessa, I. S., Vasconcelos, K. L., Bernucci, L. B., Beja, I. A., & Chaves, J. M. (2014). *Análise de propriedades físicas e mecânicas de misturas asfálticas recicladas a frio com emulsão asfáltica e cimento Portland e a influência de cada material*. In: 28º Congresso de Pesquisa e Ensino em Transportes. Associação Nacional de Pesquisa e Ensino em Transportes. Curitiba, PR.

Al-Qadi, I. L., Elseifi, M., & Carpenter, S. H. (2007). *Reclaimed asphalt pavement – a literature review*. Report no. FHWA-ICT-07-001. Illinois Department of Transportation. Springfield, IL. 23p.

Al-Qadi, I. L., Carpenter, S. H., Roberts, G., Ozer, H., Aurangzeb, Q., Elseifi, M., & Trepanier, J. (2009). *Determination of usable residual asphalt binder in RAP*. Research Report No. FHWA-ICT-09-031. Illinois Center for Transportation. Springfield, IL. 64p.

Amirkhanian, S.N., & Williams, B. (1993). Recyclability of moisture-damaged flexible pavements. *Journal of Materials in Civil Engineering.* 5(4), 510–530.

Arrambide, J., and Duriez, M. (1959). *Liants Routiers et Enrobés: Matériaux de Protection, Plâtre, Agglomérés, Bois.* Moniteur des Travaux Publics, Dunod.

Aragão, F. T. S., Kim, Y., Karki, P., & Little, D. (2010). Semi empirical, analytical, and computational predictions of dynamic modulus of asphalt concrete mixtures. *Transportation Research Record*. 2181, 19–27.

Aragão, T. S. F., Hartmann, D., Kim, Y.-R., Motta, L., & Haft-Javaherian, M. (2014). Numerical–experimental approach to characterize fracture properties of asphalt mixtures at low temperatures. *Transportation Research Record.* 2447, 42–50.

Aragão, T. S. F., & Kim, Y.-R. (2012). Mode I fracture characterization of bituminous paving mixtures at intermediate service temperatures. *Experimental Mechanics*. 52(9), 1423–1434.

Aragão, T. S. F., Kim, Y.-R., Lee, J., & Allen, D. H. (2011). Micromechanical model for heterogeneous asphalt concrete mixtures subjected to fracture failure. *Journal of Materials in Civil Engineering.* 23(1), 30–38.

Arambula, E., Masad, E., & Martin, A. E. (2007). Moisture susceptibility of asphalt mixtures with known field performance evaluated with dynamic analysis and crack growth model. *Transportation Research Record*. 2001, 20–28.

Arega, Z. A., Bhasin, A., & de Kesel, T. (2013). Influence of extended aging on the properties of asphalt composites produced using hot and warm mix methods. *Construction and Building Materials.* 44, 168–174.

Asli, H., Ahmadinia, E., Zargar, M., & Karim, M. R. (2012). Investigation on physical properties of waste cooking oil – rejuvenated bitumen binder. *Construction and Building Materials.* 37, 398–405.

Asphalt Institute (1986). *Asphalt hot-mix recycling*. *The asphalt institute manual*. Series No. 20 (MS-20), Second Edition.

Aurangzeb, Q., & Al-Qadi, I. (2014). Asphalt pavements with high reclaimed asphalt pavement content: economic and environmental perspectives. *Transportation Research Record: Journal of the Transportation Research Board.* 2456, 161–169.

Aurangzeb, Q., Al-Qadi, I., Abuawad, I., Pine, W., & Trepanier, J. (2012). Achieving desired volumetrics and performance for mixtures with high percentage of Reclaimed Asphalt Pavement. *Transportation Research Record.* 2294, 34–42.

Balbo, J. T. (2007). *Pavimentação asfáltica: materiais, projeto, e restauração.* Oficina de Textos.

Balbo, J.T., & Bodi, J. (2004). *Reciclagem a quente de misturas asfálticas em usinas: alternativa para bases de elevado módulo de elasticidade*. In: 18º Congresso de Pesquisa e Ensino em Transportes. Associação Nacional de Pesquisa e Ensino em Transportes. Florianópolis, SC.

Bessa, I. S., Almeida, L. R., Vasconcelos, K. L., & Bernucci, L. L. (2016). Design of cold recycled mixes with asphalt emulsion and Portland cement. *Canadian Journal of Civil Engineering*. 43, 773–782.

Bhasin, A. (2006). *Development of methods to quantify bitumen-aggregate adhesion and loss of adhesion due to water*. Ph.D. dissertation, Texas A&M University. College Station, TX.

Bhasin, A., Little, N. D., Bommavaram, R., & Vasconcelos, K. (2008). A framework to quantify the effect of healing in bituminous materials using material properties. *Road Materials and Pavement Design*. 9(1), 219–242.

Boriack, P., Katicha, S., & Flintsch, G. (2014). A laboratory study on effects of high RAP and binder content. Stiffness, fatigue resistance and rutting resistance. *Transportation Research Record.* 2445, 64–74.

Brownidge, J. (2010). *The role of an asphalt rejuvenator in pavement preservation: use and need for asphalt rejuvenation*. In: 1st International Conference on Pavement Preservation, (p.351–364).

Burr, B., Davison, R., Jemison, H., Glover, C., & Bullin, J. (1991). Asphalt hardening in extraction solvents. *Transportation Research Record.* 1323, 70–76.

Carey, D.E., & Paul, H.R. (1982). *Quality control of recycled asphaltic concrete.* Research Report n.158, Louisiana Department of Transportation and Development.

Caro, S., Beltran, D. P., Alvarez, A. E., & Estakhri, C. (2012). Analysis of moisture damage susceptibility of warm mix asphalt (WMA) mixtures based on dynamic mechanical analyzer (DMA) testing and a fracture mechanics model. *Construction and Building Materials*. 35, 460–467.

Caro, S., Masad, E., Airey, G., Bhasin, A., & Little, D. N. (2008). Probabilistic analysis of fracture in asphalt mixes caused by moisture damage. *Transportation Research Record.* 2057, 28–36.

Caro, S., Masad, E., Bhasin, A., & Little, D. (2010). Micromechanical modeling of the influence of material properties on moisture-induced damage in asphalt mixtures. *Construction and Building Materials*. 24, 1184–1192.

Carpenter, S.H., & Wolosick, J.R. (1980). Modifier influence in the characterization of hot-mix recycled material. *Transportation Research Record.* 777, 15–22.

Castelo Branco, V. T. F. (2008). *A unified method for the analysis of nonlinear viscoelasticity and fatigue cracking of asphalt mixes using the dynamic mechanical analyzer.* Ph.D. Dissertation, Texas A&M University. College Station, TX. 220p.

Castelo Branco, V. T. F., Masad, E., Bhasin, A., & Little, D. (2008). Fatigue analysis of asphalt mixtures independent of mode of loading. *Transportation Research Record*. 2057, 149–156.

Christensen, R. M. (1982) *RICHARD M. Theory of viscoelasticity: An Introduction*. [s.l.] Academic Press.

Copeland, A. (2008). *Sustaining our highways: a national perspective on rap usage and best practices for recycled asphalt pavements.* Presented at Pavement Performance Prediction Symposium, Laramie, WY.

Copeland, A. (2011). *Reclaimed asphalt pavement in asphalt mixtures: state of the practice*. Publication FHWA-HRT-11-021, Turner-Fairbank Highway Research Center, Federal Highway Administration, McLean, VA, 49p.

Costa, C., Pinto, S. (2011). O uso de reciclagem de pavimentos como alternativa para o desenvolvimento sustentável em obras rodoviárias no brasil. *Revista Engenharia*. 602, 96–102.

Cravo, M. C. C. (2016). *Efeitos do envelhecimento térmico e fotoquímico em ligantes asfálticos, mástique e matriz de agregados finos*. Ph.D. Thesis, UFRJ – Federal University of Rio de Janeiro. Rio de Janeiro, RJ.

Cucalon, L. G., Kassem, E., Little, D. N., & Masad, E. (2017). Fundamental evaluation of moisture damage in warm-mix asphalts. *Road Materials and Pavement Design.* 18(S1). 258–283.

Daniel, J. S., & Kim, Y. R. (2002). Development of a simplified fatigue test and analysis procedure using a viscoelastic continuum damage model. *Journal of the Association of Asphalt Paving Technologists*. 71, 619–650.

Daniel, J., Pochily, J., & Boisvert, D. (2010). Can more reclaimed asphalt pavement be added? Study of extracted binder properties from plant-produced mixtures with up to 25% reclaimed asphalt pavement. *Transportation Research Record: Journal of the Transportation Research Board*. 2180, 19–29.

David, D. (2006). *Misturas asfálticas recicladas a frio: estudo em laboratório utilizando emulsão e agente de reciclagem emulsionado*. Masters Dissertation. Federal University of Rio Grande do Sul. Porto Alegre, RS. 117p.

Domingues, M.P., & Balbo, J.T. (2006). *Estudo de características de misturas asfálticas recicladas a quente com o emprego de usinas transportáveis de pequeno porte*. In: 20º Congresso de Pesquisa e Ensino em Transportes. Associação Nacional de Pesquisa e Ensino em Transportes. Brasília.

EAPA (2015). *Asphalt in figures*. Available in: http://www.eapa.org/asphalt.php

Epps, J. A., Little, D. N., Holmgreen, R. J., & Terrel, R. L. (1980). *Guidelines for recycling pavement materials*. NCHRP Report. (224).

Freire, R. A. (2015). *Evaluation of the coarse aggregate influence in the fatigue damage using fine aggregate matrices with different maximum nominal sizes.* Master's Dissertation. Federal University of Ceará. Fortaleza – CE.

Freire, R. A., Babadopulos, L. F. A. L., Castelo Branco, V. T. F., & Bhasin, A. (2017). Aggregate maximum nominal sizes' influence on fatigue damage performance using different scales. *Journal of Materials in Civil Engineering.* 29(8), 04017067.

Freire, R. A., Castelo Branco, V. T. F., & Vasconcelos, K. (2014). Avaliação da resistência ao trincamento de misturas asfálticas compostas por agregados miúdos com diferentes tamanhos máximos nominais. *Revista Transportes*. 22(3). 117–127.

Ghabchi, R., Barman, M., Singh, D., Zaman, M., & Mubaraki, M. A. (2016). Comparison of laboratory performance of asphalt mixes containing different proportions of RAS and RAP. *Construction and Building Materials*. 124, 343–351.

Gong, X., Romero, P., Dong, Z., & Sudbury, D. S. (2016). The effect of freeze–thaw cycle on ohe low-temperature properties of asphalt fine aggregate matrix utilizing bending beam rheometer. *Cold Regions Science and Technology.* 125, 101–107.

Gudipudi, P., & Underwood, B. S. (2015). Testing and modeling of fine aggregate matrix and its relationship to asphalt concrete mix. *Journal of the Transportation Research Board.* 2507, 120–127.

Haghshenas, H., Nabizadeh, H., Kim, Y-R., & Santosh, K. (2016). *Research on high-RAP asphalt mixtures with rejuvenators and WMA additives*. Report nº SPR-P1(15) M016. Nebraska Department of Roads. Lincoln, NE.

Hajj, E., Souliman, M., Alavi, M., & Loría Salazar, L. (2013). *Influence of hydrogreen bioasphalt on viscoelastic properties of reclaimed asphalt mixtures*. In: 92th TRB Annual Meeting. Transportation Research Board, Washington, DC.

Hansen, K. R., & Newcomb, D. E. (2011). *Asphalt pavement mix production survey on reclaimed asphalt pavement, reclaimed asphalt shingles, and warm-mix asphalt usage*. Nov. Grant No.: DTFH-61-1–P-00084. National Asphalt Pavement Association. Lanham, MD.

He, Y., Alavi, M. Z., Jones, D., & Harvey, J. (2016). Proposing a solvent-free approach to evaluate the properties of blended binders in asphalt mixes containing high quantities of reclaimed asphalt pavement and recycled asphalt shingles. *Construction and Building Materials.* 114, 172–180.

Hill, B., Oldham, D., Behnia, B., Fini, E., Buttlar, W., & Reis, H. (2013). Low-temperature performance characterization of biomodified asphalt mixtures that contain reclaimed asphalt pavement. *Transportation Research Record: Journal of the Transportation Research Board.* (2371), 49–57.

Hu, X., Nie, Y., Feng, Y., & Zheng, Q. (2012). Pavement performance of asphalt surface course containing Reclaimed Asphalt Pavement (RAP). *Journal of Testing and Evaluation.* 40(7), 1–7.

Huang, B., Zhang, Z., & Kinger, W. (2004). *Fatigue crack characteristics of HMA mixtures containing RAP.* Proceedings, 5th International RILEM Conference on Cracking in Pavements. Limoges, France.

Im, S. (2012). *Characterization of viscoelastic and fracture properties of asphaltic materials in multiple lenght scales*. Ph.D. Dissertation, University of Nebraska–Lincoln. Lincoln, NE.

Im, S., Zhou, F., Lee, R., & Scullion, T. (2014). Impacts of rejuvenators on performance and engineering properties of asphalt mixtures containing recycled materials. *Construction and Building Materials.* 53, 596–603.

Im, S., You, T., Ban, H., & Kim, Y.-R. (2015). Multiscale testing-analysis of asphaltic materials considering viscoelastic and viscoplastic deformation. *International Journal of Pavement Engineering.* 8436(October), 1–15.

Islam, R. M., Mannan, U. A., Rahman, A. A., & Tarefder, R. A. (2014). *Effects of recycled asphalt pavement on mix and binder properties and performance in the laboratory*. In: 93th TRB Annual Meeting. Transportation Research Board, Washington, DC.

Izadi, A. (2012). *Quantitative characterization of microstructure of asphalt mixtures to evaluate fatigue crack growth*. Ph.D. dissertation, Texas A&M University. Austin, TX.

Kanaan, A., Ozer, H., & Al-Qadi, I. (2014). Testing of fine asphalt mixtures to quantify effectiveness of asphalt binder replacement using recycled shingles. *Transportation Research Record.* 2445(1), 103–112.

Kandhal, P. S. (1997). Recycling of asphalt pavements-an overview. *Journal of the Association of Asphalt Paving Technologists*, 66.

Kandhal, P. S., & Mallick, R. B. (1997). Pavement recycling guidelines for state and local governments. Federal Highway Administration, U. S. Department of Transportation. FHWA-SA-98-042. Washington, DC.

Kandhal, P. S., Rao, S. S., Watson, D. E., & Young, B. (1995). Performance of recycled hot mix asphalt mixtures. *Auburn: National Center for Asphalt Technology.* 7(1), 28-45.

Karki, P. (2014). *An integrated approach to measure and model fatigue damage and healing in asphalt composites*. Ph.D. dissertation, Texas A&M University. Austin, TX.

Karki, P., Bhasin, A., & Underwood, B. S. (2016). Fatigue performance prediction of asphalt composites subjected to cyclic loading with intermittent rest periods. *Transportation Research Record*. 2576, 72–82.

Karki, P., Kim, Y.-R., & Little, D. N. (2015a). Dynamic modulus prediction of asphalt concrete mixtures through computational micromechanics. *Journal of the Transportation Research Board.* 2507, 1–9.

Karki, P., Li, R., & Bhasin, A. (2015b). Quantifying overall damage and healing behavior of asphalt materials using continuum damage approach. *International Journal of Pavement Engineering.* 16(4), 350–362.

Karlsson, R., & Isacsson, U. (2006). Material-related aspects of asphalt recycling – state-of-the-art. *Journal of Materials in Civil Engineering*, 81(1), 81–92.

Kemp, G.R., & Predoehl, N.H. (1981). A comparison of field and laboratory environments on asphalt durability. *Association of Asphalt Paving Technologists*, 50, 492–537.

Kim, S., Sholar, G.A., Kim, J., & Byron, T., (2009a). *Performance of polymer modified asphalt mixture with reclaimed asphalt pavement*. Transportation Research Board Annual Meeting. Washington, D.C.

Kim, W., Lim, J., & Labuz, J. F. (2009b). *Cyclic triaxial testing of recycled asphalt pavement and aggregate base*. In: 88th TRB Annual Meeting. Transportation Research Board, Washington, DC.

Kim, Y. R., Seo, Y., King, M., & Momen, M. (2004). Dynamic modulus testing of asphalt concrete in indirect tension mode. *Transportation Research Record*. 1891, 163–173.

Kim, Y.-R., Allen, D. H., & Little, D. N. (2005). Damage-induced modeling of asphalt mixtures through computational micromechanics and cohesive zone fracture. *Journal of Materials in Civil Engineering.* 17(5), 477–484.

Kim, Y.-R., & Aragão, F. T. S. (2013). Microstructure modeling of rate-dependent fracture behavior in bituminous paving mixtures. *Finite Elements in Analysis and Design*. 63, 23–32.

Kim, Y.-R., Little, D. N., & Lytton, R. L. (2003a). Fatigue and healing characterization of asphalt mixtures. *Journal of Materials in Civil Engineering*. 15(1), 75–83.

Kim, Y.-R., Little, D. N., & Song, I. (2003b). Effect of mineral fillers on fatigue resistance and fundamental material characteristics. *Transportation Research Record*. 1832, 03-3454.

Kim, Y.-R., & Little, N. D. (2005). D*evelopment of specification-type tests to assess the impact of fine aggregate and mineral filler on fatigue damage*. Report No. FHWA/TX-05/0-1707-10. Federal Highway Administration, U.S. Department of Transportation and Texas Transportation Institute, 116 p.

Kodippily, S., Holleran, G., Wilson, D., & Henning, T. F. P. (2015). *Effects of polymer modified binder on the deformation and cracking performance of recycled asphalt paving mixes*. In: 94th TRB Annual Meeting. Transportation Research Board, Washington, DC.

Kubo, K. (2014). *Recycling in Japan*. TRB Circular, n.E-C188, p.60-66.

Lavin, P. (2003). *Asphalt Pavements: A practical guide to design, production and maintenance for engineers and architects*. CRC Press. London, Spon. 444p.

Lee H.-J. (1996). *Uniaxial constitutive modeling of asphalt concrete using viscoelasticity and continuum damage theory*. Ph.D. Dissertation. Raleigh, NC: North Carolina State University.

Lee, H.-J., Daniel, J. S., & Kim, Y. R. (2000). Continuum damage mechanics-based fatigue model of asphalt concrete. *Journal of Materials in Civil Engineering*, 12 (2), 105–112.

Lee, H.-J., & Kim, Y. R. (1998a). Viscoelastic continuum damage model of asphalt concrete with healing. *Journal of Engineering Mechanics*, 124 (11), 1224–1232.

Lee, H.-J., & Kim, Y. R. (1998b). Viscoelastic constitutive model for asphalt concrete under cyclic loading. *Journal of Engineering Mechanics*, 124 (1), 32–40.

Li, J., Ni, F., Huang, Y., & Gao, L. (2014). New additive used in hot in-place recycling to improve performance of RAP mix. *Transportation Research Record*. 2445, 39–46.

Li, X., Marasteanu, M., Williams, R., & Clyne, T. (2008). Effect of reclaimed asphalt pavement (proportion and type) and binder grade on asphalt mixtures. *Transportation Research Record.* 2051, 90-97.

Li, Y. (1999). *Asphalt pavement fatigue cracking modeling*. Ph.D. Dissertation. Louisiana State University. Ann Arbor, MI.

Lima, A.T. (2003). *Caracterização mecânica de misturas asfálticas recicladas a quente*. Master's Dissertation. Federal University of Ceará. Fortaleza, CE. 99p.

Little, D. H., Holmgreen Jr, R. J., & Epps, J. A. (1981). Effect of recycling agents on the structural performance of recycled asphalt concrete materials. *Association of Asphalt Paving Technologists*. 50, 32-63.

Lo Presti, D., Brown, L., Kranthi, K., Grenfell, J., Airey, G., Collop, A., & Scarpas, T. (2012). *Mechanical characterization of reclaimed asphalt mixes for modeling purposes*. In: 7th International Conference on Maintenance and Rehabilitation of Pavements, Auckland, New Zealand.

Ma, T., Huang, X, & Hussain, U.B. (2011). Evaluation of reclaimed asphalt pavement binder stiffness without extraction and recovery. *Journal of Central South University of Technology*. 18(4), 1316–1320.

Mannan, U. A., Islam, M. R., & Tarefder, R. A. (2015). *Fatigue behavior of asphalt containing Reclaimed Asphalt Pavements*. In: 94th TRB Annual Meeting. Transportation Research Board, Washington, DC.

Masad, E. A., Zollinger, C., Bulut, R., Little, D. N., & Lytton, R. L. (2006). Characterization of HMA moisture damage using surface energy and fracture properties. *Journal of the Association of Asphalt Paving Technologists*. 75, 713–754.

Masad, E., Castelo Branco, V. T. F., Little, D. N., & Lytton, R. (2008). A unified method for the analysis of controlled-strain and controlled-stress fatigue testing. *International Journal of Pavement Engineering*. 9(4), 233–246.

Masad, E., Jandhyala, V. K., Dasgupta, N., & Somadevan, N. (2002). Characterization of air void distribution in asphalt mixes using x-ray computed tomography. *Journal of Materials in Civil Engineering.* 14(2), 122–129.

Masad, E., Muhunthan, B., Shashidhar, N., & Harmanet, T. (1999). Internal structure characterization of asphalt concrete using image analysis. *Journal of Computing in Civil Engineering*. 13(2), 88–95.

Maupin Jr., G. W., Diefenderfer, S. D., & Gillespie, J. S. (2008). *Evaluation of using higher percentages of recycled asphalt pavement in asphalt mixes in Virginia*. VTRC Report VTRC08-R22, Charlottesville, Virginia, 26p.

Maupin Jr., G., Diefenderfer, S. D., & Gillespie, J. S. (2009). Virginia's Higher Specification for Reclaimed Asphalt Pavement: Performance and Economic Evaluation. *Transportation Research Record: Journal of the Transportation Research Board,* 2126, 142–150.

McDaniel, R. S., Soleymani, H., Anderson, R. M., Turner, P., & Peterson, R. (2000). *Recommended use of reclaimed asphalt pavement in the Superpave mix design method*. NCHRP Web Document 30, Project D9-12: Contractor´s Final Report.

McDaniel, R., & Anderson, R.M. (2001). *Recommended use of reclaimed asphalt pavement in the Superpave mix design method: technician's manual*. NCHRP Report 452. Washington, DC. 49p.

McMillan, C., & Palsat, D. (1985). Alberta's experience in asphalt recycling. *Canadian Technical Asphalt Association.* 30, 148–167.

Mogawer, W. S., Austerman, A. J., Bonaquist, R., & Roussel, M. (2011). Performance characteristics of thin lift overlay mixtures containing high RAP content, RAS, and warm mix asphalt technology. *Transportation Research Record*. 2208, 17–25.

Mogawer, W. S., Austerman, A. J., Kluttz, R., & Puchalski, S. (2015). *Achieving conventional mixture performance in high reclaimed asphalt pavement mixtures using rejuvenators and polymer-modified asphalt.* In: 94th TRB Annual Meeting. 15–1602. Washington, DC.

Mogawer, W. S., Bennert, T., Daniel, J. S., Bonaquist, R., Austerman, A. J., & Booshehrian, A. (2012). Performance characteristics of plant produced high RAP mixtures. *Journal of the Association of Asphalt Paving Technologists*. 81, 403–440.

Mogawer, W. S., Booshehrian, A., Vahidi, S., & Austerman, A. J. (2013). Evaluating the effect of rejuvenators on the degree of blending and performance of high RAP, RAS, RAP/RAS mixtures. *Journal of the Association of Asphalt Paving Technologists*. 82, 193–213.

Mogawer, W. S., Fini, E. H., Austerman, A. J., Booshehrian, A., & Zada, B. (2016). Performance characteristics of high reclaimed asphalt pavement containing bio-modifier. *Road Materials and Pavement Design*. 17(3), 753–767.

Mohammad, L. N., Negulescu, I. I., Wu, Z., Daranga, C., Daly, W. H., & Abadie, C. (2003). Investigation of the use of recycled polymer modified asphalt binder in asphalt concrete pavements. *Journal of the Association of Asphalt Paving Technologists.* 72, 551–594.

Mohammadafzali, M., Ali, H., Musselman, J. A., Sholar, G. A., Kim, S., & Nash, T. M. (2015). *A study on long-term aging of recycled binders using performance grade tests with extended aging time*. In: 94th TRB Annual Meeting. Transportation Research Board, Washington, DC.

Momm, L., & Domingues, F. A. A. (1995). *Reciclagem de pavimentos à frio "in situ" superficial e profunda.* Annual Pavement Meeting. 29th Edition. Cuiabá, PR.

Moreira, H.S. (2005). *Comportamento mecânico de misturas asfálticas a frio com diferentes teores de agregado fresado incorporado e diferentes modos de compactação*. Master's Dissertation. Federal University of Ceará. Fortaleza, C.E. 94p.

Motamed, A., Bhasin, A., & Izadi, A. (2012). *Fracture properties and fatigue cracking resistance of asphalt binders.* Research Report nº SWUTC/12/161122-1. University of Texas. Center for Transportation Research. Austin, TX.

Moya, J. P. A., Hong, F., & Prozzi, J. A. (2011). *RAP: save today, pay later*? In: TRB 90th Annual Meeting. 11–1017. Washington, DC.

Nabizadeh, H. (2015). *Viscoelastic, fatigue damage, and permanent deformation characterization of high rap bituminous mixtures using fine aggregate matrix (FAM).* Ph.D. Dissertation, University of Nebraska–Lincoln. Lincoln, NE.

Nascimento, M. D. V., Almeida, J. A., Lucena, A. E. F. L., Lucena, L. C. F. L., & Costa, S. C. F. E. (2013). Comportamento mecânico de misturas asfálticas recicladas com uso de compactação por impacto e por amassamento. *Ciência & Engenharia*. 22 (2), 115–120.

Newcomb, D. E., Brown, E. R., & Epps, J. A. (2007). *Designing HMA mixtures with high RAP content. A practical guide.* Quality Improvement Series 124. National Asphalt Pavement Association. Lanham, MD.

Olard, F., & Pouget, S. (2014). *Current status of RAP application in France*. TRB Circular. E-C188, 42–50.

Ongel, A., & Hugener, M. (2015). Impact of rejuvenators on aging properties of bitumen. *Construction and Building Materials*. 94, 467–474.

O'Sullivan, K. A. (2011). *Rejuvenation of reclaimed asphalt pavement (RAP) in hot mix asphalt recycling with high RAP contente.* Master's Thesis. Worcester Polytechnic Institute. Worcester, MA. 45p.

Ozer, H., Ma, J., Al-Qadi, I. L., & Sharma, B. K. (2017). *Rheological characterization of short- and long-term aged binders recovered from recycled asphalt mixes*. In: 96th TRB Annual Meeting. Transportation Research Board, Washington, DC.

Palvadi, N. S. (2011). *Measurement of material properties related to self-healing based on continuum and micromechanics approach*. Ph.D. dissertation, Texas A&M University. Austin, TX.

Palvadi, S., Bhasin, A., & Little, D. N. (2012). Method to quantify healing in asphalt composites by continuum damage approach. *Transportation Research Record*. 2296, 86–96.

Park, S. W., Kim, Y. R., & Schapery, R. A. (1996). A viscoelastic continuum damage model and its application to uniaxial behavior of asphalt concrete. *Mechanics of Materials.* 24 (4), 241–255.

Park, S. W., & Schapery, R. A. (1996). A viscoelastic constitutive model for particulate composites with growing damage. *International Journal of Solids and Structures.* 34 (8), 931–947.

Paul, H.R. (1996). Evaluation of recycled projects for performance. *Journal of the Association of Asphalt Paving Technologists.* 65, 231–254.

Pazos, A. G., Sacramento, F. T., & Motta, L. M. G. (2015). *Efeitos de Propriedades Morfológicas de Agregados no Comportamento Mecânico de Misturas Asfálticas*. 44ª RAPV – Annual Meeting of Paving. Foz do Iguaçu, PR.

Pereira, P. A., Oliveira, J. R., & Picado-Santos, L. G. (2004). Mechanical characterization of hot mix recycled materials. *International Journal of Pavement Engineering*, v.5, p.211–220.

Peterson, R.L., Soleymani, H.R., Anderson, R.M., & McDaniel, R.S. (2000). Recovery and Testing of RAP Binders from Recycled Asphalt Pavements. *Journal of the Association of Asphalt Paving Technologists.* 69, 72–91.

PIARC (2008). Review of the growth and development of recycling in pavement construction. PIARC Technical Committee C4.3 Road Pavements, 203p.

Pinto, S., Guarçoni, D.S., Ramos, C.R., & Guerreiro, F. (1994). *Recuperação de Pavimentos através da Reciclagem à Frio "in situ" com a Utilização de Agente Rejuvenescedor Emulsionado* – Case Studies. In: International Business Communications – Workshop. Rio de Janeiro, RJ.

Plancher, H., & Petersen, J. C. (1982). U.S. Patent No. 4,325,738. Washington, DC: U.S. Patent and Trademark Office.

Poulikakos, L. D., dos Santos, S., Lee, J., & Partl, M. N. (2014). *Moisture susceptibility of recycled asphalt concrete: a multi-scale approach*. In: TRB 93rd Annual Meeting. Washington, DC. (14–0041).

Reese, R. (1997). Properties of Aged Asphalt Binder Related to Asphalt Concrete Fatigue Life*. Journal of the Association of Asphalt Paving Technologists*. 66, 604–632.

Rowe, G. M. (1993). Performance of Asphalt Mixtures in the Trapezoidal Fatigue Test. *Journal of the Association of Asphalt Paving Technologists*. 62, 344–384.

Rowe, G. M., & Bouldin, M. G. (2000). *Improved Techniques to Evaluate the Fatigue Resistance of Asphaltic Mixes*. Proc., 2nd Eurasphalt and Eurobitume Congress. Barcelona.

Sabahfar, N., Hossain, M., & Hobson, C. (2016). *Low-temperature performance of Superpave mixtures with recycled asphalt pavement*. In: 95th TRB Annual Meeting. Transportation Research Board. Washington, DC.

Salman, B., Salem, O. S., Garguilo, D. T., & He, S. (2017). *Innovative maintenance, repair, and reconstruction techniques for asphalt roadways: a survey of State Departments of Transportation*. In: 96th TRB Annual Meeting. Transportation Research Board. Washington, DC. (17–04946).

Sargious, M., & Mushule, N., (1991). Behavior of recycled asphalt pavement at low temperatures. *Canadian Journal of Civil Engineering.* 18, 428–435.

Schapery, R. A. (1975). A theory of crack initiation and growth in viscoelastic media iii. analysis of continuous growth. *International Journal of Fracture.* 11, 549–562.

Schapery, R. A. (1984). Correspondence principles and a generalized J integral for large deformation and fracture analysis of viscoelastic media. *International Journal of Fracture.* 25, 195–223.

Schapery, R. A. (1990). A theory of mechanical behavior of elastic media with growing damage and other changes in structure. *J. Mech. Phys. Solids.* 38, 215–253.

Schimmoller, V. E., Holtz, K., Eighmy, T. T., Wiles, C., Smith, M., Malasheskie, G., Rohrbach, G. J., Schaftlein, S., Helms, G., Campbell, R. D., Deusen, Charles H. V. D., Ford, B., & Almborg, J. A. (2000). *Recycled materials in European highway environments: uses, technologies, and policies*. Federal Highway Administration, Washington, DC, 132p.

Shah, A., McDaniel, R. S., Huber, G. A., & Gallivan, V. L. (2007). Investigation of properties of plantproduced RAP mixtures. *Transportation Research Record:* 1998, 103–111.

Shen, J., Amirkhanian, S., & Lee, S. J. (2005). The effects of rejuvenating agents on recycled aged CRM binders. *International Journal of Pavement Engineering*, v.6, n.4, p.273–279.

Shen, J., Amirkhanian, S., & Aune Miller, J. (2007a). Effects of rejuvenating agents on Superpave mixtures containing Reclaimed Asphalt Pavement. *Journal of Materials in Civil Engineering*, v.19, n.5, p.376-384.

Shen, J., Amirkhanian, S., & Tang, B. (2007b). Effects of rejuvenator on performance-based properties of rejuvenated asphalt binder and mixtures. *Construction and Building Materials*, v.21, p.958–964.

Silva, A. H. M. (2011). *Avaliação do comportamento de pavimentos com camada reciclada de revestimentos asfálticos a frio com emulsão modificada por polímero*. Master's Degree Thesis. São Paulo, SP. University of São Paulo.

Silva, H. M. R. D., Oliveira, J. R. M., & Jesus, C. M. G. (2012). Are totally recycled hot mix asphalts a sustainable alternative for road paving? *Resources, Conservation and Recycling.* 60, 38–48.

Smiljanic, M., Stefanovic, J., Neumann, H. J., Rahimian, I., & Javonovic, J. (1993). Ageing of asphalt on paved roads. Characterization of asphalts extracted from the wearing course of the Belgrade. Niš highway. *Erdöl und Kohle, Erdgas, Petrochemie vereinigt mit Brennstoff-Chemie*. 46(6), 238-244.

Sondag, M. S., Chadbourn, B. A., & Drescher, A. (2002). *Investigation of recycled asphalt pavement (RAP) mixtures*. Report No. MN/RC – 2002-15. Minnesota Department of Transportation. 93p.

Song, I. (2004). *Damage analysis in asphalt concrete mixtures based on parameter relationships*. Ph.D. dissertation, Texas A&M University. College Station, TX.

Souza, L. T., Kim, Y.-R., Souza, F. V., & Castro, L. S. (2012). Experimental testing and finite-element modeling to evaluate the effects of aggregate angularity on bituminous mixture performance. *Journal of Materials in Civil Engineering*. 24(3), 249–258.

Sullivan, J. (1996). *Pavement recycling executive summary and report*. Report FHWA-AS-95-060, Washington, DC, 119p.

Tam, K. K., Joseph, P. E., & Lynch, D. F. (1992). Five-year experience of low-temperature performance of recycled hot mix. *Transportation Research Record*, n.1362, p.56-65.

Tavakol, M., Hossain, M., & Heptig, B. (2017). *Minimum required virgin binder content for recycled Superpave mixtures*. In: 96th TRB Annual Meeting, Transportation Research Board, Washington, DC.

Taylor, N. H. (1978). *Life expectancy of recycled asphalt paving. Recycling of bituminous pavements.* L. E. Wood, ed., American Society for Testing Materials, Philadelphia, 3–15.

Terrel, R., & Epps, J. (1989). *Using additives and modifiers in Hot-Mix Asphalt*. Lanham, MD: Quality Improvement Series (QIP 114 A), NAPA, 9p.

Terrel, R. L., Epps, J. A., Joharifard, M., & Wiley, P. (1997). *Progress in hot in-place recycling technology*. In 8th International Conference on Asphalt Pavements (ICAP). Seattle, WA, USA.

Tong, Y., Luo, R., & Lytton, R. L. (2013). Modeling water vapor diffusion in pavement and its influence on fatigue crack growth of fine aggregate mixture. *Transportation Research Record*. 2373. 71–80.

Tong, Y., Luo, R., & Lytton, R. L. (2015). Moisture and aging damage evaluation of asphalt mixtures using the repeated direct tensional test method*. International Journal of Pavement Engineering*. 16(5), 397–410.

Trichês, G., Lazzarin, C., & Bezem, W. (2000). *Estudo sobre o aproveitamento do material fresado no revestimento de vias urbanas*. In: 1º Simpósio Internacional de Manutenção e Restauração de Pavimentos e Controle Tecnológico. São Paulo, p.487-498.

Underwood, B. S., & Kim Y. R. (2011). Experimental investigation into the multiscale behavior of asphalt concrete. *International Journal of Pavement Engineering.*12(4), 357–370.

Underwood, B. S., & Kim, Y. R. (2013). Effect of volumetric factors on the mechanical behavior of asphalt fine aggregate matrix and the relationship to asphalt mixture properties. *Construction and Building Materials*. 49, 672–681.

Vasconcelos, K. L., Bhasin, A., & Little, D. N. (2010). Influence of Reduced Production Temperatures On the Adhesive Properties of Aggregates and Laboratory Performance of Fine Aggregate-Asphalt Mixtures. *International Journal of Road Materials and Pavement Design.* 11(1), 47–64.

Vasconcelos, K. L., Bhasin, A., Little, D. N., & Lytton, R. L. (2011). Experimental Measurement of Water Diffusion through Fine Aggregate Mixtures. *Journal of Materials in Civil Engineering.* 23(4).

Vasconcelos, K.L., & Soares, J.B. (2003). *Projeto de misturas de concreto betuminoso reciclado a quente com diferentes teores de material fresado*. In: XII Congreso Iberolatinoamericano del Asfalto, Quito.

Vasconcelos, K.L., & Soares, J.B. (2004). *Influência do percentual de fresado e do envelhecimento de curto prazo na dosagem de misturas asfálticas recicladas a quente*. In: XVI Congresso de Ensino e Pesquisa em Transportes, Associação Nacional de Pesquisa e Ensino em Transportes – ANPET, Florianópolis.

Ventura, A., Monéron, P., & Jullien, A. (2008). Environmental impact of a binding course pavement section, with asphalt recycled at varying rates: use of life cycle methodology. *Road Materials and Pavement Design*, *9*(sup1), 319-338.

Vincent, J. (2012). Basic Elasticity and Viscoelasticity. *Structural Biomaterials*: Third Edition (1–28). Princeton University.

Visintine, B. (2011). *An Investigation of Various Percentages of Reclaimed Asphalt Pavement on the Performance of Asphalt Pavements*. Ph.D. Dissertation. Raleigh, NC: North Carolina State University.

West, R. C., Rada, G. R., Willis, J. R., & Marasteanu, M. O. (2013). Improved mix design, *evaluation, and materials management practices for Hot-Mix Asphalt with high Reclaimed Asphalt Pavement content*. NCHRP Report n.752, Washington, DC, 152p.

West, R., Kvasnak, A., Tran, N., Powell, B., & Turner, P. (2009). Testing of Moderate and High Reclaimed Asphalt Pavement Content Mixes. Laboratory and Accelerated Field Performance Testing at the National Center for Asphalt Technology Test Track. *Journal of the Transportation Research Board.* 2126. 100–108.

Willis, J.R., & West, R. (2014). *Current status of Reclaimed Asphalt Pavement application in the United States*. TRB Circular, n.E-C188, p.3-16.

Winkle, C. V., Mokhtari, A., Lee, H. D., Williams, R. C., & Schram, S. (2016). Laboratory and Field Evaluation of HMA with High Contents of Recycled Asphalt Pavement. *Journal of Materials in Civil Engineering*, 29(2), 04016196.

Xu, J., Huang, S., & Qin, Y. (2014). Asphalt Pavement Recycling in Mainland China. *Transportation Research Circular.* E-C188: Application of RAP and RAS in Hot-Mix Asphalt. p. 51–60.

You, Z., Adhikari, S., & Kutay, M. E. (2009). Dynamic Modulus Simulation of the Asphalt Concrete Using the X-Ray Computed Tomography Images. *Materials and Structures*. 42(5), 617–630.

Yu, X., Zaumanis, M., Dos Santos, S., & Poulikakos, L. D. (2014) Rheological, microscopic, and chemical characterization of the rejuvenating effect on asphalt binders. *Fuel*, n.135, p.162-171.

Zaumanis, M., Mallick, R. B., & Frank, R. (2014a). Determining optimum rejuvenator dose for asphalt recycling based on Superpave performance grade specifications. *Construction and Building Materials*, 69, 159-166.

Zaumanis, M., Mallick, R., & Frank, R. (2013). Evaluation of Rejuvenator's Effectiveness with Conventional Mix Testing for 100% Reclaimed Asphalt Pavement

Mixtures. *Transportation Research Record: Journal of the Transportation Research Board*, (2370), 17-25.

Zaumanis, M., Mallick, R. B., Poulikakos, L., & Frank, R. (2014b). Influence of six rejuvenators on the performance properties of Reclaimed Asphalt Pavement (RAP) binder and 100% recycled asphalt mixtures. *Construction and Building Materials*, 71, 538–550.

Zhang, K., Wen, H., & Hobbs, A. (2015). Laboratory Tests and Numerical Simulations of Mixing Superheated Virgin Aggregate with Reclaimed Asphalt Pavement Materials. *Journal of the Transportation Research Board*. 2506, 62–71.

Zhang, K., Muftah, A., Wen, H., Bayomy, F., & Santi, M. (2016). *Performance-related design method for asphalt mixes that contain Reclaimed Asphalt Pavement (RAP).* In: 95th TRB Annual Meeting, Transportation Research Board, Washington, DC.

Zhu, J., Alavi, M. Z., Harvey J., Sun, L., & He, Y. (2017) Evaluating Fatigue Performance of Fine Aggregate Matrix of Asphalt Mix Containing Recycled Asphalt Shingles. *Construction and Building Materials*. 139, 203–211.

Zollinger, C. J., (2005). *Application of Surface Energy Measurements to Evaluate Moisture Susceptibility of Asphalt and Aggregates*. Master's Thesis. Texas A&M University. College Station, TX.

Appendix A – General information of the FAM samples

	FINGERPRINT						DAMAGE TEST							OBSERVATIONS
	SAMPLE	AIR VOIDS (%)	Glve (Pa)	m	α	DATE	STRESS (kPa)	TIME (HS)	INITIAL G* (Pa)	I	FINAL G* (Pa)	C final	Ci - Cf	
MAF 01: 100% RAP	12	5.1	3.06E+09	0.088	11.37	23/01/17	50	44.0	2.47E+09	0.81	2.23E+09	0.73	0.08	LOW STRESS
MAF 01: 100% RAP	2	4.0	2.13E+09	0.199	5.02	14/02/17	100	-	-	-	-			TEMPERATURE VARIATION
MAF 01: 100% RAP	3	3.9	5.12E+09	0.141	7.10	07/02/17	100	131.0	4.30E+09	0.84	3.41E+09	0.67	0.17	
MAF 02: N.A. + 50/70	2	1.2	5.05E+08	0.547	1.83	17/01/17	50	16.6	4.98E+08	0.98	3.08E+08	0.61	0.38	
MAF 02: N.A. + 50/70	4	1.3	5.12E+08	0.544	1.84	14/12/16	60	43.6	3.51E+08	0.69	2.94E+08	0.58	0.11	
MAF 02: N.A. + 50/70	5	1.3	4.16E+08	0.520	1.92	14/12/16	60	95.5	3.68E+08	0.88	3.56E+08	0.86	0.03	TEMPERATURE VARIATION
MAF 07: 20% RAP + 50/70	7	1.2	1.00E+09	0.351	2.85	14/03/17	150	43.7	8.44E+08	0.84	5.93E+08	0.59	0.25	
MAF 07: 20% RAP + 50/70	9	1.2	7.08E+08	0.356	2.81	13/03/17	250	43.6	6.74E+08	0.95	2.94E+08	0.42	0.54	
MAF 08: 40% RAP + 50/70	1	3.0	7.37E+08	0.129	7.74	24/03/17	150	1.7	5.57E+08	0.76	3.68E+08	0.50	0.26	
MAF 08: 40% RAP + 50/70	7	2.5	1.72E+09	0.206	4.84	19/06/17	350	8.5	1.35E+09	0.78	8.47E+08	0.49	0.29	
MAF 08: 40% RAP + 50/71	6	2.3	1.36E+09	0.181	5.52	07/06/17								
MAF 08: 40% RAP + 50/71	14	2.9	1.60E+09	0.247	4.05	25/05/17								
MAF 09: 20% RAP + 85/100	5	0.9	8.49E+08	0.415	2.41	20/04/17	150	122.7	7.24E+08	0.85	4.95E+08	0.58	0.27	
MAF 09: 20% RAP + 85/101	3	1.0	7.40E+08	0.402	2.49	29/06/17								
MAF 10: 40% RAP + 85/100	3	1.0	1.43E+09	0.250	3.99	05/05/17	180	43.6	1.34E+09	0.93	1.18E+09	0.83	0.11	
MAF 10: 40% RAP + 85/100	7	1.2	1.40E+09	0.304	3.29	05/05/17	250	140.1	1.25E+09	0.89	1.00E+09	0.72	0.17	
MAF 10: 40% RAP + 85/101	9	1.0	1.46E+09	0.283	3.53	02/05/17								
MAF 10: 40% RAP + 85/100	12	0.9	1.40E+09	0.264	3.79	05/05/17	180	16.7	1.01E+09	0.72	7.33E+08	0.52	0.20	
MAF 11: 20% RAP + 50/50 (LIG/ÓLEO)	1	4.1	1.04E+09	0.351	2.85	24/05/17	150	4.0	1.00E+09	0.96	6.60E+08	0.64	0.33	
MAF 11: 20% RAP + 50/50 (LIG/ÓLEO)	4	3.3	9.27E+08	0.406	2.46	27/03/17	100	1.0	8.75E+08	0.94	7.41E+08	0.80	0.15	
MAF 11: 20% RAP + 50/50 (LIG/ÓLEO)	6	3.1	1.15E+09	0.345	2.90	24/03/17								
MAF 11: 20% RAP + 50/50 (LIG/ÓLEO)	8	3.9	1.36E+09	0.299	3.35	22/05/17	100	5.6	1.14E+09	0.84	6.78E+08	0.50	0.15	TEMPERATURE VARIATION
MAF 12: 20% RAP + 0/100 (LIG/ÓLEO)	9	4.0	1.42E+09	0.299	3.35	04/04/17	100	19.0	1.25E+09	0.88	8.09E+08	0.57	0.31	
MAF 12: 20% RAP + 0/100 (LIG/ÓLEO)	12	4.0	9.91E+08	0.318	3.14	30/05/17	60	-	-	-	-	-	-	TEMPERATURE VARIATION
MAF 12: 20% RAP + 0/100 (LIG/ÓLEO)	14	5.0	4.03E+08	0.208	4.81	14/06/17	200			0.00		0.00	0.00	
MAF 13: 40% RAP + 50/50 (LIG/ÓLEO)	2	5.7	1.57E+09	0.190	5.27	10/04/17	120	10.0	1.29E+09	0.82	8.17E+08	0.52	0.30	
MAF 13: 40% RAP + 50/50 (LIG/ÓLEO)	7	4.8	1.89E+09	0.273	3.66									
MAF 13: 40% RAP + 50/50 (LIG/ÓLEO)	13	7.2	1.78E+09	0.289	3.47	19/06/17				0.00		0.00	0.00	
MAF 14: 40% RAP + 0/100 (LIG/ÓLEO)	2	7.2	1.24E+09	0.281	3.56	20/01/17	230	58.0	1.16E+09	0.94	6.22E+08	0.50	0.44	
MAF 14: 40% RAP + 0/100 (LIG/ÓLEO)	3	7.0	1.09E+09	0.216	4.62	04/12/16	200	189.0	9.97E+08	0.92	7.92E+08	0.73	0.19	
MAF 14: 40% RAP + 0/100 (LIG/ÓLEO)	6	7.3	1.87E+09	0.234	4.27	27/01/17	230	46.7	1.18E+09	0.63	7.31E+08	0.39	0.24	
MAF 14: 40% RAP + 0/100 (LIG/ÓLEO)	7	6.8	1.35E+09	0.193	5.18	23/11/16	200	96.0	1.11E+09	0.82	8.95E+08	0.66	0.16	LOW STRESS